AUBURN
UNIVERSITY

SAMUEL GINN
COLLEGE OF ENGINEERING

Analysis and potential solutions to sediment deposition in Dean Road Bridge watershed, Midland City, AL

FINAL REPORT

Prepared by

Jose G. Vasconcelos, Ph.D.
Xing Fang, Ph.D., P.E.
J. Brian Anderson, Ph.D., P.E.
Sagar Tamang
Wenjun Song

Department of Civil Engineering
Auburn University

Submitted to

Alabama Department of Transportation
Montgomery, Alabama

NOVEMBER 2018

Highway Research Center
Harbert Engineering Center
Auburn, Alabama 36849

www.eng.auburn.edu/research/centers/hrc.html

1. Report No.	2. Government Accession No.	3. Recipient Catalog No.

4 Title and Subtitle	5 Report Date
ANALYSIS AND POTENTIAL SOLUTIONS TO SEDIMENT DEPOSITION IN DEAN ROAD BRIDGE WATERSHED, MIDLAND CITY, AL	November 2018
	6 Performing Organization Code

7. Author(s)	8 Performing Organization
Jose G. Vasconcelos, Ph.D., Xing Fang, Ph.D., P.E., J. Brian Anderson, Ph.D., P.E., Sagar Tamang, and Wenjun Song	Report No. ALDOT 930-925-1

9 Performing Organization Name and Address	10 Work Unit No. (TRAIS)
Highway Research Center Department of Civil Engineering 238 Harbert Engineering Center Auburn, AL 36849	11 Contract or Grant No.

12 Sponsoring Agency Name and Address	13 Type of Report and Period Covered
Alabama Department of Transportation 1409 Coliseum Boulevard Montgomery, AL 36130-3050	14 Sponsoring Agency Code

15 **Supplementary Notes**

16 Abstract

Land use changes in watersheds can create dramatic impacts to the environment as well to existing transportation infrastructure. A severe aggradation process is ongoing in Soapstone Branch, located in Dale County, Alabama, a tributary of the Little Choctawhatchee River. This aggradation has compromised most of the conveyance of the Dean Road Bridge (BIN 12930) as it crosses Soapstone Branch. Between February 2011 and April 2014, the clearance under the bridge, which exceeded 6 ft., dropped to near zero due to sediment accumulation brought from the upstream reaches of the watershed. Given this scenario, this research intended to: 1) study the causes for the ongoing sedimentation process in this stream, considering various competing processes happening within the watershed; and 2) propose alternative solutions to improve conveyance at Dean Road Bridge, with the goal of avoiding the need of a bridge replacement. This research included field investigations to help the calibration of hydrological and hydraulic modeling tools. The calibrated hydrological model supplied flow data for detailed, two-dimensional hydraulic simulations. The hydrological modeling also indicated that in recent years there was a 35% increase of 35% in sediment yield in the watershed. Hydraulic modeling showed that a stream modification strategy based on increasing stream slopes near Soapstone Branch consistently increased shear stresses in the stream bed, reducing the likelihood of sediment accumulation near the bridge. Further modeling indicate that, for long-term conditions including sediment transport in the stream, the solution is sustainable, and could be seen as a lower-cost alternative to bridge replacement at Dean Road.

17 Key Words	18 Distribution Statement
Scour, soil erosion, bridges, erosion functions	No restrictions.

19 Security Classification (of this report)	20 Security Classification (of this page)	21 No. of pages	22 Price
Unclassified	Unclassified	102	None

Final Report 930-925-1

Analysis and potential solutions to sediment deposition in Dean Road Bridge watershed, Midland City, AL

Submitted to

The Alabama Department of Transportation

Prepared by

Jose G. Vasconcelos, Ph.D.
Xing Fang, Ph.D., P.E.
J. Brian Anderson, Ph.D., P.E.
Sagar Tamang
Wenjun Song

NOVEMBER 2018

DISCLAIMERS

The contents of this report reflect the views of the authors, who are responsible for the facts and the accuracy of the data presented herein. The contents do not necessarily reflect the official views or policies of the Alabama Department of Transportation or the Auburn University Highway Research Center. This report does not constitute a standard, specification, or regulation. Comments contained in this paper related to specific testing equipment and materials should not be considered an endorsement of any commercial product or service; no such endorsement is intended or implied.

NOT INTENDED FOR CONSTRUCTION, BIDDING, OR PERMIT PURPOSES

Jose G. Vasconcelos, Ph.D.
Xing Fang, Ph.D., P.E.
J. Brian Anderson, Ph.D., P.E.

Research Supervisors

Acknowledgements

This project was sponsored by the Alabama Department of Transportation (ALDOT). Material contained herein was obtained in connection with a research project "Analysis and potential solutions to sediment deposition in Dean Road Bridge watershed, Midland City, AL" ALDOT Project 930-925, conducted by the Auburn University Highway Research Center. The funding, cooperation, and assistance of many individuals from each of these organizations are gratefully acknowledged.

Abstract

Land use changes in watersheds can create dramatic impacts to the environment as well to existing transportation infrastructure. A severe aggradation process is ongoing in Soapstone Branch, located in Dale County, Alabama, a tributary of the Little Choctawhatchee River. This aggradation has compromised most of the conveyance of the Dean Road Bridge (BIN 12930) as it crosses Soapstone Branch. Between February 2011 and April 2014, the clearance under the bridge, which exceeded 6 ft., dropped to near zero due to sediment accumulation brought from the upstream reaches of the watershed. Given this scenario, this research intended to: 1) study the causes for the ongoing sedimentation process in this stream, considering various competing processes happening within the watershed; and 2) propose alternative solutions to improve conveyance at Dean Road Bridge, with the goal of avoiding the need of a bridge replacement.

This research included field investigations to help the calibration of hydrological and hydraulic modeling tools. The calibrated hydrological model supplied flow data for detailed, two-dimensional hydraulic simulations. The hydrological modeling also indicated that in recent years there was a 35% increase of 35% in sediment yield in the watershed. Hydraulic modeling showed that a stream modification strategy based on increasing stream slopes near Soapstone Branch consistently increased shear stresses in the stream bed, reducing the likelihood of sediment accumulation near the bridge. Further modeling indicate that, for long-term conditions including sediment transport in the stream, the solution is sustainable, and could be seen as a lower-cost alternative to bridge replacement at Dean Road.

TABLE OF CONTENTS

LIST OF TABLES

LIST OF FIGURES

1. Introduction

Changes in land uses caused by human activities in watersheds are known to create impacts to natural systems, including streams, rivers and other water bodies. Among the various types of impacts, of particular relevance are those related to watershed and stream bank erosion. This issue is recognized in technical literature, and Castro and Reckendorf (1995) presented a summary of the various impacts of sediments to various water bodies, both in terms of water quality and quantity. The authors state that sediment impacts are complex, multifold, and have cumulative effects in streams and rivers that are difficult to reproduce in laboratory conditions.

Human activities that are linked to severe sediment loadings include construction sites (Harbor, 1995), clearcutting of forested areas (Brown and Krygier, 1971), and poorly managed agricultural practices. When these activities occur close to water bodies, the potential for these impacts are increased. Other factors may trigger gradual increase in sediments in water bodies, such as short-term climatic events, instream alterations or changes in land management. Impacts in water quality and quantities in streams are immediate to aquatic species such as fish and macroinvertebrates.

However, changes in river/stream hydrology, sediment generation and sediment transport can also create severe impacts to man-made structures such as bridges and culverts. For instance, watershed urbanization may contribute to larger peak runoff flows and volumes, which in turn may lead to increase in stream flow velocities, stream bank erosion, stream bank failure, and scouring. Activities such as forest clearcutting can generate a significant increase in sediment loadings that can enter streams and lead to aggradation. Poor agricultural practices can also be a source of sediments to streams, which in turn may also lead to aggradation.

More than 600,000 bridges in the National Bridge Inventory (NBI) are built over streams. There are a large proportion of these bridges built over alluvial streams that are continually adjusting their beds and banks. Stream instability includes aggradation, degradation, bank erosion, and lateral channel shift during the bridge's useful life. Federal Highway Administration's (FHWA) Hydraulic Engineering Circular (HEC) No. 20 provides guidance for stream stability analyses (Lagasse et al., 2012). Johnson et al. (2001) reported that aggradation at bridges has been experienced in the arid regions, Midwest states, such as Iowa and Tennessee, and in a number of mid-Atlantic states, such as Pennsylvania, New York, and West Virginia. For example, in 1972, Hurricane Agnes destabilized large portions of the channels in the Bentley Creek watersheds, causing a significant increase in bank erosion and subsequent movement of sediment (non-cohesive sand, gravel, cobbles, and boulders) through the channels. FHWA has the series of technical documents: HEC-18 (Arneson et al. 2012), HEC-20 (Lagasse et al., 2012), HEC-23 (Lagasse et al., 2009), and HDS 6 (Richardson et al., 2002), that provide some guidance on stream instability, but the primary focus of those documents is scour at bridge sites, and limited information is given about stream aggradation and its countermeasures. As result, there is limited guidance to DOTs as to how to address specific issues related to aggradation in streams.

1.1. Problem Statement

A severe aggradation process is ongoing in Soapstone Branch, located in Dale County, Alabama, a tributary of the Little Choctawhatchee River (USGS HUC 0314020105). As it is shown in Figure 1-1, the small stream and its watershed is near the southeast edge of Dale County. Figure

1-2 shows the aggradation condition at the Dean Road Bridge (BIN 12930) where Dean Road (Dale Co. Road 560) intercepts Soapstone Branch.

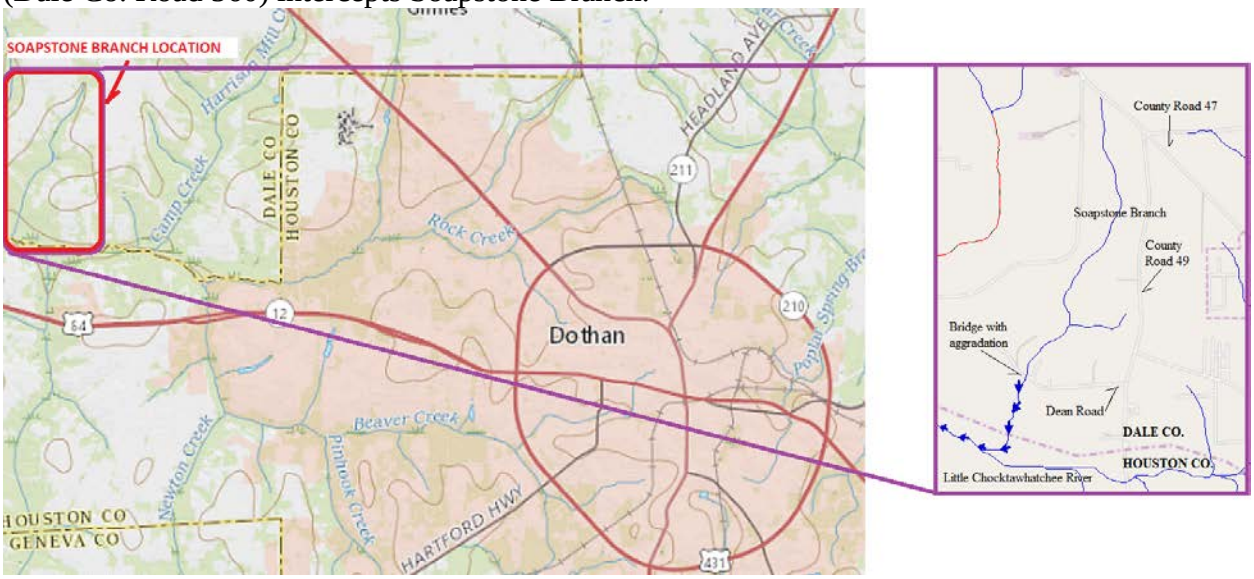

Figure 1-1: Location of Soapstone Branch and Dean Road within Dale County, AL.

Figure 1-2: Aggradation in Soapstone Branch under Dean Road Bridge (Field visit on 8/11/2015)

According to ALDOT, Dale County has diagnosed this aggradation problem in the bridge crossing in 2013, and by April 2014 there was only 2 inches of clearance beneath the bridge deck. Sediment excavation at the bridge vicinity was performed earlier in 2015, however by August 11, 2015 sedimentation had almost blocked the bridge, limiting again its flow conveyance. As result of this aggradation, the bridge has the potential of overtopping when moderate rain events were observed in the Soapstone Branch watershed, as it is illustrated in Figure 1-3.

Figure 1-3 Overtopping at Dean Road Bridge during a storm event of 02/03/2016

Several potential factors could be playing a role in the issue of sediment blockage at Dean Road Bridge. As is indicated in Figure 1-4, rainfall in the region has presented significant fluctuations in recent years, with peaks well above the long-term average. Severe rain events can create episodes of large surface runoff and exacerbate issues of sediment generation within watershed, stream bank failure, and stream bank erosion. Moreover, as Figure 1-5 indicates, since 2011 there has been land use changes, including construction of structures and forest clearcutting. These changes can help in increase processes such as surface erosion and streambank failures.

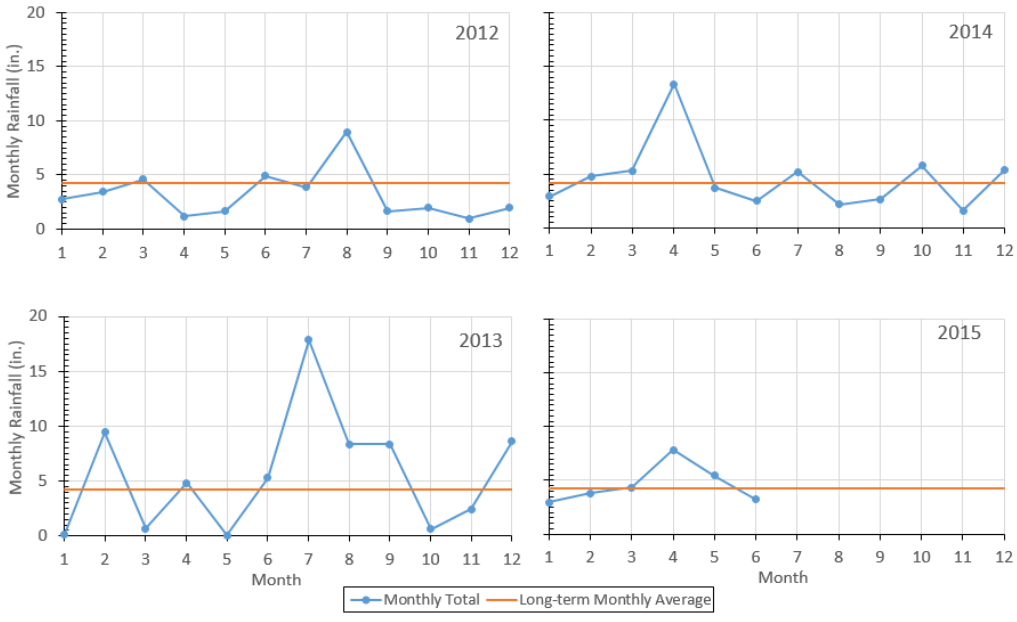

Figure 1-4: Monthly rainfall recorded at Dothan Regional Airport meteorological station since 2012. This meteorological station is 6.5 miles away from Dean Road Bridge

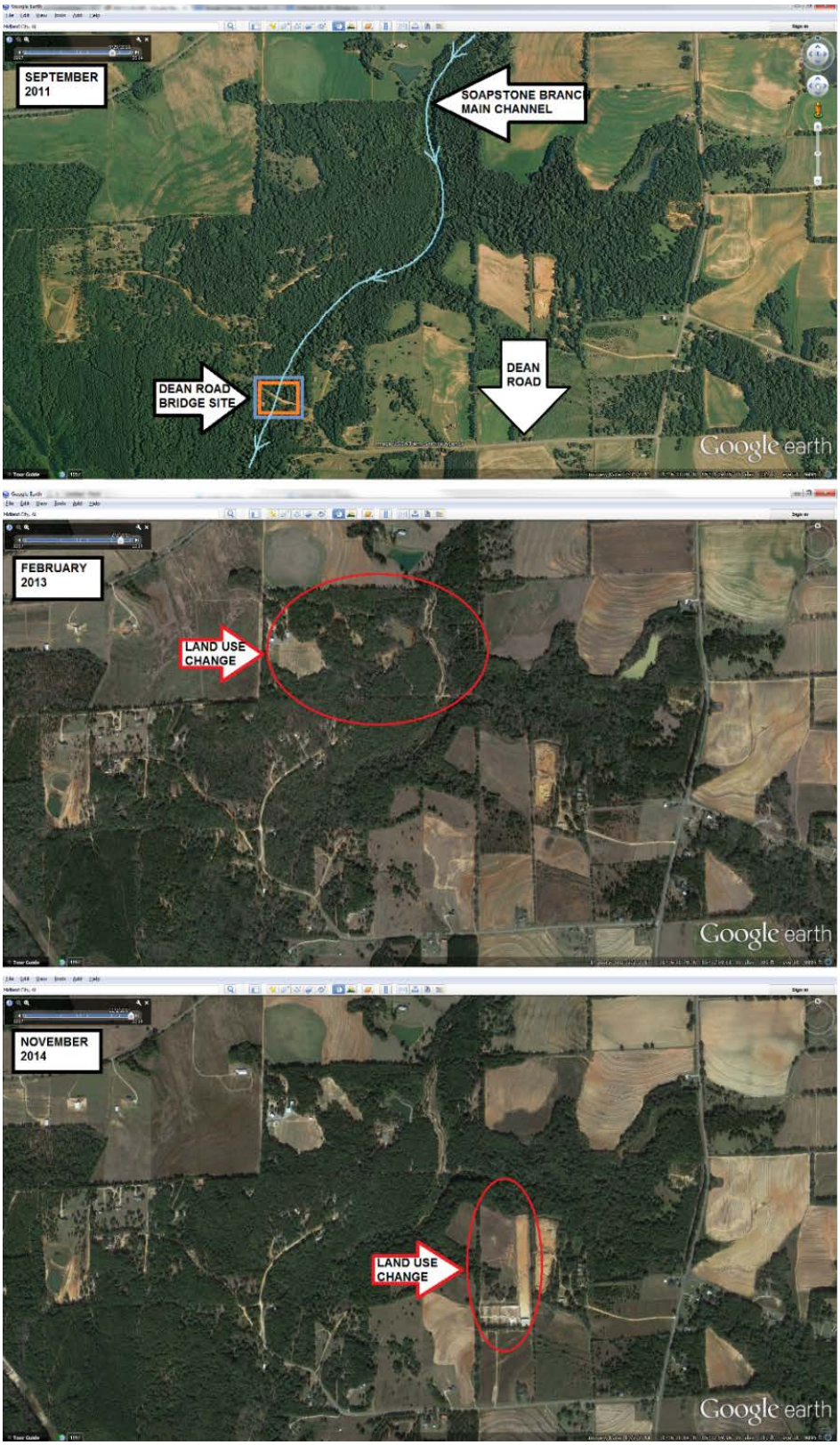

Figure 1-5: Land use changes identified in aerial images from Soapstone Branch watershed with reference to 09/2011 (top), in 02/2013 (middle), and 11/2014 (bottom).

1.2. Background

This background section is divided in two main parts. The first part presents fundamental aspects related to watershed hydrology and sediment generation and motion due to runoff, as well related modeling tools. The second part of the background focuses on modeling tools that are used to calculate flow characteristics in streams, as well the ability of such models to yield accurate solutions and to account for the transport of sediments.

1.2.1. Hydrological Cycle and Soil Erosion

Soil erosion is the process of detachment of top layer of soils by mechanical forces of wind or water. Negative impacts of soil erosion include and not limited to severe draughts in arid and semi-arid regions, reduction in the conveyance of channel resulting in flood, and a decrease in agricultural productivity. In the world, around 80% of agricultural land experience severe to moderate erosion and 10% experience moderate erosion (Speth 1994). It costs the US economy about $30–$40 billion dollars annually due to on and off site effects such as loss in agricultural productivity, blockage of conveyance of irrigation channel, etc. (Morgan 2009). Unlike mountainous regions where soil erosion limits land use and impacts agricultural productivity, lowland areas are more affected by erosion that induces blockage of flow in streams, bridges, and culverts. Such aggradation problems if not treated develop exponentially over time and may risk the damage of such structures and cause flooding.

The process of sediment motion is inserted in a wider concept of hydrological cycle. This is defined as the process by which ocean water is transported to the atmosphere, then to the land and back to the ocean (Viessman and Lewis 2003). Earth's hydrologic cycle begins with the evaporation of water from the surface of ocean, sea or other water bodies (Figure 1.6). As the water vapor moves upward, it condenses to form clouds. These clouds carry the moisture around the world and fall to the earth's surface in the form of precipitation (rain, dew, snow, etc.). a part of this precipitation infiltrates into the ground whereas, the remaining precipitation appears as surface overland flow. Infiltrated volume of water is stored in the groundwater and then appears as groundwater flow to supplement the streams. These streams then flow down to replenish seas and oceans. The process of transformation of precipitation into the overland flow, groundwater flow, and streamflow can be modeled using a hydrologic model.

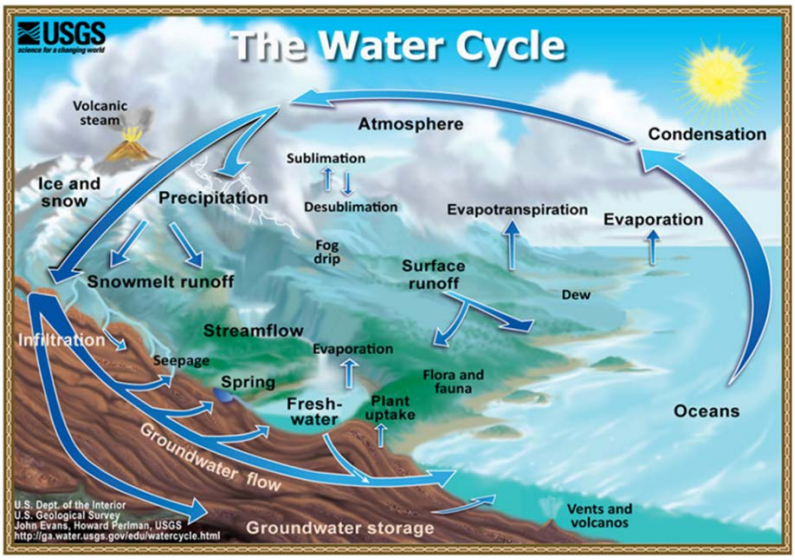

Figure 1-6: Earth's Hydrologic Cycle (Source: US Geological Survey)

The hydrologic model can be considered as an approximation of actual physical, chemical and biological processes going on in a catchment. The catchment is defined as the land area that drains to a specific point of interest in a stream. The physical process of interception, overland flow, infiltration, groundwater flow etc. are simplified by using model parameters, which mimic the real physical phenomenon. Also, the processes of nutrient transfer, chemical yields from agricultural land, effects on the biotic composition, the function of riparian ecosystems, etc. can be simulated using hydrologic model. In terms of representation of reality, a hydrologic model can be classified as a physical, analog or mathematical model (Feldman 2000). A physical hydrologic model is a miniature representation of real world system. This type of models when constructed at lab consists of surfaces altered to represent the land use, soil type, surface slope etc. of the watershed. The second type of hydrologic model, i.e., the analog model is developed to represent the flow of water with the flow of electricity in a circuit. This type of models has widespread use in computing subsurface flow. A mathematical hydrologic model consists of a set of equations to represent the flow of water with a change in a hydrometeorological variable. Further classification of a mathematical hydrologic model can be done based on whether it can simulate a single storm, i.e., an event-based model or it can simulate the hydrological response from a catchment for a longer period (both wet and dry), i.e., continuous hydrologic model.

In the context of the present research, numerical modeling of the local hydrology is adopted, since this will enable the development of more detailed hydraulic modeling of the flow conditions at the vicinity of Dean Road Bridge. In the process of using a hydrological model, calibration of hydrological parameters is a fundamental need. However, one challenge is how to perform such complex modeling given that the watershed is not gauged. One means by which ungauged catchments can be modeled well by borrowing parameters from an analogue donor catchment.

There exist three popular regionalization procedures to transfer the parameter from a donor-gauged catchment to a target-ungauged catchment:

- Regression analysis: a regression equation is developed and used to relate stream and catchment characteristics with the model parameters. Generally, multiple linear regression is used in which catchment attributes are treated as independent variables and model parameter as a dependent variable. This approach assumes that the relationship between catchment attributes and model parameters is well behaved, however, it has been found that model parameters are significantly affected by the calibration period and input accuracies. Furthermore, it assumes that the selected catchment attribute provides enough information on the behavior of ungauged catchment (Oudin et al. 2008).
- Physical similarity approach: In this procedure, parameters from donor (gauged) catchments that are “physically” similar to ungauged catchments are transferred. The rationale behind this approach is that catchments with similar physical properties behave hydrologically similar. Generally, this approach includes defining several physical properties and then ranking them based on similarity to identify the donor catchment.
- Spatial proximity approach: Parameters from donor (gauged) catchments that are near to ungauged catchments are transferred. It follows the assumption that the catchments nearby have similar climatic and catchment condition. It has been found that this approach performs better than physical similarity and regression analysis (Oudin et al. 2008; Zhang and Chiew 2009), and will be the method used in this research to calibrate the hydrological model to represent Soapstone Branch watershed and soil erosion.

Once parameters are transferred and hydrological modeling is enabled, it becomes possible to compute soil erosion created by the runoff. The Universal Soil Loss Equation (USLE) is one of the most widely adopted methods for estimating soil erosion. Equations used to estimate the amount of soil erosion began in the 1940's, and included effects of soil slope length and steepness (Zingg, 1940), crop and support practice factors (Smith, 1941), and tolerable soil loss limit equation through soil erodibility factor. A national committee in Ohio in 1946 developed a rainfall factor. A combination of all these studies helped in the development of USLE. The mathematical expression for USLE is given in

$$A = R * K * LS * C * P \quad (1.1)$$

Where,
A = soil loss per unit area with units depending on the units selected for K and R
R= rainfall erosivity factor
K= Soil erodibility factor
LS = topographic factor considering the effect of slope length and steepness of the slope
C = cover and management factor
P = support practice factor

After the development of USLE, additional research included revised isoerodent maps (spatial distribution of R factor), a new equation to reflect slope length and steepness, etc. All these improvements to the original USLE were incorporated into the Revised Universal Soil Loss Equation (RUSLE). However, issues with the application of USLE and RUSLE included determining sediment yield and failure to consider the runoff effect on soil erosion. Sediment yield at a specific point on watershed is defined as the total amount of eroded soil reaching that point, regardless of the origin of detached soil particle. Since USLE and RUSLE only provided an annual estimate of soil erosion occurring on a watershed, determination of sediment yield required further estimation of sediment delivery ratio (SDR, Eqn. 1.2). Also, as the overland flow moves downstream, it gains energy and erodes more particles. Both USLE and RUSLE disregard runoff-producing sediments. This leads to incorrect estimates in event-based calculations and, thus, the annual soil erosion amount (Kinnell 2005). The value of SDR is computed as:

$$SDR = \frac{Y}{E} \quad (1.2)$$

Where,
SDR= Sediment Delivery Ratio
Y = Average annual sediment yield per unit area
E = Average annual erosion over the same area

The Modified Universal Soil Loss Equation (MUSLE) is an advancement over both originally developed USLE and RUSLE, developed by replacing the rainfall erosivity factor with the runoff energy factor (Williams 1975). Unlike USLE and RUSLE, it is an event based soil loss model which considers the effect of runoff energy on generating sediment. Furthermore, it can provide an estimation of sediment yield. Apart from the runoff energy factor, other factors used in MUSLE are same as those of USLE which include the soil erodibility factor R, topographic factor LS (slope length and slope steepness), soil cover factor C, and conservational practice factor P. It was developed by collecting the data from 18 small watersheds with areas ranging from 132 to

4,380 acres. Several combinations of the volume of runoff and peak discharge were tried and the most accurate sediment prediction equation was finalized. The mathematical expression for MUSLE is given in Equation (2.7).

$$S = 95 * (Q * q_p)^{0.56} * K * LS * C * P \quad (1.3)$$

Where,
S = Sediment yield in tons
Q = Volume of runoff in acre-feet
qp = peak flow rate in cubic feet per second

1.2.2. Streamflow modeling strategies

Flows in natural streams are an intrinsically complex phenomenon due to a variety of factors. These factors range from the interactions between the stream and the watershed (e.g. surface water-groundwater interactions), flow unsteadiness, variable cross sections, and complex geometries. Attempts to describe open-channel flows mathematically go back near 150 years with the Saint-Venant equations, which consist in a system of partial differential equations describing mass and momentum conservations of one-dimensional (1-D) free surface flows. According to Sturm (2010), these equations can be expressed as:

$$\frac{\partial A}{\partial t} + \frac{\partial Q}{\partial x} = q \quad (1.4)$$

$$\frac{\partial Q}{\partial t} + \frac{\partial}{\partial x}\left(\beta \frac{Q^2}{A} + gAh_c\right) = gA\left(S_o - S_f\right) + q_L v_L \cos\phi \quad (1.5)$$

Where,
A = cross sectional area of the open channel flow;
Q = flow rate;
q_L = Lateral flow contribution
h_c = depth of the centroid cross section;
β = momentum correction factor
g = gravity acceleration;
S_0 = channel bed longitudinal slope
S_f = frictional slope = $\tau/\gamma R$, with R as the hydraulic radius, τ as the bed shear stress, γ as the specific weight
v_L = velocity of the flow within channel lateral contribution
ϕ = angle between lateral contribution and channel flow.

However, it was only in the past decades that computers have enabled numerical solutions of these equations to be useful in the context of engineering applications. A variety of channel flow models have emerged since the 1970's, as is exemplified by the HEC-2 (USACE, 1991), Telemac (1991), HEC-RAS 4 (Brunner, 2010), among others. Initially these models had a limitation in representing natural streams because they assumed that the stream cross sections

would not vary with time (fixed beds or stable cross sections), which is not the case in rivers with mobile beds.

Recent advances enabled the development of river flow modeling tools that are capable of representing two-dimensional (2-D) flows. These models are based on the shallow water equations, which is derived from the Euler equations by assuming a free-surface boundary condition as well assuming hydrostatic conditions. Examples of these models include the most recent version HEC-RAS 5 (Brunner, 2018), SRH-2D (Lai, 2010), among others. The set of equations that are typically solved by these models are presented below

$$\frac{\partial H}{\partial t} + \frac{\partial hu}{\partial x} + \frac{\partial hv}{\partial y} = q \qquad (1.6)$$

$$\frac{\partial u}{\partial t} + u\frac{\partial u}{\partial x} + v\frac{\partial u}{\partial y} + g\frac{\partial H}{\partial x} = \nu_t\left(\frac{\partial^2 u}{\partial x^2} + \frac{\partial^2 v}{\partial y^2}\right) - c_f u \qquad (1.7)$$

$$\frac{\partial v}{\partial t} + u\frac{\partial v}{\partial x} + v\frac{\partial v}{\partial y} + g\frac{\partial H}{\partial x} = \nu_t\left(\frac{\partial^2 u}{\partial x^2} + \frac{\partial^2 v}{\partial y^2}\right) - c_f v \qquad (1.8)$$

Where:
h and H are the flow depth and piezometric elevation ($H=z+h$) respectively
u and v are the components of flow velocity at x and y axis respectively
q is the lateral contribution to the flow
ν_t is the turbulent eddy viscosity.
c_f is the bed friction factor.

This is an important development, since it enables a more precise calculation of flows near more complex geometries, such as near the vicinity of bridges. This in turn enables more accurate calculations of shear stresses, which in turn can help to determine whether aggradation issues could be addressed with stream modification strategies. In addition to 2-D modeling features, models are beginning to incorporate calculation of sediment transport. This is also useful to the goals of this report since it could help to determine whether a solution based on stream modification has the potential of failing due to aggradation in a post-modification scenario.

2. Research objectives and structure of the report

As it was presented, the aggradation of Dean Road Bridge caused by sediment carried by Soapstone Branch is very severe, and it had resulted in overtopping following moderate-intensity rain events. This research will study this problem by focusing on two main goals:

1. Study the causes for the ongoing sedimentation process in this stream, considering watershed hydrology, stream hydraulics, sediment erodibility, and the processes for sediment generation and motion within the watershed
2. Propose tentative solutions to the sediment blockage based on stream modification near Dean Road Bridge, which limits bridge conveyance characteristics.

While not a direct research objective, it is anticipated that this investigation will provide insights in this type of problems, which is ongoing in other bridge structures in Alabama. With such knowledge, it is expected that solution strategies can be better devised for such structures. It is possible that such work will result in design recommendations and/or watershed management recommendations to reduce the likelihood of this type of problem in other bridge crossings.

The structure of this Final Research Report is as follows:

- Chapter 3 presents a Literature Review associated with this research
- Chapter 4 presents the Methodology used in field investigations and in the hydrological and hydraulic modeling work
- Chapter 5 focuses on presenting and discussing the research findings associated with the hydrological modeling, sediment generation, stream flow modeling and alternative for stream modification
- Chapter 6 presents a brief discussion on permitting aspects in performing engineering solutions to improve Dean Road Bridge conveyance.
- Chapter 7 presents the conclusions, as well recommendations for future work.

3. Literature review

3.1. Erosion and aggradation processes

Land uses changes in watersheds are known to impact natural systems, including streams, rivers and other water bodies. Erosion are among those of particular relevance, both watershed and stream bank erosion. Erosion is the process of detachment of top layer of soil by mechanical forces of wind or water. Negative impacts of soil erosion include and are not limited to severe draught in arid and semi-arid regions, reduction in the conveyance of channel resulting in flood and decrease in agricultural productivity. Erosion processes occurring in any catchment may be categorized as sheet, rill, gully, and stream erosion along the river continuum (Seiden and Schwartz, 2013).

In the world, around 80% of agricultural land experience severe to moderate erosion and 10% experience moderate erosion (Speth, 1994). It costs the US economy more than $30 billion dollar annually (Morgan, 2009). Castro and Reckendorf (1995) presented a summary of the various impacts of sediments to various water bodies, both in terms of water quality and quantity. The authors state that sediment impacts are complex, multifold, and have cumulative effects in streams and rivers that are difficult to reproduce in laboratory conditions.

Erosion enable to creation of sediment-laden runoff during rain events. Human activities that are linked to severe sediment loadings include construction sites (Harbor, 1995), clearcutting of forested areas (Brown and Krygier, 1971), and poorly managed agricultural practices. When these activities occur close to water bodies, the potential for these impacts are increased. Other factors may trigger gradual increase in sediments in water bodies, such as short-term climatic events, instream alterations or changes in land management. Impacts in water quality and quantities in streams are immediate to aquatic species such as fish and macroinvertebrates.

However, changes in river/stream hydrology, sediment generation and sediment transport can also create severe impacts to man-made structures such as bridges and culverts. For instance, watershed urbanization may contribute to larger peak runoff flows and volumes, which in turn may lead to increase in stream flow velocities, stream bank erosion, stream bank failure, and scouring. Activities such as forest clearcutting can generate a significant increase in sediment loadings that can enter streams and lead to aggradation. Poor agricultural practices can also be a source of sediments to streams, which in turn may also lead to aggradation, as is further elaborated.

3.2. Hydrologic and erosion modeling

A number of erosion models currently exist to correctly model sediment dynamics within the catchment as well as developing a sedigraph (sediment time series) at the outlet. Examples of alternatives include the European Soil Erosion Model (EUROSEM), Kinematic Runoff and Soil Erosion model (KINEROS), Erosion Productivity Impact Calculator (EPIC) and so on. However, not all of these models are well suited due to issues of lower integration with GIS, higher computational effort requirement and lack of channel sediment function (Pandeya et al., 2016). Better hydrological characterization is fundamental in the context of the present research in the Soapstone Branch watershed.

The US Army Corps of Engineers (USACE) hydrologic engineering center hydrologic modeling system (HEC-HMS) is one of the competent model and performs better than well-known Soil and Water Assessment Tool (SWAT) and Hydrological simulation program – Fortran (HSPF)

for simulating the sediment generation process (Pak et al., 2015). For sediment modeling, HEC-HMS requires a calibrated precipitation-runoff model, soil data, observed channel sediment data and channel cross section data (USACE, 2015). Continuous precipitation-runoff modeling in HEC-HMS is done by soil moisture accounting (SMA) algorithm based on Precipitation-Runoff Modeling System (Fleming et al., 2004).

HEC-HMS SMA algorithm breaks down the path of rainfall through the watershed into 5 different conceptual zones accounting for canopy interception, surface depression, water retention in tension zone, interflow and deep groundwater flow. Apart from precipitation and evapotranspiration data, twelve parameters such as canopy storage capacity, soil storage capacity etc. is needed. Furthermore, five initial conditions representing the moisture level on each of the five conceptual storage zone is required (USACE, 2013). HEC-HMS SMA model is found to behave reasonably well for wide range of catchment areas ranging from smaller watershed with 21.4 sq. km area (Meselhe et al., 2009), large watershed of area 19296 sq.km (Roy et al., 2013) as well as very large watershed area of 254,230 sq. km (Bashar et al.,2005).

Sediment modeling in HEC-HMS utilizes Modified universal soil loss equation (MUSLE) to calculate the event based sediment yield. MUSLE is an advancement of originally developed universal soil loss equation (USLE) by replacing rainfall erosivity factor with runoff energy factor (Williams, 1975.). Lack of consideration of runoff in USLE or revised universal soil loss equation (RUSLE) leads to wrong estimate in event based calculation and thus, the annual soil loss (Kinnell, 2005). Apart from runoff energy factor, other factors used in MUSLE are same as that of USLE which include soil erodibility factor, topographic factor (slope length and slope steepness), soil cover factor and conservational practice factor (Wischmeier and Smith, 1965). Since, all the runoff producing precipitation would not result in sediment generation, two additional parameters viz. critical time period and critical runoff were added to apply originally developed event based MUSLE for continuous multi-rainfall simulation (Pak et al., 2008). Furthermore, in order to develop a sedigraph from lumped sediment quantity, a power function is applied which relates sediment time series with hydrograph by locally estimated empirical coefficients (Gibson et al., 2010). A user-specified gradation curve then enables to develop a sedigraph for different grain classes (USACE, 2013). Sensitivity analysis of HEC-HMS sediment model indicates that gravel ratio in reach element, MUSLE cover factor and proportion of sand in the enrichment ratio are more sensitive than any other parameters (Pak et al., 2015). In order to assist HEC-HMS with input, a Geographic Hydrologic Modeling extension (HEC-GeoHMS) has been developed by USACE. This extension assists hydrologists in visualizing spatial information, performing spatial analysis and developing inputs to HEC-HMS.

Apart from digital data, rapid geomorphic assessment may also be done to identify the key features that cannot be identified or quantified using remote sensing techniques. Channel stability index (CSI) development is one of such assessment that enables to identify stream banks that are severely affected or have higher chances of being affected and thus, adding more sediment to the stream. CSI consists of 9 instability criterion each ranging from 0-4 thus, having a maximum possible score of 36. Channel banks with a score less than 9 is considered stable, 10-20 is moderately stable and above 20 is unstable (Heeren, 2012).

3.3. Hydraulic modeling of streams and in-stream structures

Hydraulic modeling of rivers and streams is extremely relevant in the context of the Soapstone Branch aggradation process to the bridge at Dean Road, Midland City, AL. A number of numerical modeling approaches have been developed to simulate rivers in the past five decades, and over time the range of the natural processes incorporated in the modeling tools have increased. At the current stage, river models are able to simulate backwater effects and unsteady flow processes, such as flooding events, considering one-dimensional (1D) or two-dimensional (2D) flow conditions. The influence of in-stream structures has also been incorporated in such models, as well the ability of representing sediment transport. Two of these models are focused in the present discussion, the US Army Corps of Engineers HEC-RAS 5.0 (River Analysis System) and the US Bureau of Reclamation SRH-2D (Sediment and River Hydraulics-2D).

HEC-RAS is a 1D and 2D hydraulic model that is able to simulate steady and unsteady river flows, including sediment transport, movable boundary computations, in-stream structures and water quality parameters (Brunner, 2018). It has the ability of simulate long-term trends of scour and deposition in the stream. This system can be used to evaluate deposition in reservoirs, design channel contractions required to maintain navigation depth, predict the influence of dredging on the rate of deposition, estimate maximum possible scour during large flood events, and evaluate sedimentation in fixed channels (Brunner and Gibson, 2005).

The SRH-2D model is, according to Hogan (2015), a robust, finite-volume 2D model that was developed by the US Bureau of Reclamation (USBR) and is able to simulate complex 2D river flow conditions (Lai, 2010). The Federal Highway Administration (FHWA) has partnered with the USBR to further develop SRH-2D and adopt this tool as a replacement to the outdated FESWMS model (Hogan, 2015). While the model is able to perform sediment transport calculations, future versions will also add the ability of incorporating mobile bed sediment transport.

3.4. Aggradation and sediment transport modeling

Aggradation is a term used to describe the process of rising in river bed elevation. Most commonly, this is due to sediment deposition in a river system. As it has been determined in this research, the aggradation process is so severe at Dean Road Bridge that it can be overtopped by the flow in Soapstone Branch as the watershed receives moderate rain events. Such overtopping events have the potential to cause structural damage, and even structural failure, with economical and human impacts.

The ways to control and eliminate aggradation in hydraulic structures as bridges are diverse, but not all are as effective, as pointed by Johnson et al. (2001). Dredging is probably the simplest alternative, yet it is a continuous process that does not address causes of the problem and involves constant expenditures. Sediment trap construction in the upstream of the bridge is another straightforward solution alternative, which can also accommodate the change of rate in sediment load in the future, yet it requires continuous maintenance over its lifetime, and brings potential change the local sediment budget in the stream. This in turn can lead to stream bed degradation in locations downstream from the trap and streambank instability. Channelizing or adjusting stream slope near bridges and culverts are a possible, one-time intervention that needs to be considered with care to avoid issues related to scour. Also, this alternative simply transfers the aggradation

problem downstream. Bridge replacement is also an alternative, however, it is very expensive and requires an estimate of what is the new stable sediment level in the stream.

An important component related to the development of the research work is a mathematical model describing the process of aggradation. One of the such models has been developed by Zhang and Kahawita (1987). The authors derived two fundamental equations such as linear momentum conservation and continuity equations for water, continuity equation for sediment, sediment transport relation, and resistance relation. And the equations that they derived are as following:

$$\frac{\partial z}{\partial t} - K_1\left[\frac{\partial^2 z}{\partial x^2} + \frac{1}{g}\frac{\partial^2 E}{\partial x^2}\right] = 0 \qquad (3.1)$$

$$\frac{\partial G}{\partial t} - K_1\frac{\partial^2 G}{\partial x^2} = 0 \qquad (3.2)$$

$$K_1 = \frac{\partial G}{\partial s}\frac{1}{1-\lambda} = \frac{bG_0^{1-\alpha}G^{\alpha}}{3s_0(1-\lambda)} = K_0 G^{\alpha} \qquad (3.3)$$

Where:

Z = change in bed elevation;

K_1 = linear diffusion coefficient;

g = acceleration of gravity;

E = specific energy ($u^2/2 + gh$)

G=charge per unit width;

α = a dimensionless factor which has the derivation in the paper; and

λ = bed material porosity.

Further analytical solution and experimental verification were performed by Zhang and Kahawita (1987). An analytical solution for prediction of one-dimensional non-equilibrium processes in alluvial rivers due to a sudden constant increase in upstream sidemen discharge was presented by the authors. One limitation of this study is that all the tests were performed in laboratory conditions.

There have been additional work in developing solutions for aggradation and degradation processes in artificial channels. Unsteady flow and solid transport simulation processes in in artificial channels can be solved using a three-equation model, coupled with a local erosion law. Aricö and Tucciarelli (2008) derived this method to couple the scour and erosion effectiveness into three main equations (momentum equation, continuity equation, solid load balance equation).

By comparison with aggradation research, much more effort was dedicated to experimental and numerical modeling of river sediment transport processes. According to Yang (1996), the initial mathematical model formulations in this area dated from the 1950s, combining aspects of fluid dynamics and empirical sediment-water relations. Numerical 1-D sediment transportation models had been used frequently in the context of rivers, and more recently 2D models are being introduced. Sediment transportation models are becoming more complex, including non-uniform and non-equilibrium models. Yet, the most commonly used model is still the 1-D model since it requires less measured data and yields more stable results. HEC-RAS can do both 1-D and 2-D modellings and it is also able to predict a long term sediment transportation, but can only simulate 1D sediment transport. An examples of large-scale, long-term sediment transport simulation using HEC-RAS was provided by Ghimire and DeVantier (2016).

4. Methodology

4.1. Data gathering and field Investigation

4.1.1. Bridge cross section survey

Upon the start of the research ALDOT provided a history of surveys in the bridge cross section since 1992, which is presented in Figure 4-1. As is indicated the aggradation process had become a noticeable in 2013, and by 2014 the entire cross section was blocked with sediments. Despite of efforts to dredge the bridge in February 2015, by August 2015 the entire cross section was blocked again, as was shown in Figure 1-1.

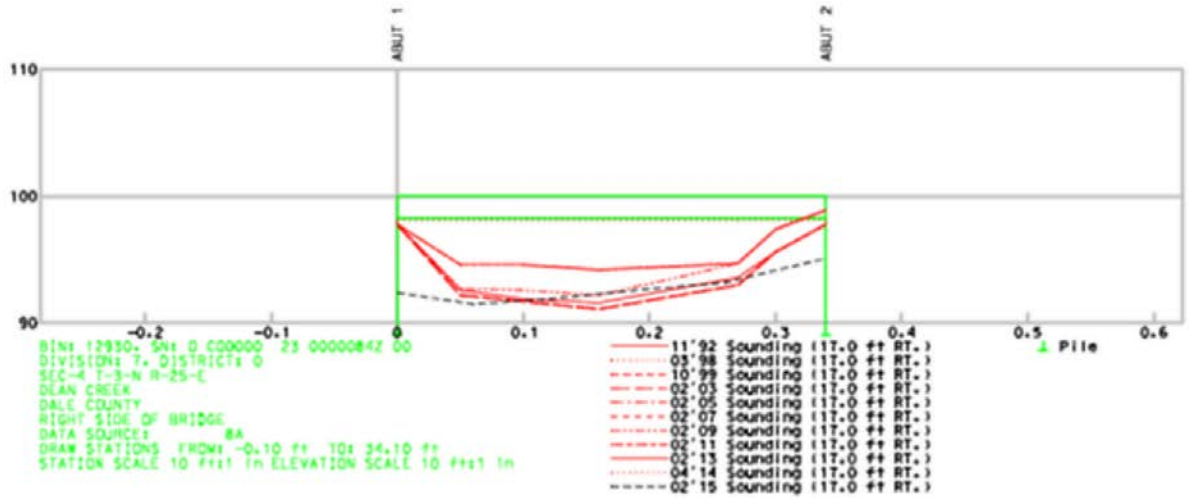

Figure 4-1: History of the Dale County Bridge (BIN 12930) cross section from 11/1992 to 02/2015. Aggradation is noticeable from 02/2013 onward, with a dredging occurring in 2015.

4.1.2. Soapstone Branch Digital Elevation Map

Dale County provided means to develop a digital elevation map (DEM) of Soapstone Branch, which is presented in Figure 4-2. The 10 m DEM obtained from USGS NED 30 is very coarse to be used for the Soapstone Branch catchment. In the case of large to medium size catchments like the donor catchment (Choctawhatchee river catchment draining near Newton, Alabama covers an area of 686 square miles), a coarser resolution DEM can be utilized without producing errors of higher degrees. However, due to the smaller size of Soapstone branch, a finer resolution DEM is required. Contour shapefile with 2 feet interval of Choctawhatchee river catchment were obtained from Dale County. This contour shapefile was then converted to 1 m resolution DEM using ArcGIS.

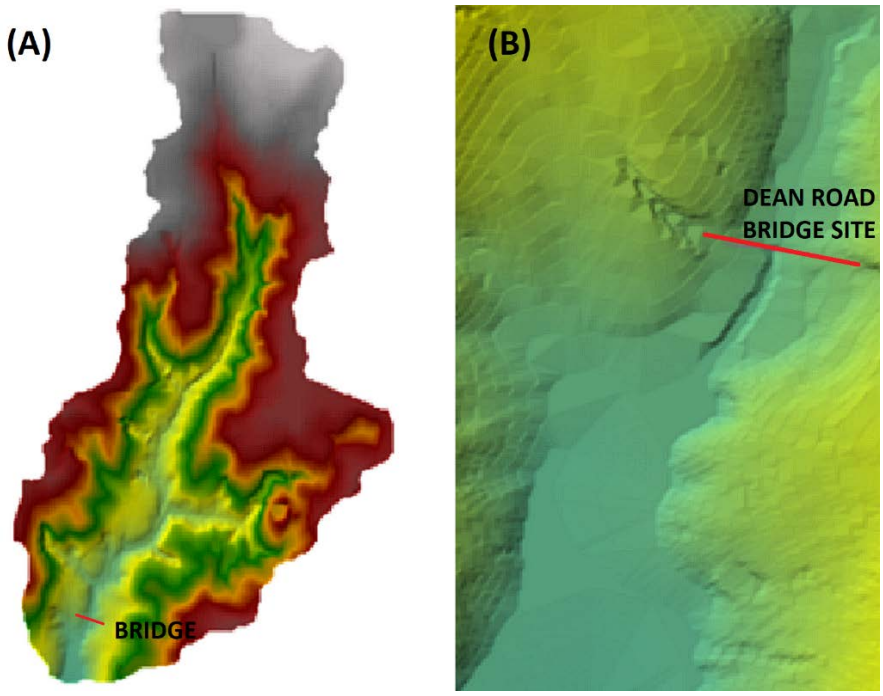

Figure 4- 2: Digital elevation map (2 ft. resolution) of Soapstone Branch Watershed (A), with a zoom near the bridge site (B)

4.1.3. Land use data and temporal changes

The National Land Cover Dataset (NLCD) provides 30 m spatial resolution land cover maps of the entire United States in a period of every 5 years. The most recent land cover data provided by NLCD is for 2011 when this project was started in 2016. This dataset is coarser in both spatial and temporal scale. As seen from Figure 1.4, using NLCD land cover dataset of 2011 fails to consider the land cover changes occurring in the catchment from 2011–2015. Furthermore, due to smaller catchment size, a finer spatial resolution is required.

Land cover maps can be generated using satellite data from Landsat platforms or using the National Agriculture Imagery Program (NAIP) dataset. The NAIP dataset has a spatial resolution of 1 m and temporal resolution of 2 years which is suitable for our study. NAIP is controlled by US Department of Agriculture's (USDA) Farm Service Agency (FSA) through Aerial Photography office in Salt Lake City. Initially, NAIP provided aerial images with natural color spectral resolution (red, green, and blue) but starting in 2007, four bands spectral resolution was available viz. red (band 1), green (band 2), blue (band 3), and near-infrared (band 4). Four band NAIP imagery was collected for the catchment for 2011 and 2015.

A satellite image collected over several bands of the electromagnetic spectrum can be displayed as false color composite images. A false color composite image is a type of color rendering methods, where arbitrary colors are selected to display the reflectance from non-visible part of electromagnetic spectrum. For example, the near-infrared reflectance is not visible to human eyes, however, this reflectance is recorded by satellite sensors. So, if a multispectral aerial imagery is displayed with a red color resembling the near-infrared reflectance, then it is a false color composite. False color composite schemes have their applications in proper identification of

vegetation in the image and thus helps in image classifications. There are a number of false color composite schemes which can be used for displaying a multispectral image. For NAIP imagery, a 4-1-2 false color composite scheme [Red = Band4 (near-infrared); Green= Band1 (red); Blue= Band2 (Green)] is utilized. A 4-1-2 false color composite map of soapstone branch catchment for 2011 and 2015 is shown in Figure 4-3.

Figure 4- 3: False Color Composite (4-1-2 scheme) Image of Soapstone Branch Catchment in 2011(Left) and 2015 (Right)

4.1.4. Precipitation and evapotranspiration data collection

Rainfall data collection is fundamental for the development of both hydrological and hydraulic data. Rainfall data from 01/2009 to 02/2016 used in this research was obtained through

a rain gauge in nearby Dothan airport, AL. From 02/2016 onward, rain data collection was performed on site through ONSET RG3 tipping bucket rain gauges installed through this research. The location of the rain gauges is presented in Figure 4-4, along with the picture showing one of the rain gauges installed in the study area. Through a combination of the Dothan Rainfall data and the locally collected rainfall a rainfall time series, presented in Figure 4-5, was developed and used in the research.

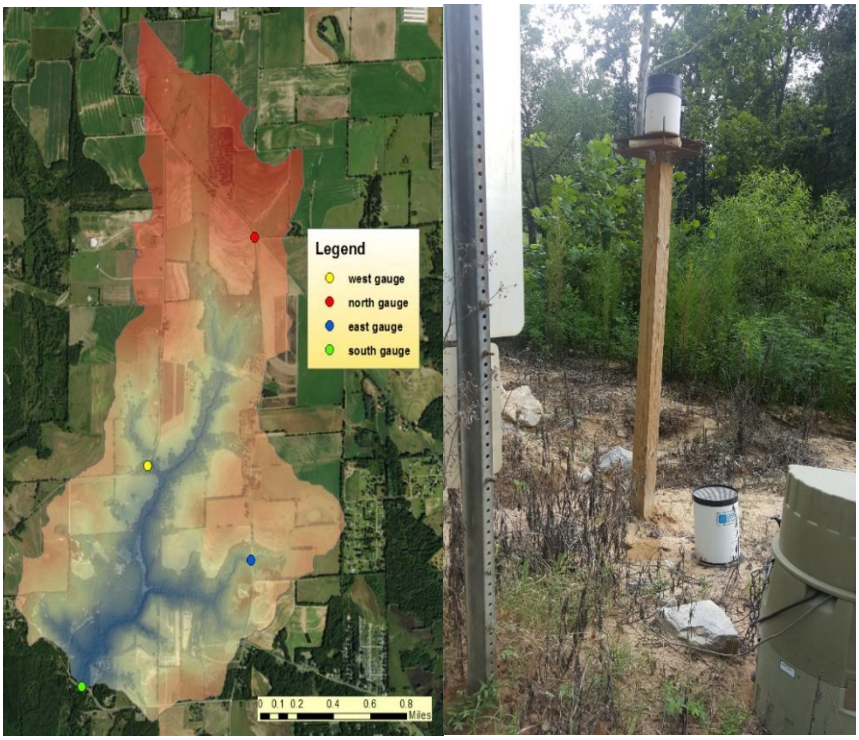

Figure 4- 4: Rain Gauge Locations in the Catchment (Left) and installed rain gauge (Right). The ONSET RG3 rain gauge can be seen in the top of the post, whereas another ISCO raingauge (used with the autosampler) is shown in the bottom (Samang 2016).

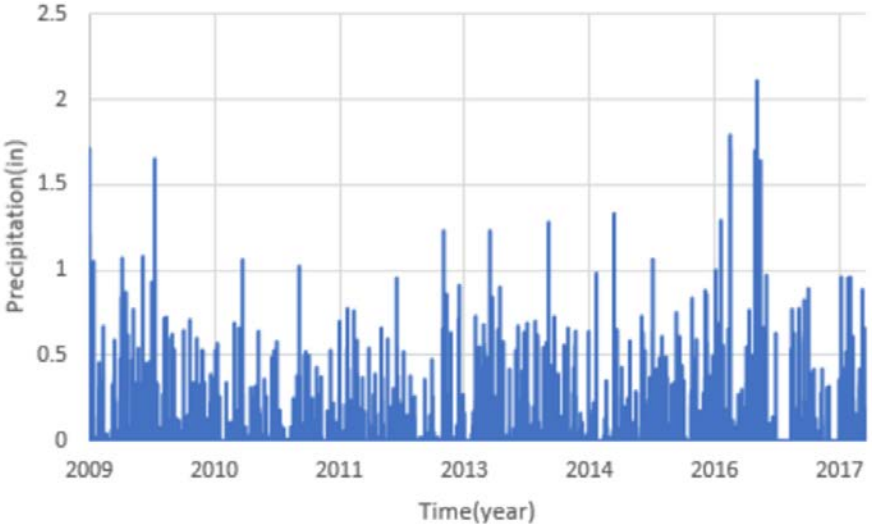

Figure 4- 5: All rainfall data used in the hydrological research within Soapstone Branch.

The ONSET rain gauge has a water collecting tipping bucket, and whenever the bucket is full, the bucket falls and tips the metallic connection at the bottom, and the rain gauge will consider this tipping as 0.01 inch of rain. The rain gauge can be connected to the computer through a data shuttle. This and other types of ONSET sensors are typically deployed for outdoor research. They have only one optical COM port on them to communicate with a computer. The data shuttle is a hardware that can transfer optical signals to digital signals that can be read by computers. The right side of Figure 4-6 are the couplers that connects the sensor and the shuttle. The coupler creates a dark environment to enable optical communication.

Daily pan evapotranspiration data were obtained for stations located in Headland, Alabama for the period of 2009–2013. For years 2014–2016 and days with missing value, monthly average pan evapotranspiration data from Class A pans for the closest station (i.e., Martin Dam) provided by NOAA (Farnsworth and Thompson 1983) was used. A correction factor of 0.7 is applied to convert pan evapotranspiration to potential evapotranspiration.

4.1.5. Particle size distribution characterization

Soil samples were collected at various locations at Soapstone Branch and grain size distribution tests were performed in these samples, with results presented in Figure 4-6. The location where these samples were collected are presented in Figure 4-7, and are mostly concentrated near the bridge site.

All samples consisted mostly of sand-sized particles by mass, with one sample having 17% of gravel sized particles and another sample containing 28% of silt/clay size particles. These result suggests that most sediments in the watershed are non-cohesive (Wang et al, 2004), which is a relevant finding for the hydraulic modeling studies.

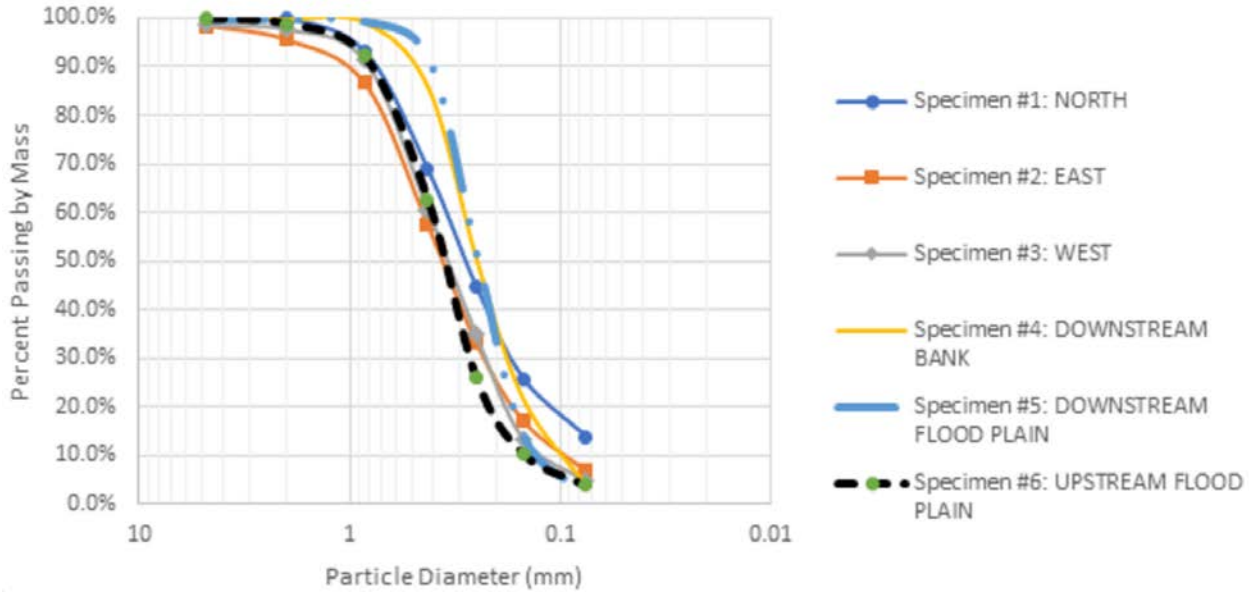

Figure 4- 6: Particle size distribution of soil samples collected in Soapstone Branch near Dean Road Bridge.

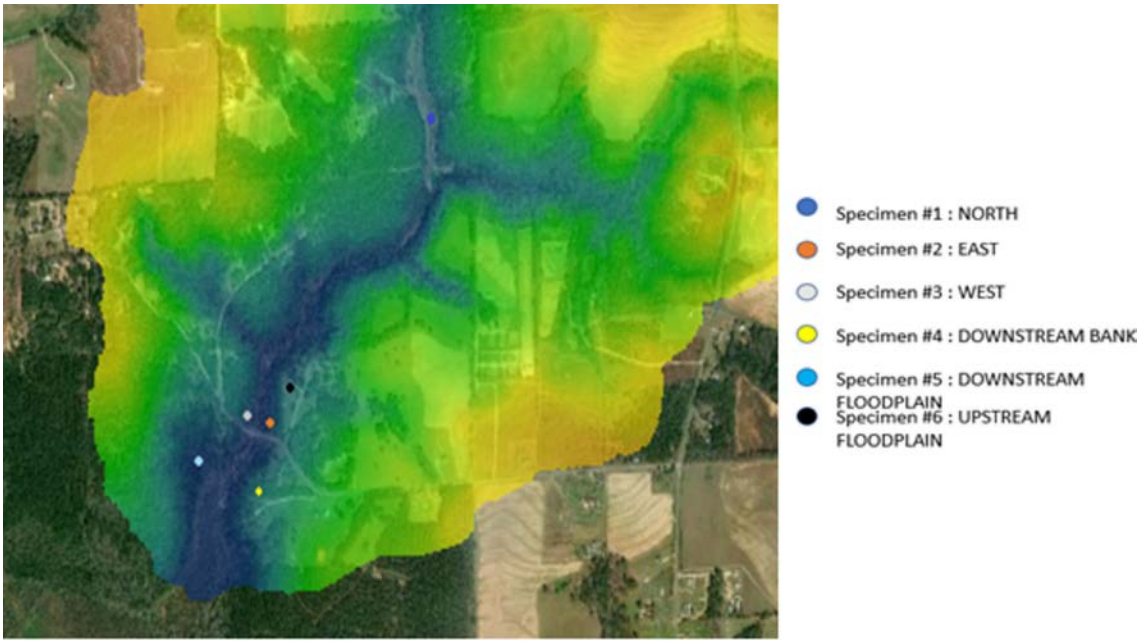

Figure 4- 7: Location where soil samples for particle size distribution were collected within Soapstone Branch watershed.

4.1.6. Stream flow depth and velocity data collection

Parameters such as the local topography, precipitation and evaporation data, land use and soil characteristics will influence runoff generation and then change stream flow depth and velocity during a given rain event. In order to characterize these variables within Soapstone Branch, different sensors were used. Level loggers ONSET HOBO U20, sampling every 15 minutes, were used to characterize flow depth in stream cross section. A Teledyne 2150 AV (area-velocity) sensor was used to collect water velocity and water depth data immediately upstream the bridge site. The HOBO U20 sensors measured pressure at the stream bed, and thus required atmospheric pressure correction, and an U20 sensor gauging atmospheric pressure was placed in together with the rain gauge near the bridge site. The 2150 AV sensor has built-in atmospheric correction, and does not need atmospheric data gathering.

One problem that could not be solved in this research was the measurement of stream flow velocity with the AV sensor. The sensor uses Doppler Effect to track motion of particles within the flow and with this determines the stream velocity. Because of large amounts of sediment carried with the stream flow, particularly during rain events, the AV sensor was often buried and thus could not record velocity (even though pressure recording was still possible). As shown in Figure 4-8, for many long periods the AV sensor velocity was zero or even negative, which was not feasible.

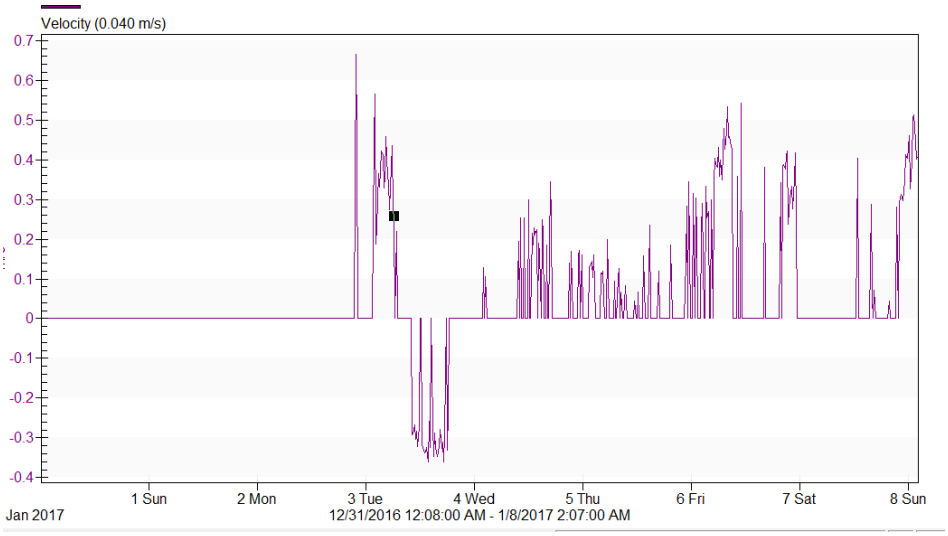

Figure 4- 8: Results from velocity measurements with AV sensor. Zero and negative velocities are attributed to the Soapstone Branch sediment load burying the sensor.

4.1.7. Sediment sampling during rain events

This research intended to establish a relationship between turbidity levels measured in the stream and the concentration of sediments in the flow, characterized by the Total Suspended Sediments (TSS) parameter. To attain this goal, a Teledyne ISCO 6700 Autosampler, shown in Figure 4-9, was deployed in the bridge site to perform sample collections. Samples collected within the bottles of the autosampler were later taken back to Auburn so that TSS tests were made, along with turbidity measurement.

Figure 4- 9: Teledyne ISCO 6700 Autosampler used in turbidity and TSS characterization of samples taken from Soapstone Branch during rain events.

An alternative way for sediment characterization was also attempted by using a turbidity sensor, model INW Turbo, with range up to 3000 NTUs, shown in Figure 4-10. This sensor was also placed in the bottom of Soapstone Branch next to the AV sensor that was measuring stream velocity. However, like the AV sensor, it was frequently buried by the Soapstone Branch sediments and did not provided useful data.

Figure 4- 10: INW Turbo turbidity sensor, with logger box, that was used in the Soapstone Branch sediment characterization. Sediment loading covered the sensor head (black), preventing the correct sensor operation.

4.2. Hydrological modeling

4.2.1. Catchment delineation and stream definition

Catchment delineation and stream processing for both donor and receiver catchments, as well for Soapstone Branch watershed, were done with the help of Hydrologic Engineering Center's Geospatial Hydrologic Modeling System (HEC-GeoHMS). HEC-GeoHMS is an extension developed by USACE as a set of tools within ArcGIS to process and create input files for HEC-HMS. It consists of several tools such as fill, flow direction, flow accumulation, etc. which help the user in deriving the boundary area for an outlet using the elevation information from DEM. It can be further used for partitioning a catchment into subcatchments using stream definition. Stream definition refers to defining a threshold for a grid cell within the catchment which can be treated as a stream. For example, a stream definition of 1 sq.km means that if any DEM grid cell is receiving flow from 1 sq. km. upstream area then, it is a stream. There is no available guideline for selection of stream definition and completely depends on the experience and expertise of modeler and modeling purpose. For the donor catchment, the catchment area was divided into 15 subcatchments using a stream definition of 75 sq. km. Using a smaller value of stream definition

will increase the number of subcatchments. For example, a new stream definition of 45 sq.km. results in 21 subcatchments.

4.2.2. Parameter estimation for HEC-HMS SMA model

Twelve parameters of the SMA model mimic the natural process of the interception, surface depression, surface runoff and groundwater flow. Each of these parameters requires an initial value before it can be calibrated. Five of these parameters, i.e., the maximum surface depression storage, maximum infiltration rate, soil percolation rate, maximum soil profile storage and maximum tension zone storage were derived from soil data, four parameter values, i.e., the groundwater layer 1 storage, groundwater layer1 coefficient, groundwater layer2 storage and groundwater layer 2 coefficient were obtained using streamflow data, the canopy interception value was obtained from landcover data, and the groundwater layer 1 percolation was determined during the calibration.

Interception refers to the amount of precipitation held by the objects present above the ground and is only returned to the atmosphere through evaporation. Interception is an important part of the hydrologic cycle as around 10-20 percent of precipitation is intercepted during the growing season (Viessman and Lewis 2003). Interception loss is high during the initial storm period, however, drops down to zero very rapidly during a storm event. Various factors such as precipitation type, rainfall intensity, volume, wind condition, season etc. affect the canopy interception. Bennett (1998) has provided interception values for different types of vegetation which are shown in Table 4.1. Land cover classes from NLCD 2011 were categorized into three types of vegetation and each was assigned respective canopy interception values.

Table 4- 1: Canopy Interception Values for Different Types of Vegetation (Bennett, 1998)

Types of Vegetation	Canopy Interception (in.)
General Vegetation	0.05
Grasses and Deciduous Trees	0.08
Trees and Coniferous Trees	1

The information about the soil components and their properties is linked in the SSURGO database for each map unit which represents a geographical area with dissimilar soil properties than the nearby soil areas. A map unit may include major components and minor components which are a single soil series. Each of these components is further classified into horizons or horizontal layers of soil, as shown in Figure 4-11. Initial estimates for five different SMA parameters viz. the maximum surface depression storage, maximum infiltration rate, soil percolation rate, maximum soil profile storage, and maximum tension zone storage were obtained from SSURGO database. A single value for each parameter was calculated for each map unit which was then converted into raster format using ArcGIS.

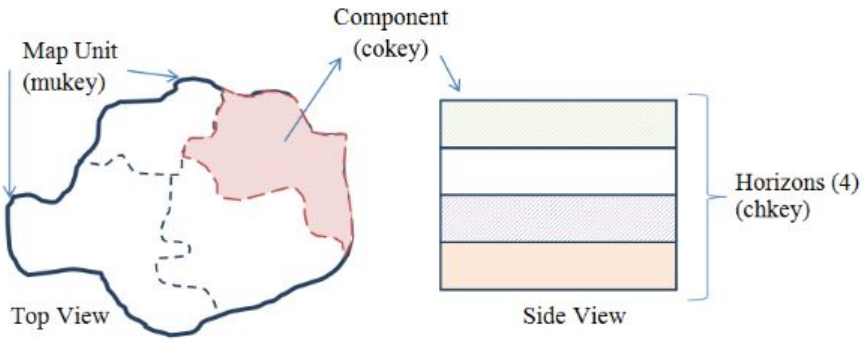

Figure 4- 11: Organization of SSURGO Map Data (Holberg 2015)

Initial estimates for surface depression storage have been suggested using the information on the slope of the land surface (Bennett 1998). Land areas with steeper slopes have less depression storage as the water flows out of them quickly due to higher energy gradient whereas flat lands can store more water. Slope information for each component is available from SSURGO database which is then averaged for map units and then associated with the maximum surface depression storage using Table 4.2.

Table 4- 2: Surface Depression Storage Values (Bennett 1998)

Description	Slope (%)	Surface Storage (in)
Paved Impervious Areas	NA	0.125-0.25
Steep, Smooth Slopes	>30	0.04
Moderate to Gentle Slopes	5-30	0.25-0.5
Flat, Furrowed Land	0-5	2

Soil Infiltration rates are defined as the rate at which the soil can absorb rainfall or irrigation. Previous studies (Bennett 1998) have suggested that the initial estimates for maximum infiltration rate can be considered equal to the saturated hydraulic conductivity. Saturated hydraulic conductivity for a soil can be obtained from its texture class (12 soil texture classes defined by USDA). It has been found that the soil texture class is the most significant soil property related to the soil moisture parameters (Cosby et al. 1984). A previous study (Rawls et al. 1982) suggests the value of saturated hydraulic conductivity for each of the soil texture classes which is presented in Table 4.3.

Table 4- 3: Texture Classes and Saturated Hydraulic Conductivities

Soil Texture Class	Saturated Hydraulic Conductivity (in/hr)
Sand	8.27
Loamy Sand	2.41
Sandy Loam	1.02
Loam	0.52
Silt Loam	0.27
Sandy Clay Loam	0.17
Clay Loam	0.09
Silty Clay Loam	0.06
Sandy Clay	0.05
Silty Clay	0.04
Clay	0.02

Percolation rate defines the rate at which water is transferred through soil and groundwater layers under the force of gravity or sometimes even due to capillary forces. Previous studies (Bennett 1998; Fleming 2002) have shown that vertical average value of saturated hydraulic conductivity can reasonably estimate the maximum percolation rate. Therefore, saturated hydraulic conductivity values were associated with respective soil texture classes (Table 4.3) for each of the soil horizons and then averaged vertically to obtain a single percolation value for each component. Percolation rate was then finally converted into raster format using ArcGIS.

Soil profile storage represents the amount of water held within soil pores which can be removed by the process of percolation and evapotranspiration (Feldman 2000). It is obtained by multiplying soil depth to the deepest soil horizon with the porosity of the soil. Porosity is defined as the ratio of the volume of the void to the volume of soil. The obtained soil storage for each soil component is then converted into raster file format using ArcGIS.

Tension zone storage represents the volume of water attached to the soil particles (Feldman 2000) and can be related to the field capacity of the soil (Fleming 2002). The field capacity is defined as the soil moisture content in field conditions with uninterrupted subsurface drainage (Colman 1947). It is obtained by multiplying soil depth to the deepest soil horizon with the field capacity. The obtained tension zone storage for each soil component is then converted into raster file format using ArcGIS. The upper zone storage is not required to be entered by the user as it is calculated as the difference of the soil profile storage and the tension zone storage by HEC-HMS in each simulation time step.

Any streamflow is comprised of surface runoff, interflow, and groundwater flow. The lines of decreasing slope on recession curve of streamflow hydrograph can help derive different contributing storage volumes when it is plotted on semi-logarithmic graph (Fleming 2002). Two parameters within the simplified SMA loss method, i.e., the groundwater 1 storage and the groundwater 1 recession constant can be derived from streamflow hydrograph.

The lower end of the recession curve in streamflow hydrograph represents only the groundwater flow as surface flows and interflows have subsided. To separate the groundwater flow from streamflow, a line is projected backwards from the tail end to the time of peak with the same

slope as the tail end of streamflow hydrograph. From the rising head of the streamflow hydrograph, a similar line is projected towards the time of peak. The combination of these two lines represents the groundwater flow. The recession curve of hydrograph can be represented by Eqn. (4.1).

$$q_t = q_0 \times K^t = q_0 \times \exp(-\propto t) \quad (4.1)$$

Where,

q_t = future flow in time t

q_0 = initial flow

K = recession constant

$\propto$ = -ln(K)

The value of $\propto$ is calculated at each step and the average value of $\propto$ is calculated. The groundwater recession coefficient is then given by

$$\text{Groundwater recession coefficient} = \frac{1}{\propto} \quad (4.2)$$

Integration yields an expression for groundwater storage (S_t) at time t for basin area A:

$$S_t = \frac{q_t}{\propto \times A} \quad (4.3)$$

The maximum value of storage is the most accurate value of groundwater storage that can be obtained from streamflow regression analysis (Holberg 2015). The value of groundwater layer 1 recession coefficient and storage were computed from baseflow for each of the four storms.

Figure 4-11 shows streamflow hydrograph for an isolated storm of 15th March 2009 plotted on a semi-logarithmic scale. The parameters derived from streamflow data are highly variable and therefore, were obtained after isolating the streamflow from storms in various months. Four different storms of 1st September 2005, 15th December 2007, 15th March 2009, and 28 June 2010 were selected, and the average values of groundwater parameters derived from the four storms were used as initial estimates of these parameters. The value of groundwater parameters for each storm and their average values are given in Table 4-4.

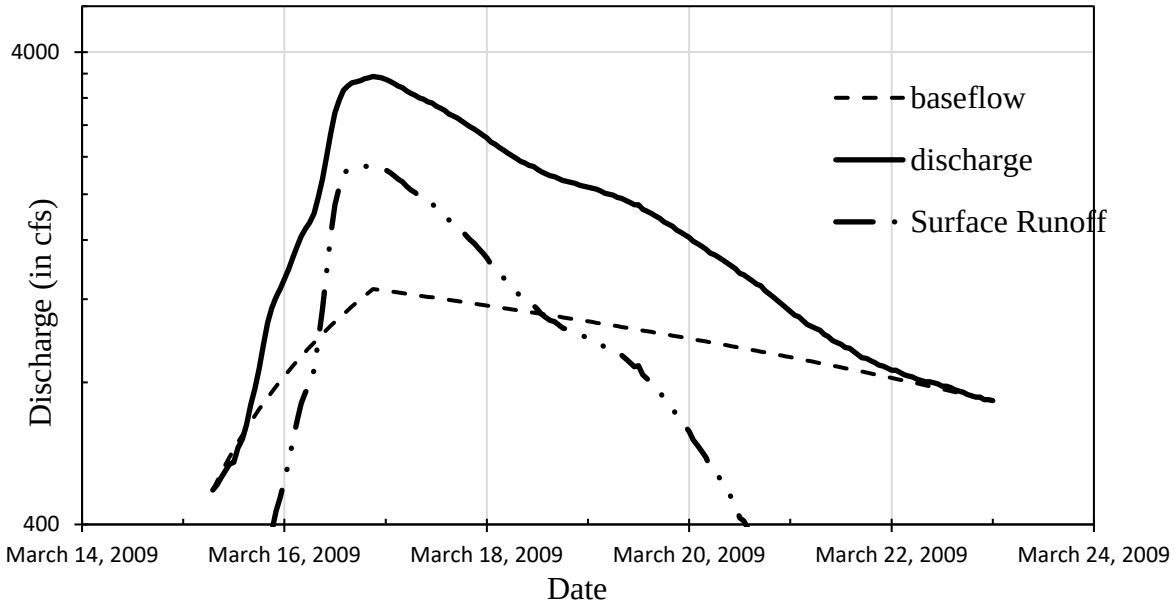

Figure 4- 12: Baseflow Separation for Storm of 15th March 2009

Table 4- 4: Groundwater Parameter Values for Selected Storms and their Averages

Storm event	Groundwater1 Coefficient (hr)	Groundwater1 storage (in.)	Groundwater2 Coefficient (hr)	Groundwater2 storage (in.)
28th June 2010	49.7	0.04	285.3	0.30
11th Nov 2009	47.9	0.01	449.3	0.55
15th March 2009	55.5	0.31	296.2	0.43
17th July 2011	35.0	0.05	162.8	0.05
Average	47.0	0.1	298.4	0.33

4.2.2. Curve number development and basin lag

For the adopted hydrological modeling, soils are divided into four different hydrologic soil groups (HSGs) viz. A, B, C, and D depending on their runoff potential and infiltration rates. The classification of soil into these classes is dependent on intake and transmission of water, freezing condition of soil etc. (USDA 1972). Soils in the group A have low runoff potential when they are wet and typically have a composition of <10% clay and >90% sand. Soils in the group B have moderately low runoff potential. The composition of this group of soils has 10%–20% clay and 50%–90% sand. Soils with moderately high runoff potential are placed in the group C and have a composition of about 20%–40% clay and <50% sand. Soils in the group D have high runoff potential and water movement is restricted. The composition of soils in this group is >40% clay and <50% sand. Hydrologic soil group in combination with land cover data can help calculate the curve number (CN). The Soil Data Viewer can map HSGs based on the SSURGO data of county provided by the user.

The curve number is an empirical parameter which provides information on the amount of runoff from a given precipitation and was developed by the Soil Conservation Services (SCS) (now the National Resources Conservation Service or NRCS) for application in small rural catchments. Apart from land cover and HSG, different conditions such as antecedent moisture condition, hydrologic condition, etc. affect the value of curve number. To avoid complexity in the determination of curve number, available landcover classes were merged together to form four land cover classes (Table 4-5). Table 4-6 was then developed to assign CN for each of the four HSGs and the four land cover classes. Combining the information from land cover, HSG and Table 4-6, curve number grids were created. Curve number is an important precipitation loss computing parameter in event-based modeling. In the continuous modeling, it can be used for calculation of the basin lag which is defined as the time difference between the center of mass of rainfall excess and unit hydrograph peak.

Table 4- 5: Simplified Land Cover Classes from NLCD Land Cover Classification

Grid Code	Description	Grid Code	Description
11 90 95	Open water Woody wetlands Emergent herbaceous wetlands	1	Water
21 22 23 24	Developed, open space Developed, low intensity Developed, medium intensity Developed, high intensity	2	Medium residential
41 42 43	Deciduous forest Evergreen forest Mixed forest	3	Forest
31 52 71 81 82	Barren land Shrub/Scrub Grassland/herbaceous Pasture/hay Cultivated crops	4	Agricultural land

Table 4- 6: Curve Number Values for Corresponding Land Cover and Hydrologic Soil Group

Land Cover Classes\ HSG	A	B	C	D
Water	100	100	100	100
Residential	57	72	81	86
Forest	30	58	71	78
Agricultural	67	77	83	87

The SMA model is a loss model which calculates the volume of water that has intercepted, infiltrated, evaporated, and stored in different zones. It does not provide the discharge which is the model output of HEC-HMS. The calculation of transforming the runoff volume (rainfall excess) to discharge is done by suitable transform methods available within HEC-HMS. For this study, the SCS unit hydrograph method was used because of required minimum number of parameters. The SCS unit hydrograph method requires the user to enter only one parameter, i.e., lag time. Based on lag time, the program computes time of concentration and rescales the SCS dimensionless unit hydrograph. Basin lag can be calculated from curve number using Eqn. (4.4).

$$\text{Basin Lag} = \frac{(L^{0.8} \times (S+1)^{0.7})}{(1900 \times Y^{0.5})} \qquad (4.4)$$

Where,

L= Hydraulic length in feet

Y= slope of watershed in percentage

and

$$S = \frac{1000}{CN} - 10 \qquad (4.5)$$

4.2.3. HEC-HMS model setup

After all the soil and streamflow parameters required for HEC-HMS model have been calculated, HEC-GeoHMS was used for transferring both the spatial information and information on parameter values for each subcatchment to HEC-HMS. HEC-GeoHMS also develops the background map file and distributed-basin schematic model file. It performs the tasks of the automatic naming of reaches and subcatchments, checks for errors in the catchment and connectivity of streams.

Thiessen polygon method is one of the most common methods of determining average precipitation over a catchment. In this method, the catchment (or subcatchments in our study) is divided into a number of polygons utilizing rain gauges as centers. These polygons are then assigned a precipitation value corresponding to their respective gauges and then a weighted average of precipitation value is computed for hydrologic

The model warmup period is defined as an initial length of simulation time at the end of which model parameters are converged to values independent of initial estimated values (Johnston and Pilgrim 1976). HEC-HMS SMA model consists of five separate zones viz. canopy, surface depression, soil, Groundwater 1 (GW1), and Groundwater 2 (GW2). Apart from the parameters developed so far, the model setup requires defining initial moisture content in each one of the five storage zones. As an attempt to find the warmup period, the model was run by increasing moisture content for each zone to 90% one at a time and then, resulting hydrographs were compared with the initial model run with 10% moisture content for each zone.

Any model parameter is subjected to unprecedented changes and errors. Sensitivity analysis is the investigative procedure of identifying the effects of changes or errors in model parameter to the model output. A large number of uses of sensitivity analysis includes but not limited to allowing the decision maker to select assumptions, identifying sensitive or important variables, testing optimal solutions' robustness, etc. (Pannell 1997). The goal of sensitivity analysis in this study was to identify the order of sensitivity of key model parameters which would further help in calibration of the model. There are two types of sensitivity analysis, i.e., global and local. In the global sensitivity analysis, all model parameters are varied over their ranges at the same time. While in the local sensitivity analysis, each model parameter is varied separately by keeping all other model parameters constant.

As identified by Fleming (2002), changing either soil storage or tension zone storage produces same results, so that the soil storage was eliminated for sensitivity analysis. Furthermore, since GW2 percolation rate can only be calculated during calibration, it was not included in the sensitivity analysis. For this study, a local sensitivity analysis was performed where model parameters were varied within the range of ± 40% (at an interval of 10%) of initial estimates individually by keeping remaining parameters constant. The effect of model parameter variation in NSE and PEV were plotted as shown in Figure 4-13.

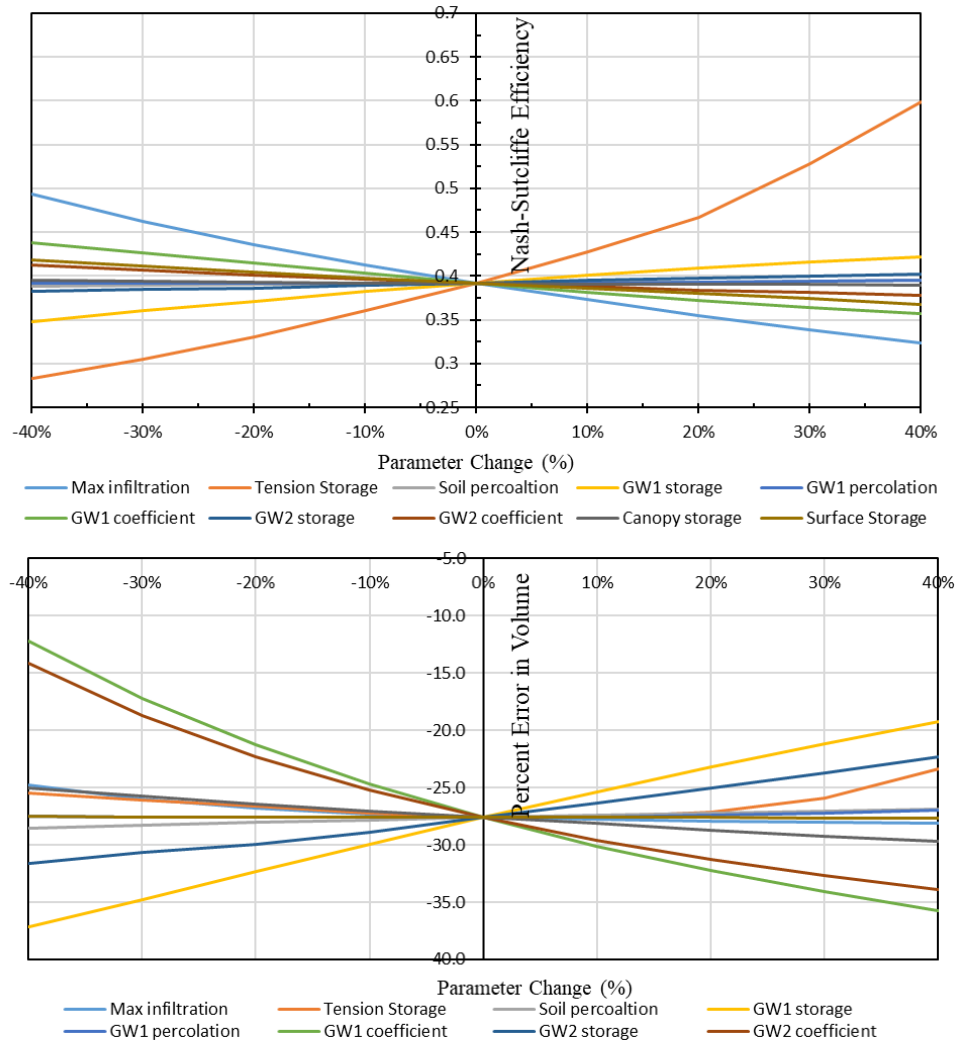

Figure 4- 13: Nash-Sutcliffe Efficiency (NSE) and Percent Error in Volume (PEV) of the Model Output due to Percent Change in Parameter Values

For the purpose of ranking the parameters in terms of their relative sensitivity to the objective functions (NSE or PEV), sensitivity parameter (S) was calculated using Eqn. (4.6).

$$S = \frac{(\frac{O_2 - O_1}{O_{12}})}{(\frac{I_2 - I_1}{I_{12}})} \quad (4.6)$$

Where,

I_1 = least value of input parameter

I_2 = highest value of input parameter

I_{12} = average value of I_1 and I_2

O_1 = output value of I_1

O_2 = output value of I_2

O_{12} = average value of O_1 and O_2

4.3. Hydraulic modeling

4.3.1. Initial and boundary conditions for hydraulic calculation

The initial condition adopted for all hydraulic models (HEC-RAS and SRH-2D) was to assume that stream was dry, which then required that models were run for enough time until base flow conditions were attained. One point to make is that the numerical scheme used by HEC-RAS is not unconditionally stable. If the guessed initial water elevation is too far away from the actual situation, it could cause the model to diverge.

The upstream boundary condition used by both models is the surface stream flows result obtained by HEC-HMS. Such flows at a location near the bridge site was copied from HEC-HMS output and used as a time series in the hydraulic models. The downstream boundary condition for both models, located far downstream from the bridge location, was created by assuming that flow normal, with an energy slope of 0.5%. While HEC-RAS has also the ability of allowing inflows from precipitation, albeit without abstractions, this was not used in the present effort. A typical HEC-HMS outflow data, which was used as an upstream boundary condition, is presented in Figure 4-14.

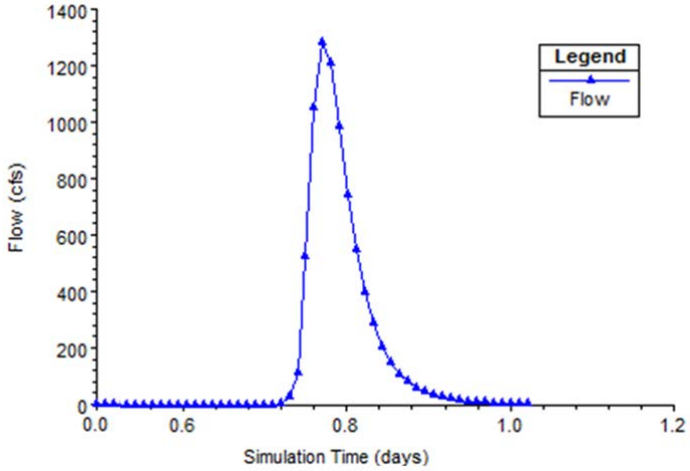

Figure 4- 14: Typical HEC-HMS outflow data, used as upstream boundary condition in the hydraulic models

4.3.2. Digital elevation map (DEM) editing

Two-dimensional hydraulic models rely heavily on topographical information to determine flow paths, depths, velocity, among other flow variables. DEM data may have some shortcomings that require adjustments before a hydraulic modeling can be used. One typical limitation is the presence of a bridge, since the stream cross section underneath the bridge deck is not represented. Also, in the case of a stream that has a very large amount of sediment load, one expects changes in its morphology. Due to these limitations, it was necessary to edit the DEM obtained from Dale County near the site of Dean Road Bridge.

The original DEM was clipped to a relatively small data file with only about 700m long along the reach. The upstream boundary of the clip is about 100 meters away from a station where flow data was obtained from HEC-HMS. The profile along the reach was incorrectly depicted in the DEM, with a lot of cliffs and adverse slope. The various field trips to the site helped to indicate

to the research team that the stream slope was mostly uniform. Thus, the channel slope must be corrected before the modeling. It was assumed a 0.5% slope for Soapstone Branch based on these field site observations. Figure 4-15 presents the changes implemented in the DEM near the bridge site by showing the stream profile at the center of Soapstone Branch. The same methodology for DEM editing was also used to perform changes in the model and enable the study of alternative cross sections to evaluate stream modification strategies.

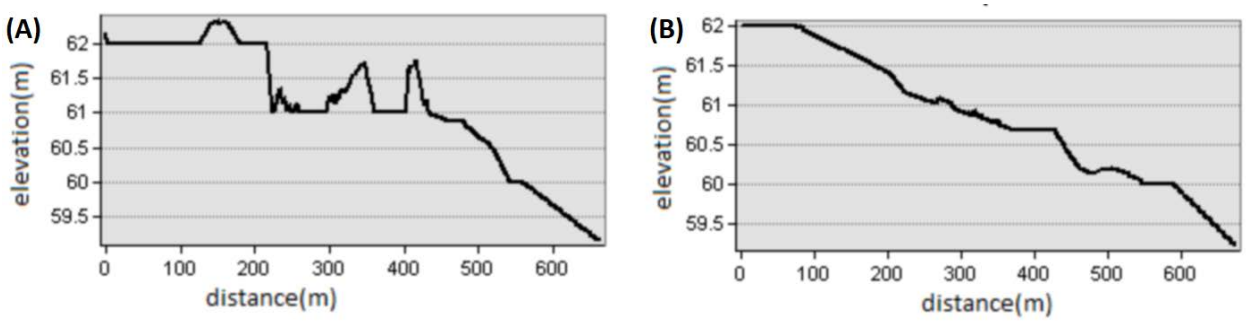

Figure 4- 15: Profile of the centerline of Soapstone Branch before (A) and after (B) the DEM editing process to eliminate inconsistencies observed in the original DEM data file. Dean Road Bridge is at the location 300 m, and originally was blocking the river flow.

4.3.2. Mesh generation

The HEC-RAS model has a uniform structured mesh with the size of 3m by 3m. Yet the mesh near the channel was unstructured and inconsistent. To make sure there would be enough mesh in the channel, at least 5 longitudinal breaklines were added along the channel so that there will be at least 5 computational cells in the channel at any station. A breakline is a line drew by the modeler representing a road or a bridge to ensure that computational cells are aligned with these and features. However, a secondary effect of enforcing a breakline in HEC-RAS is that the mesh is locally refined. This was used in the present modeling effort, so that there were more computational points within the Soapstone Branch channel, as is shown in Figure 4-16.

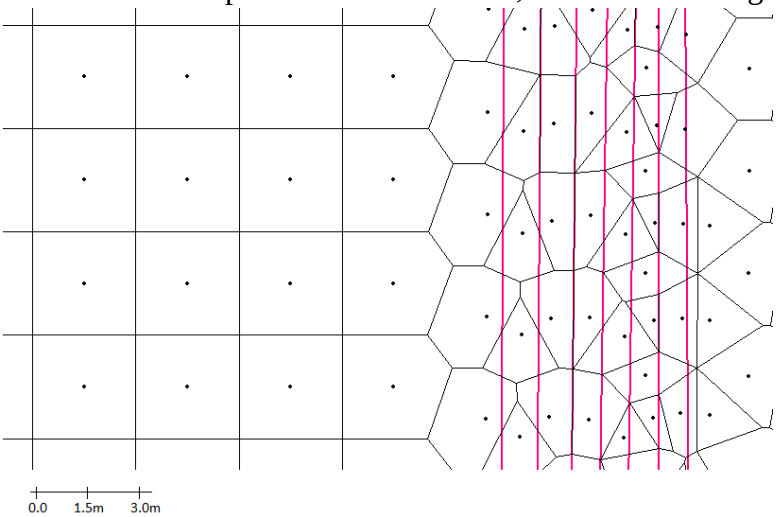

Figure 4- 16: Section of the HEC-RAS mesh used for the modeling of Soapstone Branch, indicating breaklines and a finer mesh to the right, where the stream channel is located.

Regarding mesh generation for the SRH-2D model, it relies on an pre-processing tool called Surface-water Modeling System, or SMS (EMRL, 1998). SMS generates triangular and quadrangular mesh for a SRH-2D model, and in the case of the present work a triangular, unstructured mesh was used, in which the maximum distance between the grid points in the mesh was adopted as 5 m, with a smaller maximum distance of 1.5 m used at the Soapstone Branch channel. Figure 4-17 depicts a section of the mesh used by SRH-2D to represent Soapstone Branch.

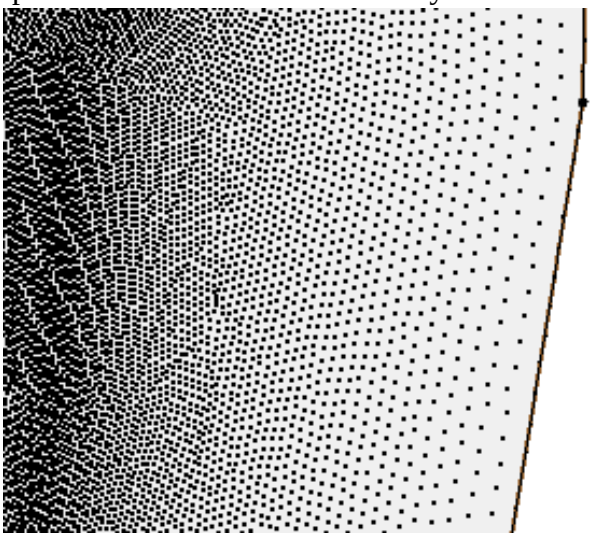

Figure 4- 17: Section of the SRH-2D grid points from the mesh generated through SMS, showing how the points are more spaced as it distances from the channel.

4.3.4. Hydraulic modeling calibration

With adequate upstream inflow information, topographical and a developed mesh it is possible to initiate the process of hydraulic modeling calibration. In the case of 2-D models this is comparatively simpler than the calibration of 1-D models, since there are fewer assumptions needed for model development. For instance, in the case of flows approaching a bridge in 1-D HEC-RAS model, it is necessary to make assumptions of ineffective flow areas. Such is not needed in the case of 2-D modeling with HEC-RAS.

Typically, the main calibration parameter for a stream model is linked to the bed roughness, as this impacts depth profiles. In the case of Soapstone Branch there is an advantage in that the types of land covers in the hydraulic modeling area is mostly comprised of forested areas and stream banks. However, there was a practical difficulty posed by the actual Dean Road Bridge and the aggradation that happens in it. During moderate to large rain events, the stream receives enough inflow to increase its velocity. Large velocities in the stream enable a partial sediment removal under the bridge deck, which increase its conveyance. As inflows keep increasing, the bridge is overtopped, and flows go either on the top or in the bottom of the bridge. This is a very complex situation, and cannot be modelled without resorting to a calibration process.

The strategy to represent the hydraulic behavior of the existing bridge cross section conveyance was to create a unique representation for the bridge cross section that was based on a two-tier discharge structure. The lower tier would be able to adequately reproduce the conditions of flow depth associated with low flows and base flows, and the upper tier with more intense stream flows. This was implemented also by editing the DEM near the bridge site, and Figure 4-18 presents the resulting elevation data after this editing was completed.

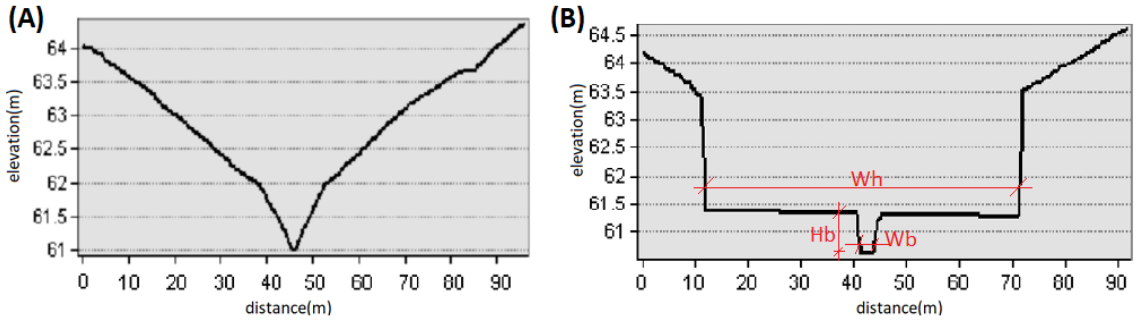

Figure 4- 18: Original and edited stream cross section near the bridge site. The edited geometry cross section parameters are presented in the right. The other selected calibration parameter was the Manning roughness n..

The process of selecting the geometric characteristics of the double-trapezoid cross section of Figure 4-18 was the key part of the hydraulic modeling calibration. The calibration variables included: low flow bottom width (Wb), assumed as either 4 ft. or 5 ft.; the low flow channel height (Hb), assumed as 0.5 ft., 0.7 ft. or 0.9 ft. The width of the high flow channel (Wh) was assumed either 20 ft., 40 ft. or 60ft. The side slopes for both channels were set at m = 2 (2 horizontal: 1 vertical). Finally, Manning number was assumed as either n=0.020, n=0.025 and n=0.030. In total, more than 50 different combinations of these variables were considered, and these geometries were tested in a selected group of rain events presented in Table 4-8. The best agreement between observed and simulated depth hydrographs was attained when Wb = 4 ft., Hb = 0.7 ft., Wh = 60 ft. and n = 0.025. An example of a flood event is presented in Figure 4-19 showing modeled and simulated depth hydrographs (using HEC-RAS) for three different set of calibration values..

Table 4- 7: Rain events recorded in Soapstone Branch watershed and used for hydraulic modeling calibration

Rain event	Date
1	23-Jan-17
2	7-Feb-17
3	3-Apr-17
4	9-May-17
5	19-Jun-17
6	16-Jul-17
7	25-Jul-17

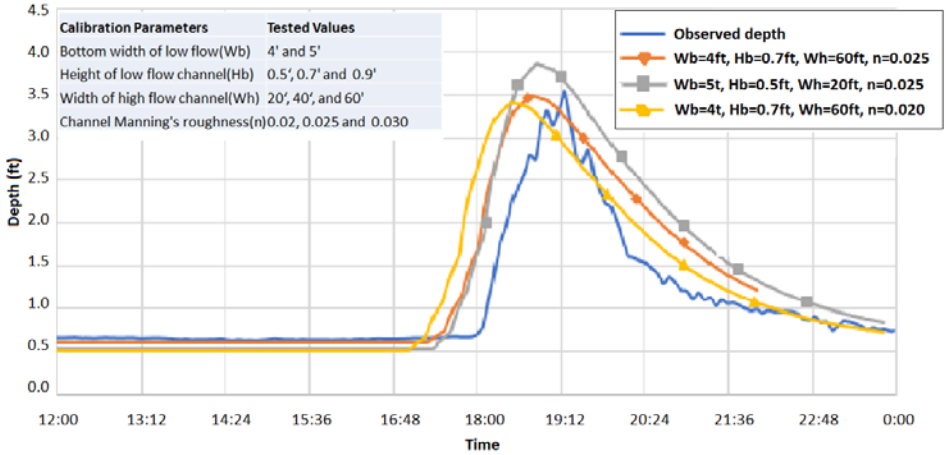

Figure 4- 19: Comparison between an observed and three modeled depth hydrographs upstream from the bridge, illustrating effects of the edited cross section geometry parameters and of Manning roughness.

5. Results and Discussion

This section is structures in two main parts. The first part focuses on the hydrological modeling results for the Soapstone Branch Watershed. The second part is the hydraulic modeling of the conditions near the bridge, and study of alternative cross sections for the stream near Dean Road Bridge, which could help mitigate the issues associated with aggradation.

5.1. Hydrological simulation

The hydrological modeling stage intends to provide estimates of inflows to the region near the bridge site, as well of sediment loading in the watershed. The subsections below are structured in include the model parameter calculation, MUSLE soil erodibility parameter calculation, HEC-HMS hydrological calculation results, and finally estimates of soil erosion in the watershed.

5.1.1. Hydrological parameter calculation

HEC-GeoHMS was used for catchment delineation from the DEM created earlier. A stream definition of 0.4 sq. km. was selected using a trial and error method to match the generated streams with the natural streams. This procedure divided the catchment into seven subcatchments, shown in Figure 5-1, and identified from W80 to W140.

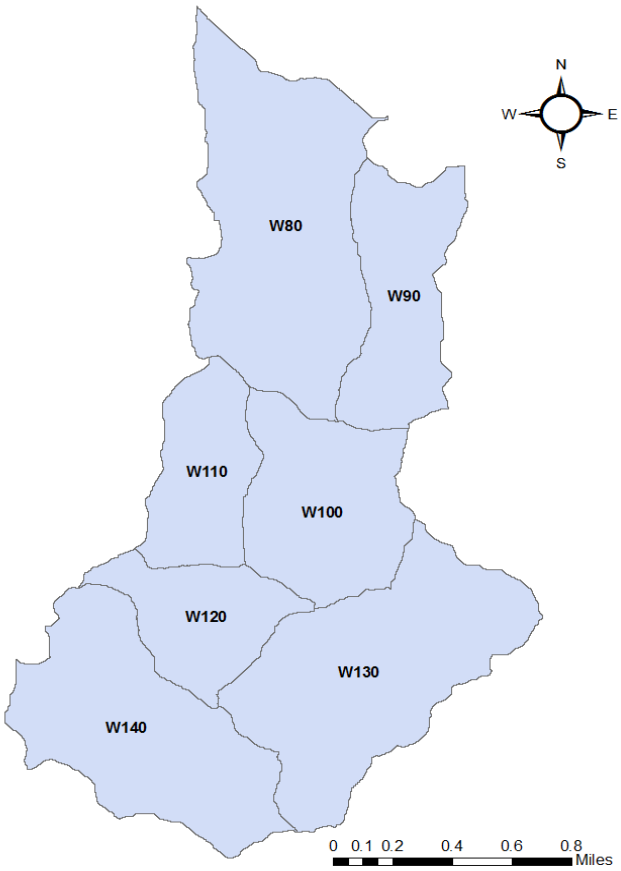

Figure 5- 1: Delineated Soapstone Branch Catchment and Partition into Subcatchments

The NAIP imagery can be converted into land cover maps using two types of classification schemes viz. unsupervised and supervised classification scheme. In unsupervised classification, users can enter the desired number of classes to which s/he desires to initially classify the original image. The software then classifies as per designed algorithm to group pixels into various spectral classes. Unlike this method, in supervised classification, the user selects training sites for each final desired class and, based on the spectral signature of those training sites, software categorizes the original image. The accuracy of unsupervised classification scheme can be further improved by using a cluster busting technique (Bossler et al. 2004). In the cluster busting technique, a subset of the image is selected, and unsupervised classification scheme is applied to the respective subset image. The overlay of the subset and the originally classified image results into an image with higher accuracy.

Two different NAIP datasets collected in 2011 and 2015 were used. Unsupervised classification using the Iterative Self-Organizing Data Analysis Technique (ISODATA) with 40 classes was applied using ERDAS IMAGINE 2016 software. Using multispectral NAIP imagery, these 40 classes were categorized into 4 different land use types viz. forest, agricultural land, water, and rangeland. Rangelands and agricultural lands have similar spectral reflectance and are often difficult to differentiate with a smaller number of classes in unsupervised classification. For improving accuracy, the cluster busting technique was applied. An area of land surrounding the forest and rangeland was clipped from the original image and then, the unsupervised classification was carried out on the clipped subset (Figure 5-2). Final overlay of the clipped and initially classified image produced the final land cover map (Figure 5-3).

Land cover maps were prepared using classification and cluster busting techniques for 2011 and 2015. Accuracy assessment for both land cover classification was performed in ERDAS Imagine software. In accuracy assessment, a number of test points is selected by the user and then ERDAS Imagine places those points over the area being classified either by random procedure or stratified random procedure (user's choice). Those distributed points are then provided a land cover class based on their spectral signature. Newly entered land cover class for those points is compared with the originally classified land cover class. The software then calculates overall accuracy and Kappa statistics based on this comparison. Overall accuracy is the simple accuracy assessment which calculates the percentage of the match during the comparison. However, Kappa statistic reflects the difference between agreement achieved and the agreement expected by chance. A Kappa value of 0.7 indicates that there is 70% better agreement than by chance alone. For 2011, overall classification accuracy was 95% and overall Kappa statistics was 0.9149 whereas, for 2015, overall classification accuracy was 100% and overall Kappa statistics was 1.0.

Rangeland area increased whereas forest area decreased from 2011 to 2015, as indicated in Figure 5.3. Statistical analysis of land cover data from 2011 to 2015 shows that forest area reduced from 34.4% to 28.7%, agricultural land increased from 56.3% to 58.1% and rangeland increased from 8.7% to 12.6%.

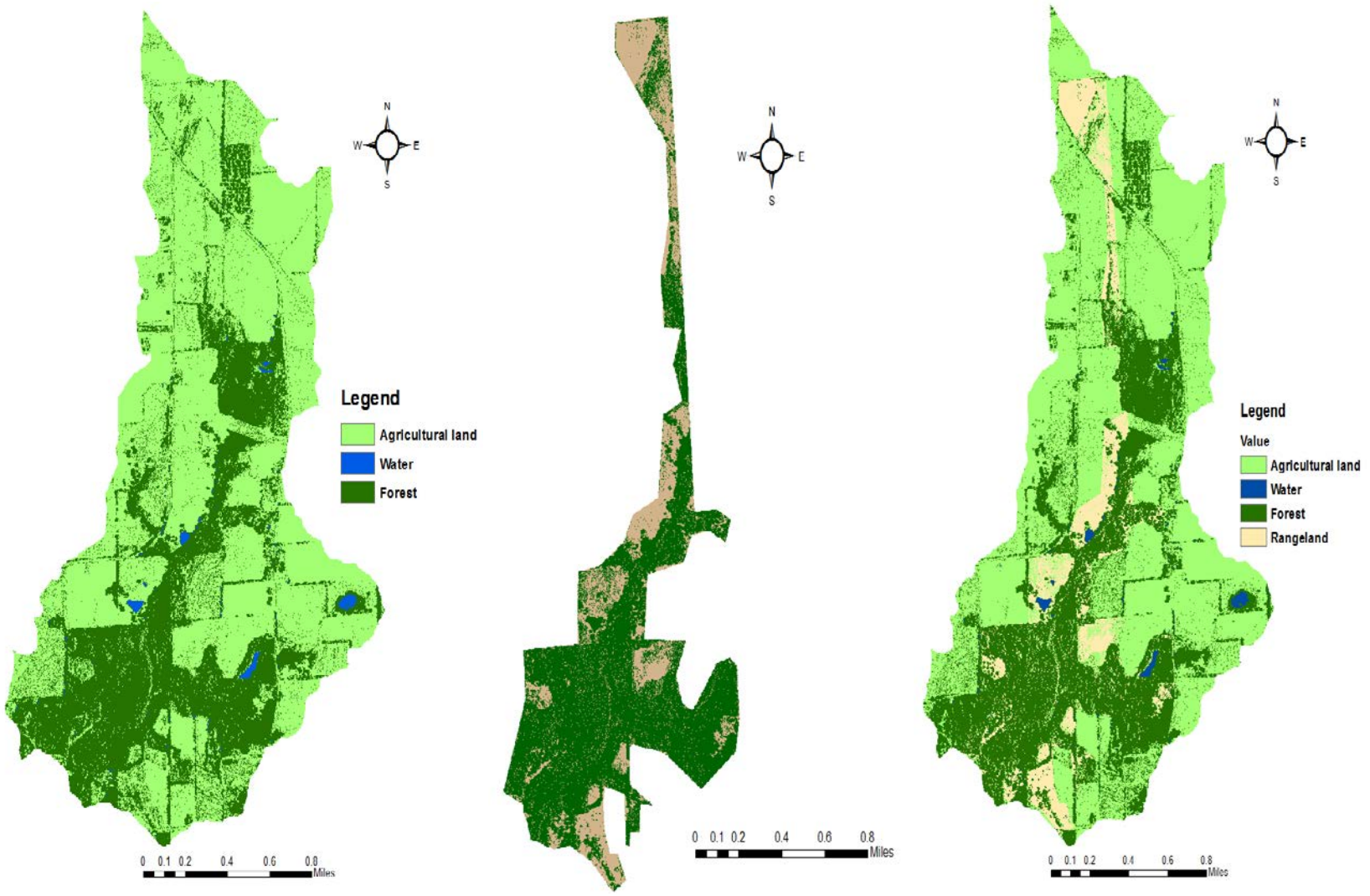

Figure 5- 2: Cluster Busting Technique Applied to Area Surrounding Forest: Before (Left), Cluster busting (Middle) and After (Right)

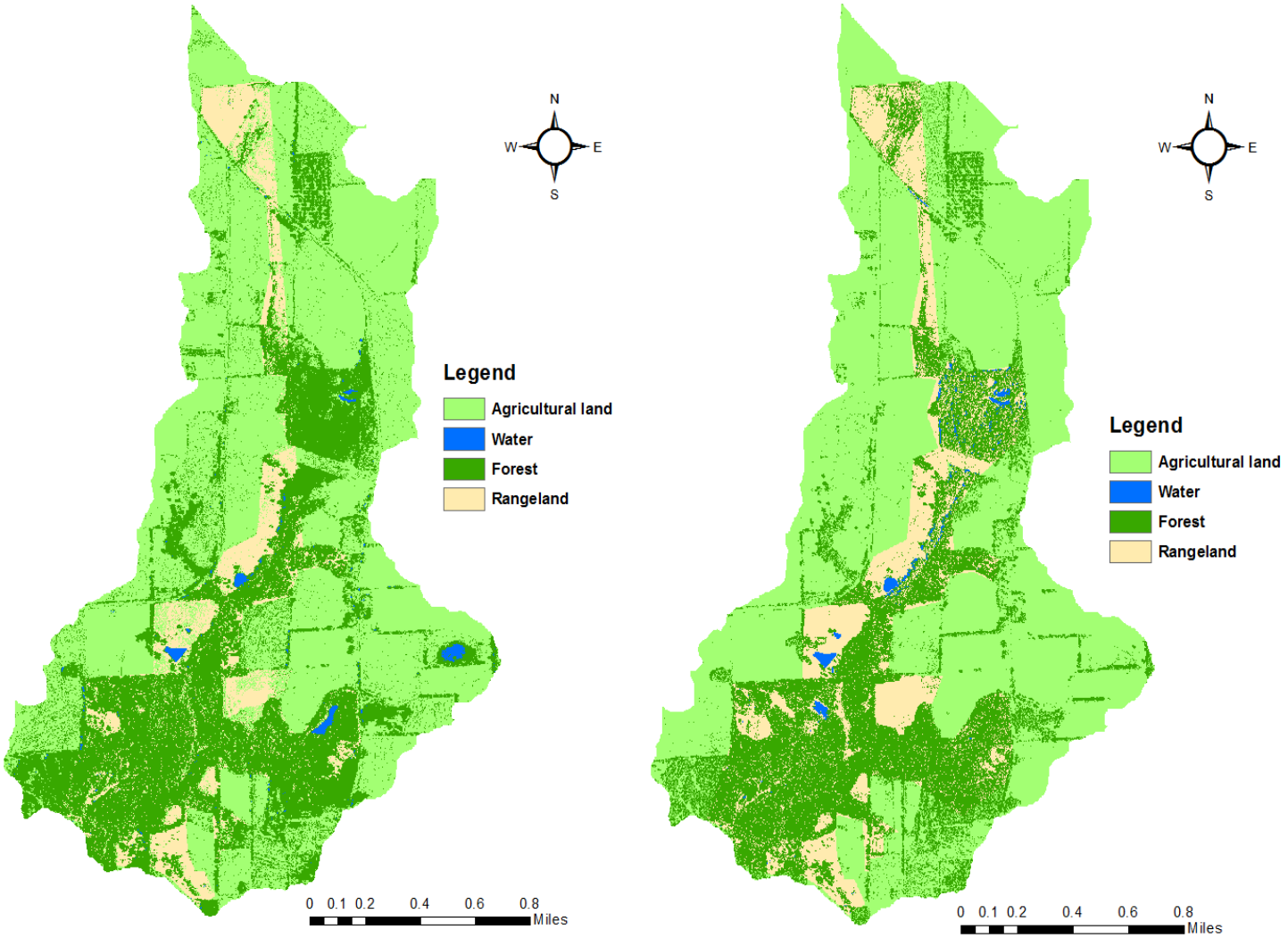

Figure 5- 3: Land Cover Map of Soapstone Branch Catchment Developed from NAIP Imagery for 2011 (Left) and 2015 (Right)

The soil data of Dale County was used for producing the HSG map for the catchment shown in Figure 5-4. The combination of HSG map and land cover map produced the CN grids of the catchment for 2011 and 2015, shown in Figure 5-5. Table 5-1 shows that curve number of each subcatchments increased by a small amount from 2011 to 2015, thus, reducing the basin lag. However, for subcatchments W140, W130 and W110, increase in curve number was higher than the increase in other subcatchments as expected since deforestation and land cover changes in this subcatchments were of significant amount than any other catchment.

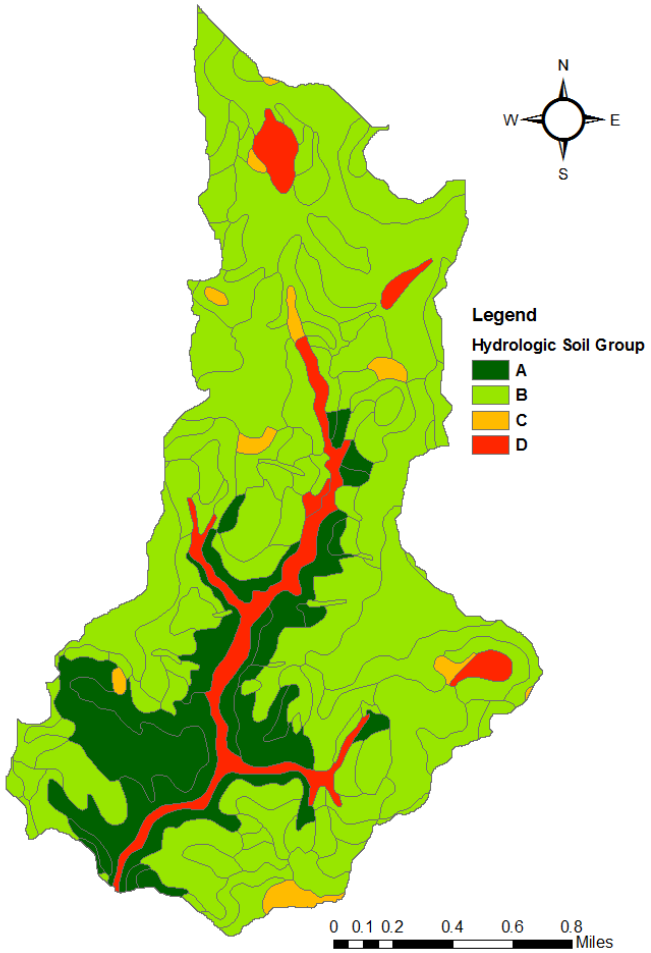

Figure 5- 4: Hydrologic Soil Group Map of Soapstone Branch Catchment

Table 5- 1: Curve Number and Basin Lag Computation at Subcatchment Scale for 2011 and 2015

Subcatchment	Curve Number (2011)	Curve Number (2015)	Basin lag 2011 (in minutes)	Basin lag 2015 (in minutes)
W140	65	66	46	44
W130	73	75	52	50
W120	67	67	37	37
W110	77	78	33	31
W100	75	75	32	32
W90	77	78	54	53
W80	78	79	64	63

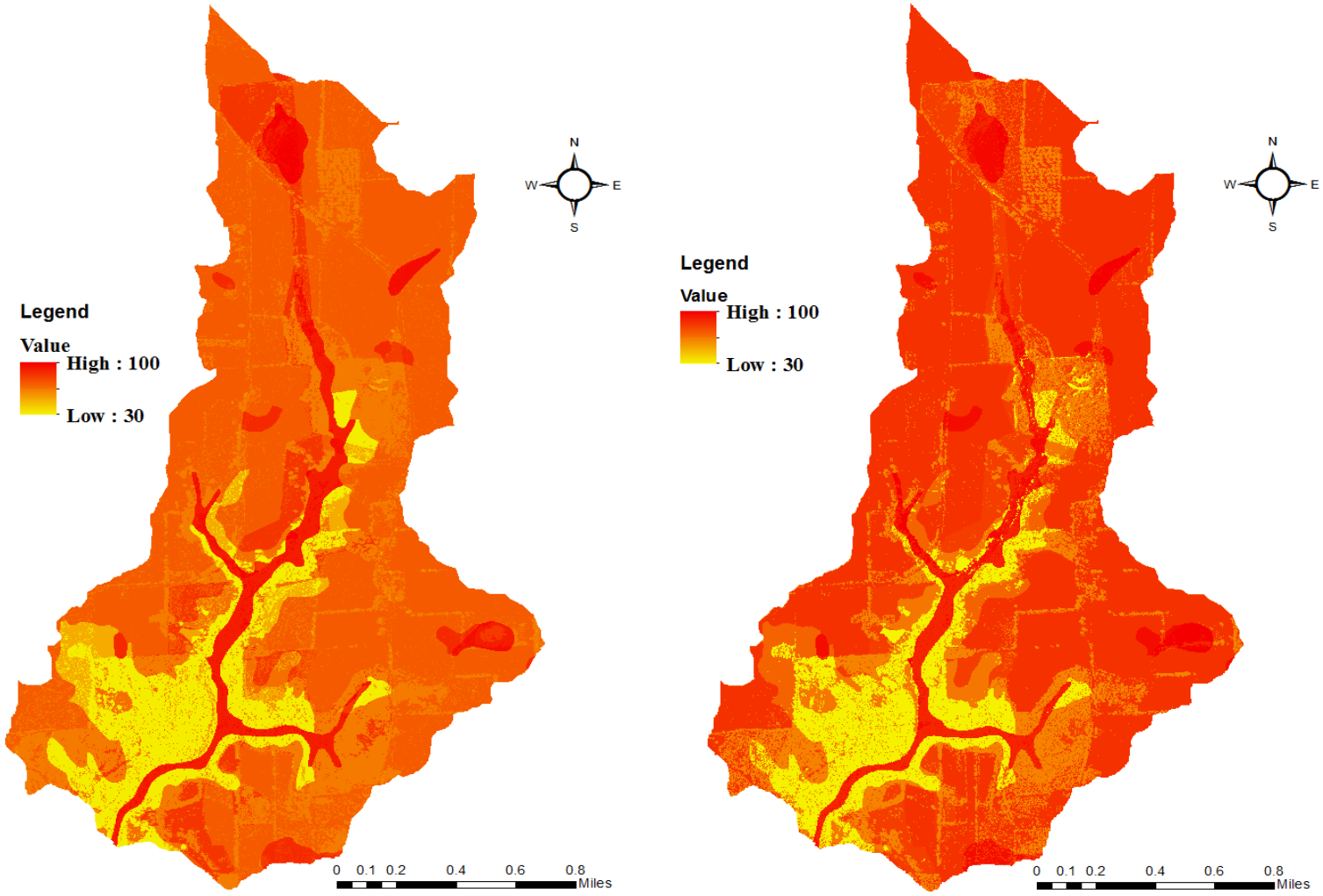

Figure 5- 5: Curve Number Grid of Soapstone Branch Catchment for 2011 (Left) and 2015 (Right)

5.1.2. Soil erosion parameter estimation for MUSLE

Soil erodibility factor (K factor) is defined as the rate of soil loss per rainfall erosion index unit measured on a unit plot of 72.6 ft. length and 9% slope. The unit plot is in clean-tilled fallow condition with tillage upslope and downslope. K factor can be obtained from soil data available at SSURGO database. USDA soil data viewer provides an easy way of mapping K factor of the soil data provided county. K factor obtained from USDA for Dale County was then clipped for the Soapstone branch catchment shown in Figure 5-6. An areal average K factor value of 0.19 was obtained for the Soapstone branch catchment.

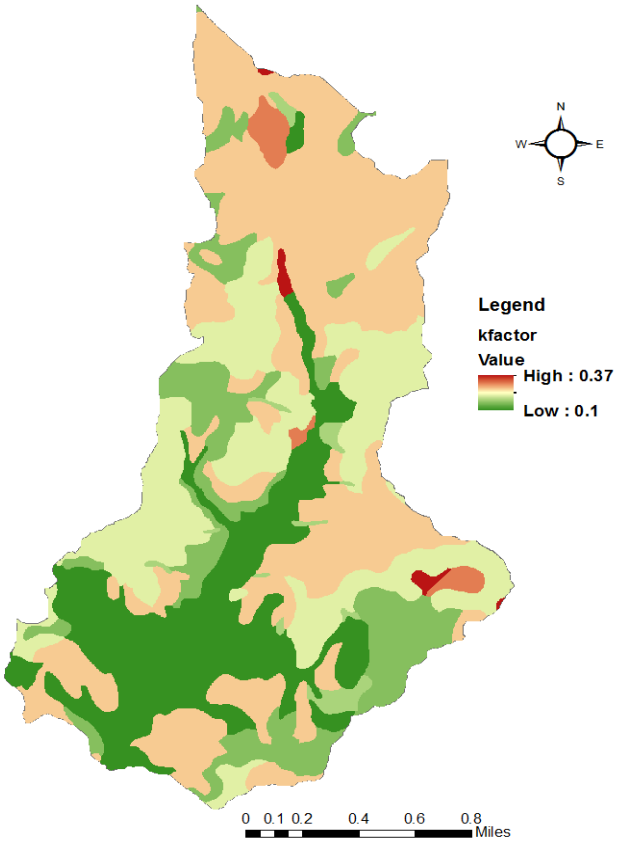

Figure 5- 6: Spatial Distribution of K factor in the Soapstone Branch Catchment

The topographic factor (LS factor) accounts for the effect of slope length and slope steepness on the quantity of soil erosion. It is the ratio of soil loss per unit area from a field slope to the amount of soil loss from a plot of 72.6 ft. length with 9% uniform slope. LS factor can be computed by using Equation 5.1

$$LS = \left(\frac{X}{72.6}\right)^{m} * (0.065 + 0.045 * S + 0.0065 * S^2) \quad (5.1)$$

Where,

X = slope length (ft.)

S = Slope gradient (%)

m = exponent depending on S and can be obtained from Table 5.2:

Table 5- 2: Exponent m-value in LS factor for different slope

Slope (in %)	m-value
>5	0.5
3-5	0.4
1-3	0.3
<1	0.2

Slope length (X) can be calculated for each raster grid using Equation 5.2.

$$X = flow\ accumulation * cell\ size \qquad (5.2)$$

From available DEM, a slope grid and flow accumulation grid were created. Then, LS factor grid (Figure 5-7) was prepared using Equation 5.1 and 5.2. An areal average LS factor value of 0.98 was computed for the Soapstone branch catchment.

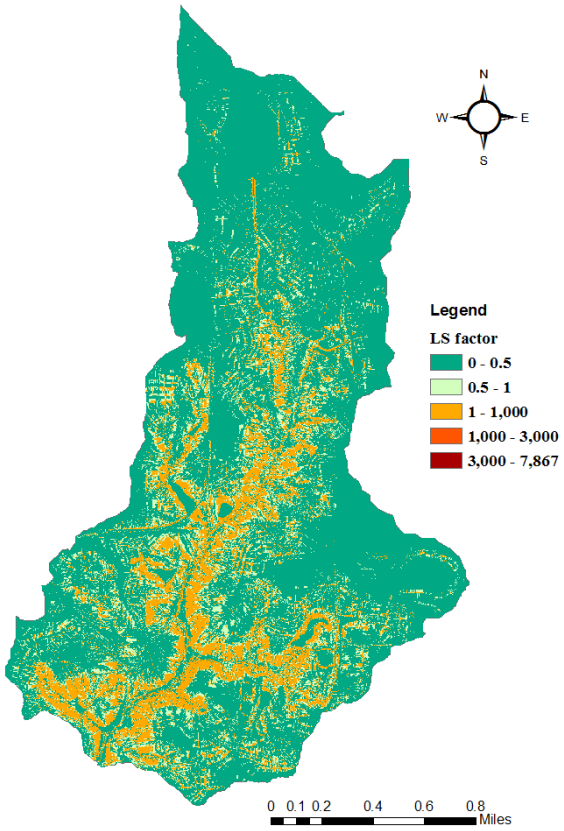

Figure 5- 7: Spatial Distribution of LS factor in the Soapstone Branch Catchment

The cover management factor (C factor) is the ratio of soil loss from a land covered by a specific crop to the soil loss under continuous bare fallow land condition. The C factor depends on a variety of factors such as the type of vegetation, their stage of growth, and their respective cover percentage. The C factor for any area can be developed using normalized difference vegetation index (NDVI). NDVI is a numerical indicator which describes the greenness, i.e., relative health and density of vegetation. The value of NDVI ranges from -1 to +1 and can be calculated using data from the visible red band and near infrared band of satellite imagery. The mathematical

expression for NDVI is given in Equation 5.3. NDVI value so produced can be used to develop cover factor using Equation 5.4 (Gitas et al. 2009).

$$NDVI = \frac{NIR - VR}{NIR + VR} \quad (5.3)$$

Where,

NIR = near infra-red

VR= visible red

and

$$C = \exp(-a\frac{NDVI}{b - NDVI}) \quad (5.4)$$

Where,

a, b = empirical constant

Gitas et al. (2009) have suggested a value of 2 and 1 for a and b, respectively. Using the near infra-red band (band 4) and visible red band (band 1) of aerial images (from NAIP) for the catchment, NDVI value raster grid was created for both 2011 and 2015.

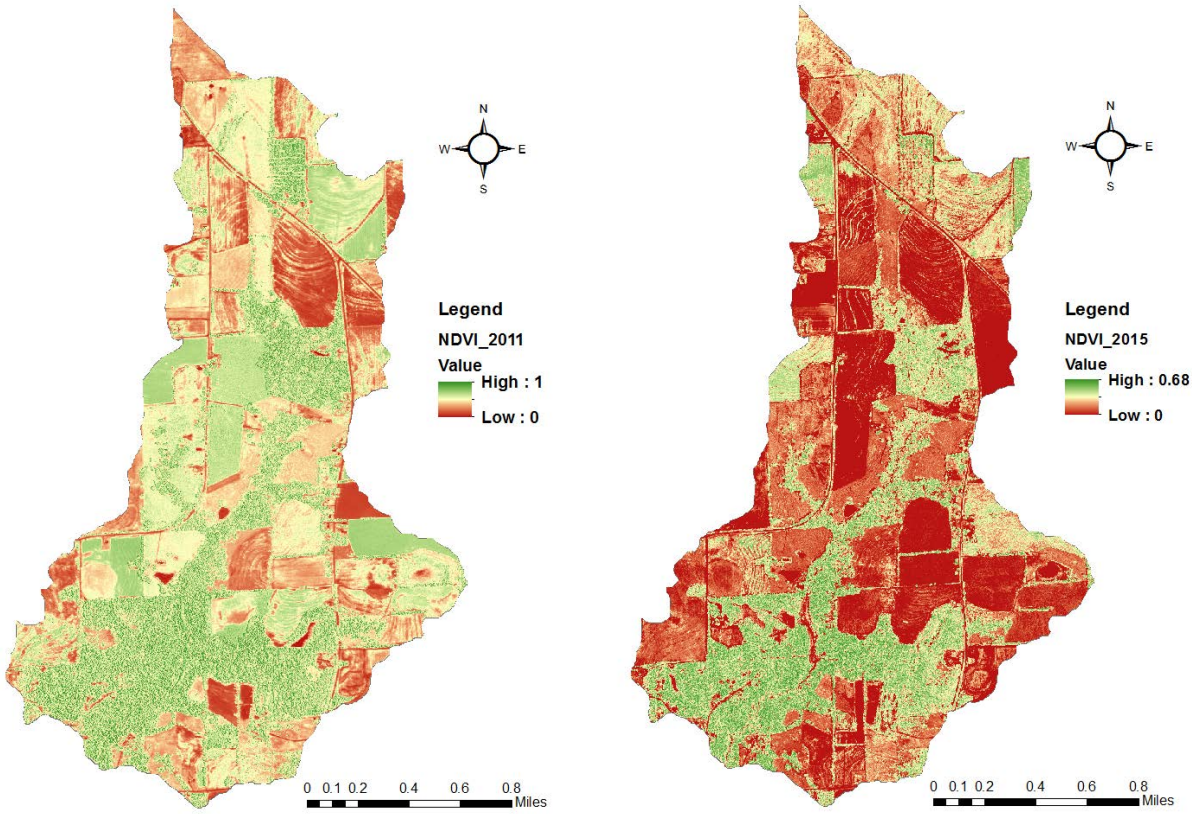

Figure 5- 8: *Spatial Variation of NDVI Values of the Soapstone Branch Catchment in 2011 (Left) and 2015 (Right)*

Raster calculation on NDVI raster grid for 2011 and 2015 (Figure 5-8) using Equation 5.4 produced C factor grid of catchment for 2011 and 2015, respectively. However, it can be noted from Figure 5-8, that, compared to 2011, 2015 has less crop in the agricultural land indicated by dark red zones with lower NDVIs. During data collection of aerial imageries of the catchment for these two years, an attempt was made to obtain data for the same month. However, due to data

limitation, aerial imageries were obtained for different months, i.e., August 2011 and September 2015. Due to the probable crop rotation going on in the agricultural land and different crop growth season, agricultural land has different NDVIs and C factor for 2011 and 2015. Since the objective of this study is to quantify the difference in sediment yield due to land cover changes and not the crop type or growth season, an additional computational step was applied.

For 2011, land cover class corresponding to agricultural land was clipped out and the average value of C factor for agricultural land was calculated. This average value was then applied to all raster grid of C factor for 2015 which correspond to agricultural land (Figure 5-9). This additional computation avoids the effect of agricultural crop growth and their seasonality on the sediment yield.

Furthermore, an attempt was made to quantify the amount of change in C factor by neglecting the effects of deforestation near stream. For this task, the forest area where major deforestation activities were experienced from 2011–2015, as observed from aerial imageries, was clipped out from the 2011 imagery and overlaid on 2015 aerial imagery. A new hypothetical C factor grid was then obtained using the procedure explained earlier (Figure 5-10).

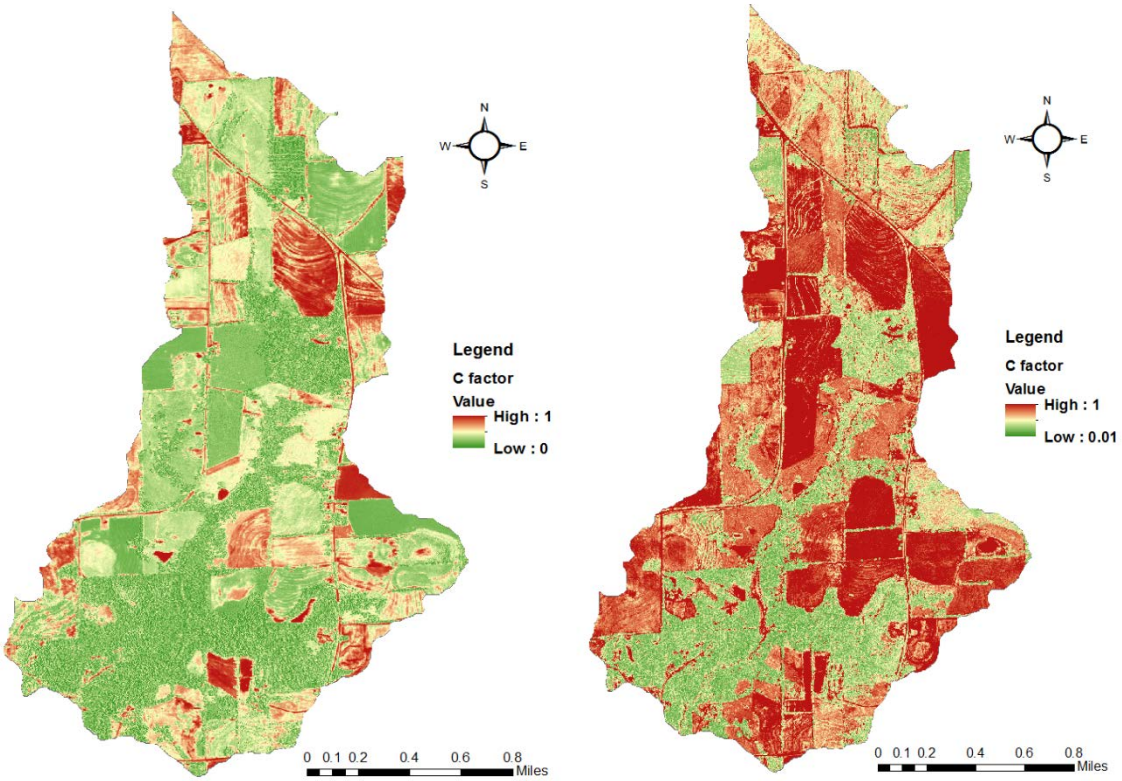

Figure 5- 9: Spatial distribution of C factor raster grid of Soapstone Branch Catchment in 2011 (Left) and 2015 (Right)

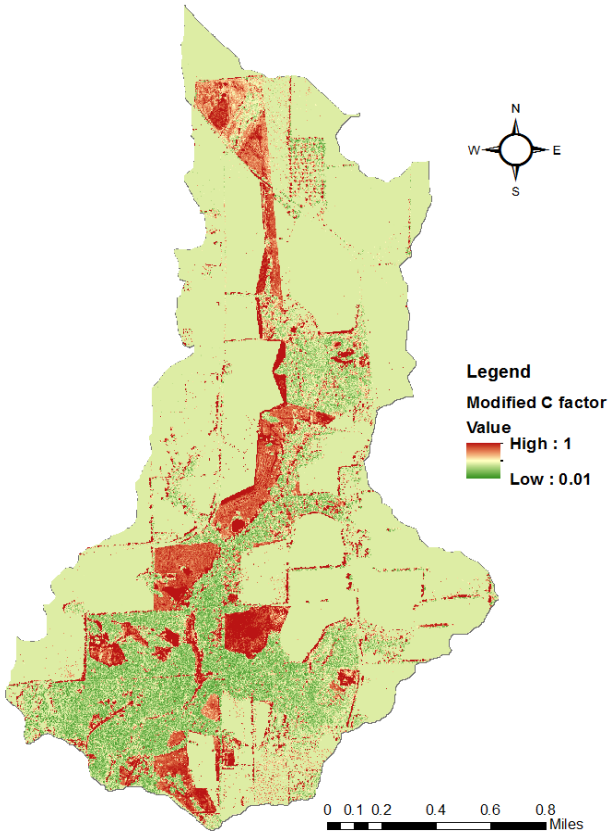

Figure 5- 10: Modified C factor raster grid of the Soapstone Branch Catchment in 2015

An areal average value of C factor grid was computed for the entire catchment both in 2011 and 2015. Average C factor value of the Soapstone branch catchment in 2011 was 0.347 which increased to 0.678 in 2015. However, the modification of C factor grid to neglect the influence of crop rotation and crop growth season produced an areal average value of 0.466 in 2015. Therefore, an overall increase of 34.3% in C factor was experienced by the Soapstone branch catchment due to deforestation.

An areal average C factor value of 0.449 was obtained by neglecting the effects of deforestation from 2011–2015 which corresponds to 29.4% increase since 2011. This indicates that only 4.9% increase in C factor was due to major deforestation activities. Remaining 29.4% increase in C factor may be due to the change in the size of rangeland, grass cover in rangeland, increase in agricultural area, thinning of forest which is not visible in aerial imagery, etc. This hypothetical C factor grid was obtained to quantify the effects of deforestation and other activities on C factor. Table 5-3 lists the areal average value of C factor and percentage increase in C factor from 2011 for different land cover conditions.

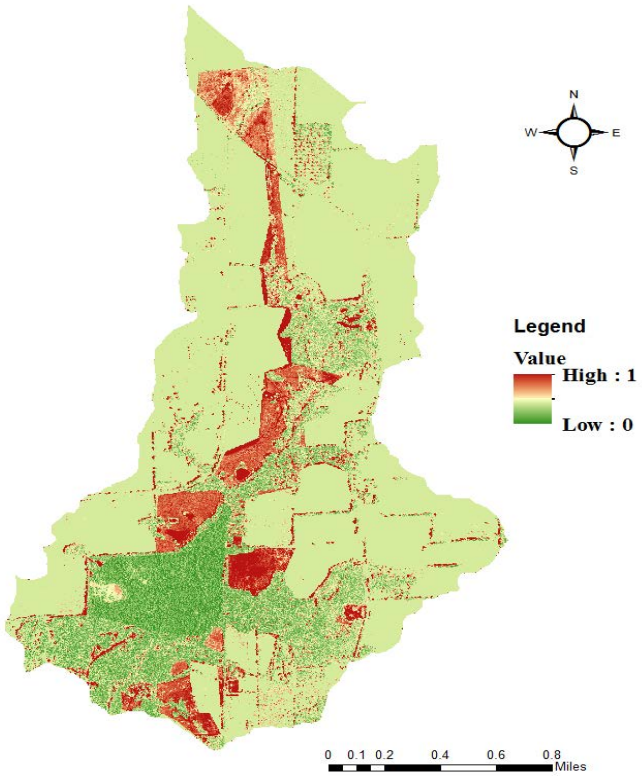

Figure 5- 11: C factor grid of Soapstone branch in 2015 obtained by neglecting the effects of deforestation

Table 5- 3: Areal Average C Factor Value and Percent Change for Different Scenarios

Scenario	Areal average C	Percent change (%) from 2011
2011 land cover condition	0.347	N/A
2015 land cover condition due to all possible changes	0.678	95.4
2015 land cover after removing crop rotation	0.466	34.3
2015 land cover after removing major deforestation and crop rotation	0.449	29.4
2015 land cover with deforestation	0.364	4.9

The support practice factor (P factor) is defined as the ratio of soil loss with support practice to the amount of soil loss with up and down hill farming. Soil conservation practices such as contouring, contour strip-cropping, and terracing reduce the soil erosion and thus have lower P factor values. The value of P factor ranges from 0 to 1. Table 5.4 provides the typical values of P factor for different practices (Kuok et al. 2013). Due to the absence of any such practices in the Soapstone branch catchment, a P factor of 1 was selected for a conservative sediment yield estimation.

Table 5- 4: P factor values for different soil conservation practices

Soil conservation	P value
None	1
Contouring	0.6
Contour strip-cropping	0.35
Terracing	0.15

5.1.3. HEC-HMS modeling

HEC-GeoHMS was used for developing the background map file and distributed-basin schematic model file. It also performed the tasks of the automatic naming of three river reaches and seven subcatchments, checks for errors in the catchment and connectivity of streams. HEC-HMS model setup is shown in Figure 5.12.

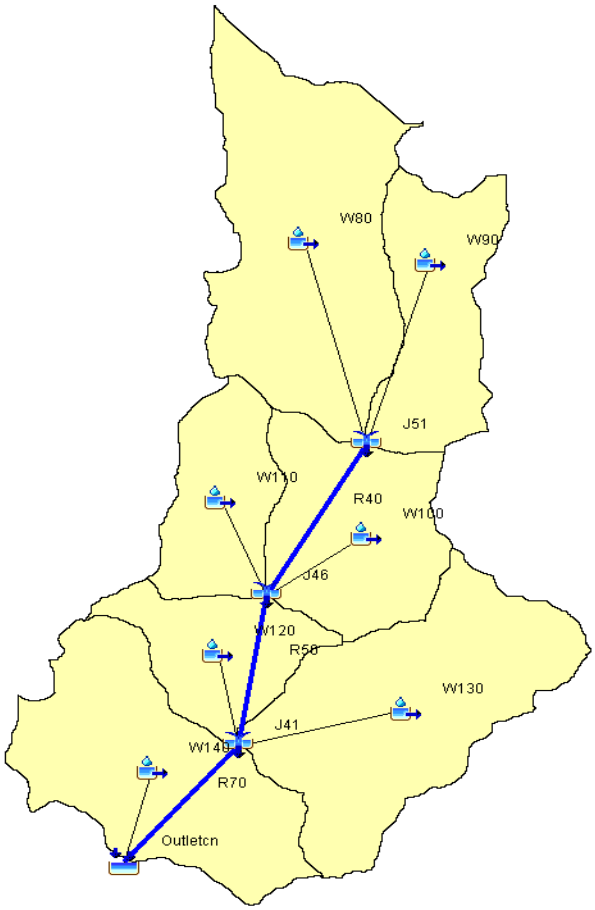

Figure 5- 12: HEC-HMS Setup for Soapstone Branch Catchment

Semi-distributed continuous SMA model of the Soapstone branch catchment was run from January 2009–September 2016 using a combination of Dothan rainfall data (January 2009–February 2016) and installed rain gauge data at the site (March 2016–September 2016). An initial warmup period of nine months was used. A 10-min simulation time interval was selected for model

run due to the smaller response time of sub-catchments. Figure 5-13 shows the simulation result from SMA model of the Soapstone branch catchment for the period of seven years (October 2009–September 2016).

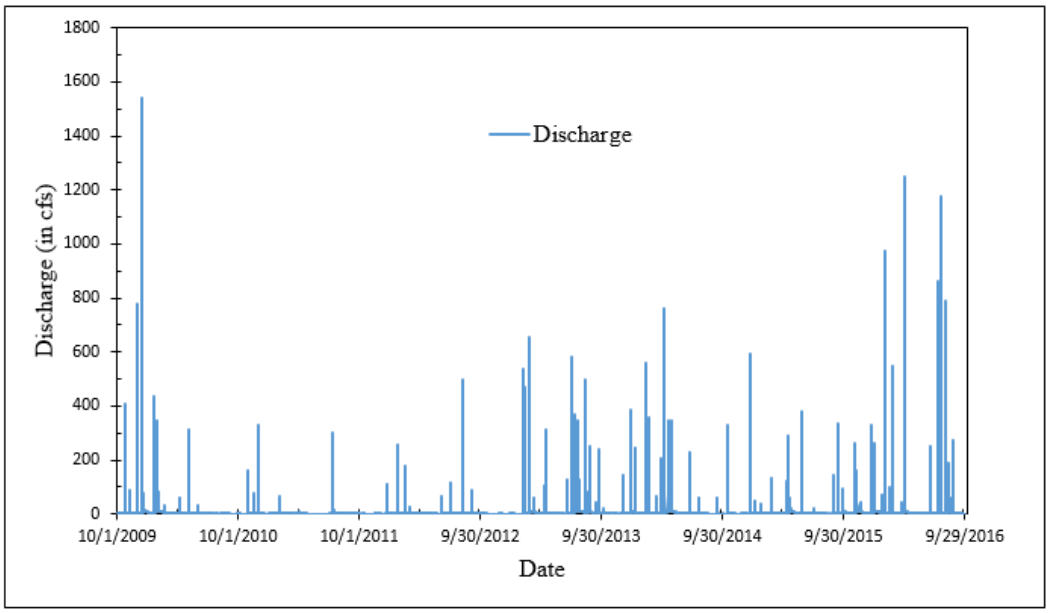

Figure 5- 13 SMA Model Result of Soapstone Branch Catchment (October 2009–September 2016)

An event based hydrologic model provides information on how the catchment responds to an individual rainfall event. The CN method discussed in earlier in this chapter can be also used for developing an event based model. CN is a dimensionless empirical parameter which determines the proportion of rainfall available as direct runoff during each storm event by considering the effects of land cover, soil type, and hydrological conditions.
The event based CN method can be expressed as:

$$Q = \frac{(P - I_a)^2}{(P - I_a) + S} \qquad (5.5)$$

Where,

Q = Direct runoff volume in inches
I_a = Initial abstraction in inches
S= Potential maximum retention after runoff begins in inches

and,

$$S = \frac{1000}{CN} - 10 \qquad (5.6)$$

CN values obtained by combining HSGs and land cover types are subjected to variability due to rainfall intensity, soil moisture conditions, etc. These reasons causing variability in CN are combined to form Antecedent Runoff Condition (ARC), previously called antecedent moisture condition. ARC is divided into three different classes viz. I for dry conditions, II for average conditions and III for wetter conditions. CN developed so far corresponds to ARC class II. The adjustment of ARC II CN to ARC I CN or ARC III CN is provided in Table 5-5 (McCuen 2005).

Table 5- 5: Adjustment of Curve Number for Dry condition (I) and Wet condition (III)

ARC II CN	Corresponding CN for ARC	
	I	III
100	100	100
95	87	99
90	78	98
85	70	97
80	63	94
75	57	91
70	51	87
65	45	83
60	40	79
55	35	75
50	31	70
45	27	65
40	23	60
35	19	55
30	15	50
25	12	45
20	9	39
15	7	33
10	4	26
5	2	17
0	0	0

Classification of catchment state into ARC classes is based on past rainfall conditions. Total 5-day antecedent rainfall which defines these three ARC of a catchment is listed in Table 5-6 (McCuen 2005).

Table 5- 6: Rainfall Limits Defining the Antecedent Runoff Condition

	Total 5-day Antecedent Rainfall (in.)	
ARC	Dormant Season	Growing Season
I	< 0.5	<1.4
II	0.5-1.1	1.4-2.1
III	>1.1	>2.1

Apart from 5-day antecedent rainfall, catchment state into ARC classes depends on the season, as shown in Table 5-6. Since the Soapstone branch catchment is an agricultural catchment, the season of the crop growth defines the ARC classes together with antecedent rainfall. Two major crops grown in the Soapstone branch catchment are corn and cotton. The growing season for corn is from March–August whereas for cotton is April–September (NASS 1997). Therefore, the period from March–September was considered as the growing season and October–February was considered as the dormant season for crops in Soapstone branch catchment. Tables 5-7 and 5-8 lists the adjustment of CN for ARC class I and class III for both 2011 and 2015. For the event based model of the Soapstone branch catchment, the 5-day antecedent rainfall and the

growing/dormant season were checked for each event and then corresponding CNs were applied for individual events.

Table 5- 7: 2011 Curve number and adjustment for ARC classes

Subbasin	2011 CN	CN (ARC I)	CN (ARC III)
W140	65	45	82
W130	73	54	87
W120	67	47	83
W110	77	59	89
W100	75	56	88
W90	77	59	89
W80	78	62	90

Table 5- 8: 2015 Curve Number and adjustment for ARC Classes

Subbasin	2015 CN	CN (ARC I)	CN (ARC III)
W140	66	46	82
W130	75	57	88
W120	67	47	83
W110	78	61	90
W100	75	57	88
W90	78	60	90
W80	79	61	91

Six storm events from three different ARC classes and, one from before 2011 and another after 2011 were selected for comparison with the SMA model. Details of each individual storm events are provided in Table 5-9.

Table 5- 9: Selected Storm Events for comparison with the SMA model

Storm Events	Total 5-day antecedent precipitation (in.)	ARC Class	Event Precipitation (in.)	Event duration (hr)
4/8/2010	0.01	I	0.99	3
2/7/2013	0.14	I	2.65	11
12/2/2009	0.8	II	3.95	23
1/23/2012	0.98	II	1.34	4
12/14/2009	3.02	III	5.28	18
2/10/2013	2.78	III	1.23	1

The uncalibrated event-based CN model produced much lower discharges than the SMA model did for all storm events as shown in Figures 5-14, 5-15 and 5-16. This underestimation is

the highest in ARC class I condition and gradually decreases as the antecedent rainfall condition in the catchment increases. The difference in discharge is the minimum for ARC class III conditions. Also, the discharge produced by calibrated SMA model and uncalibrated CN model matches quite well for intense storm events as shown in Figures 5-15 (A) and 5-16 (A) . For storm events occurring after 2011, the storm events were simulated using CNs and basin lag from both 2011 and 2015. It was found that event-based model prepared using 2015 CN performed better than event model based on 2011 CN.

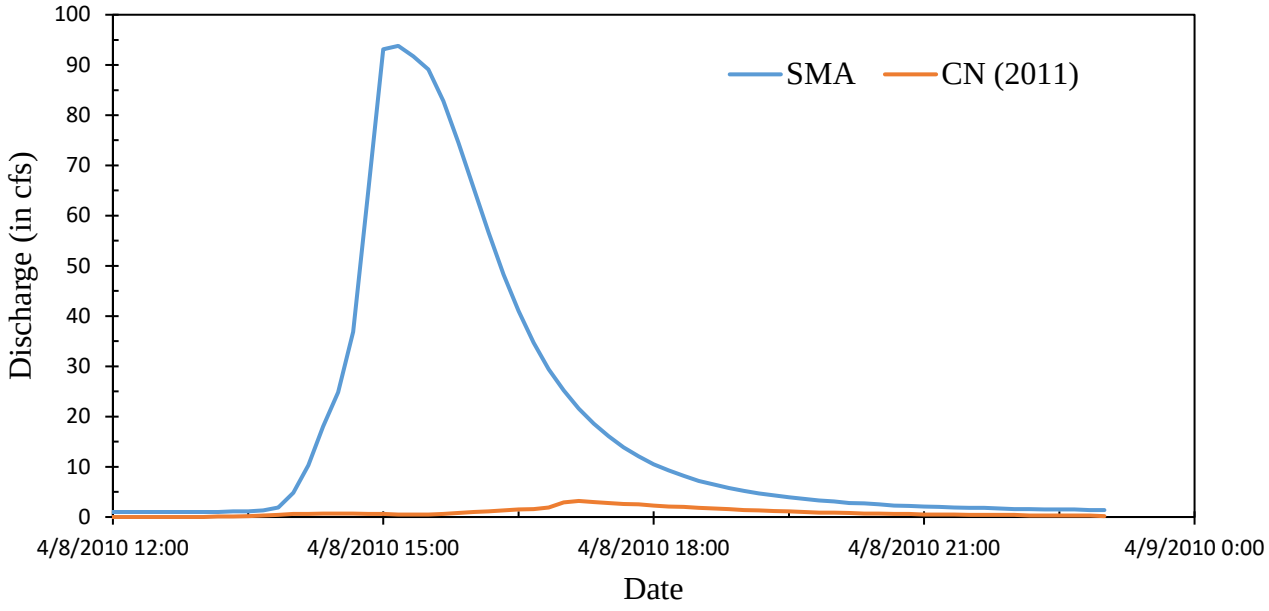

(A)

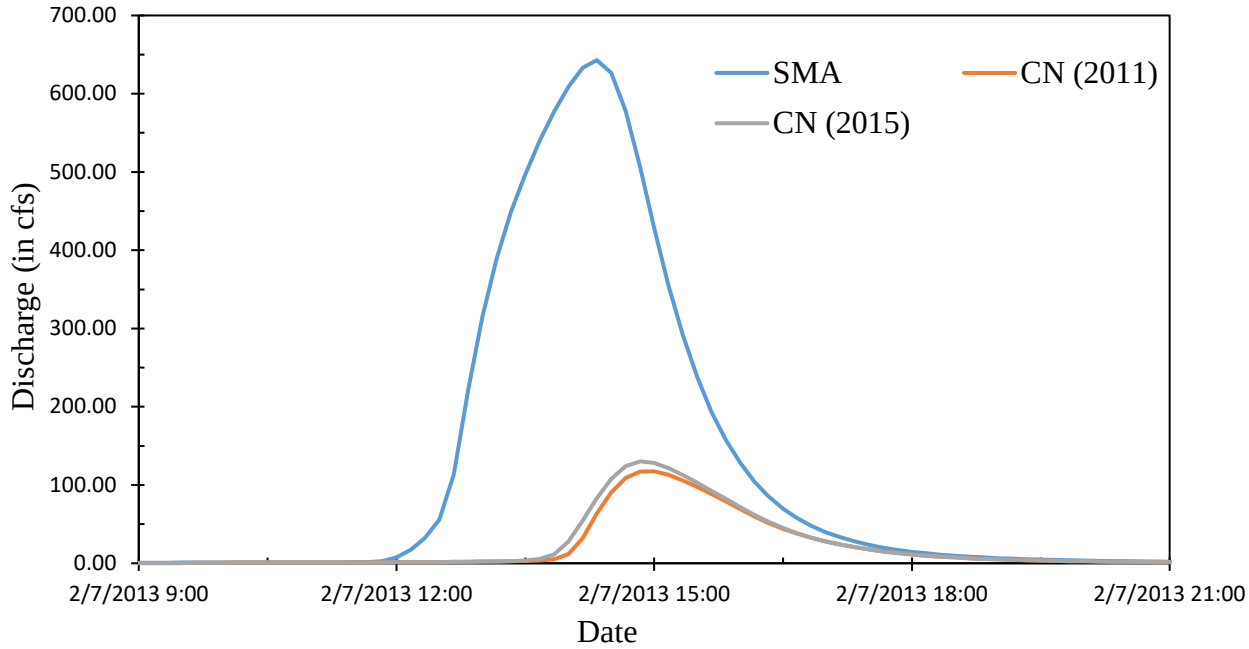

(B)

Figure 5- 14: Comparison of SMA Model with Uncalibrated Event-based CN Model for ARC Class I Condition with Storm Events Before 2011 (A) and After 2011 (B)

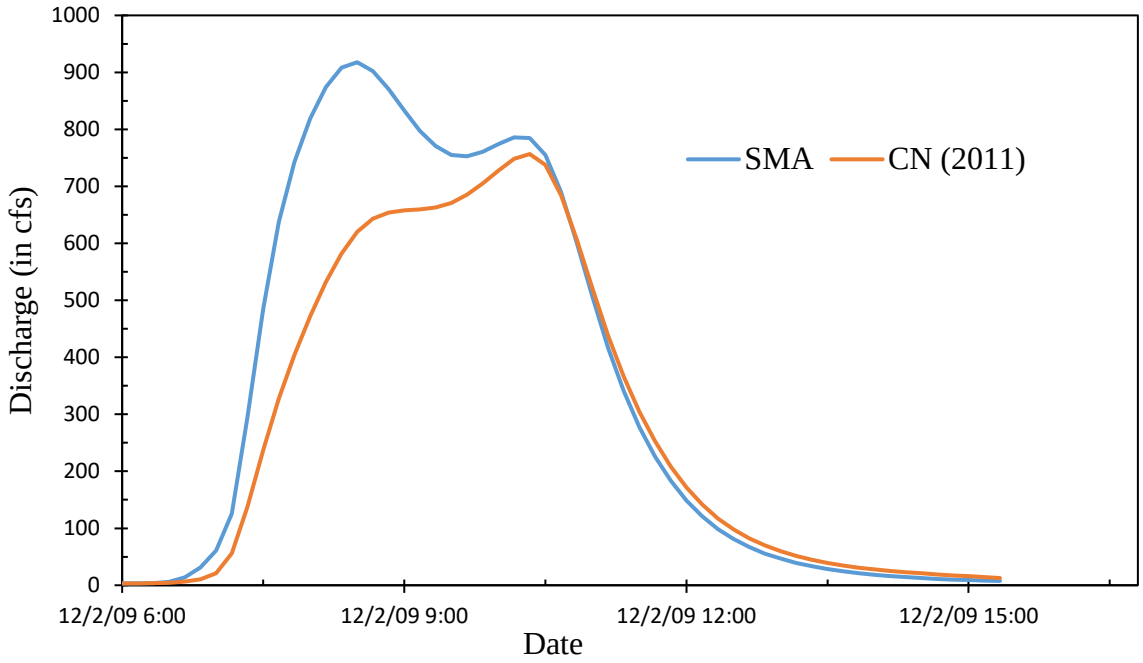

(A)

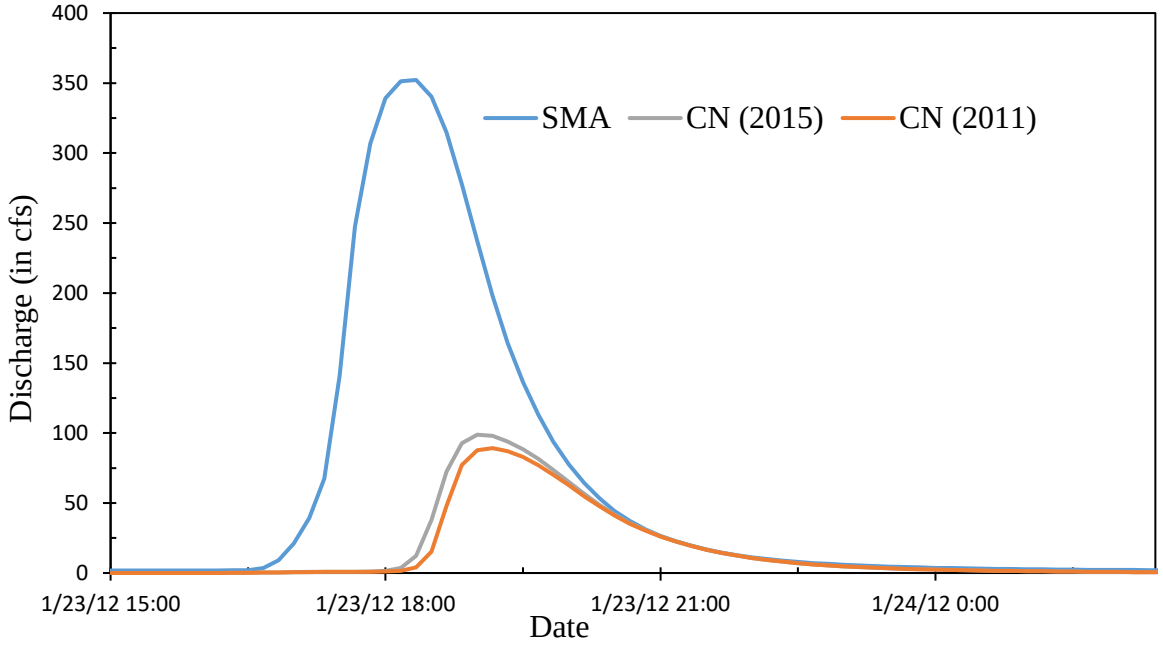

(B)

Figure 5- 15: Comparison of SMA model with Uncalibrated Event-based CN model for ARC Class II Condition with Storm Events. Before 2011 (A) and After 2011 (B)

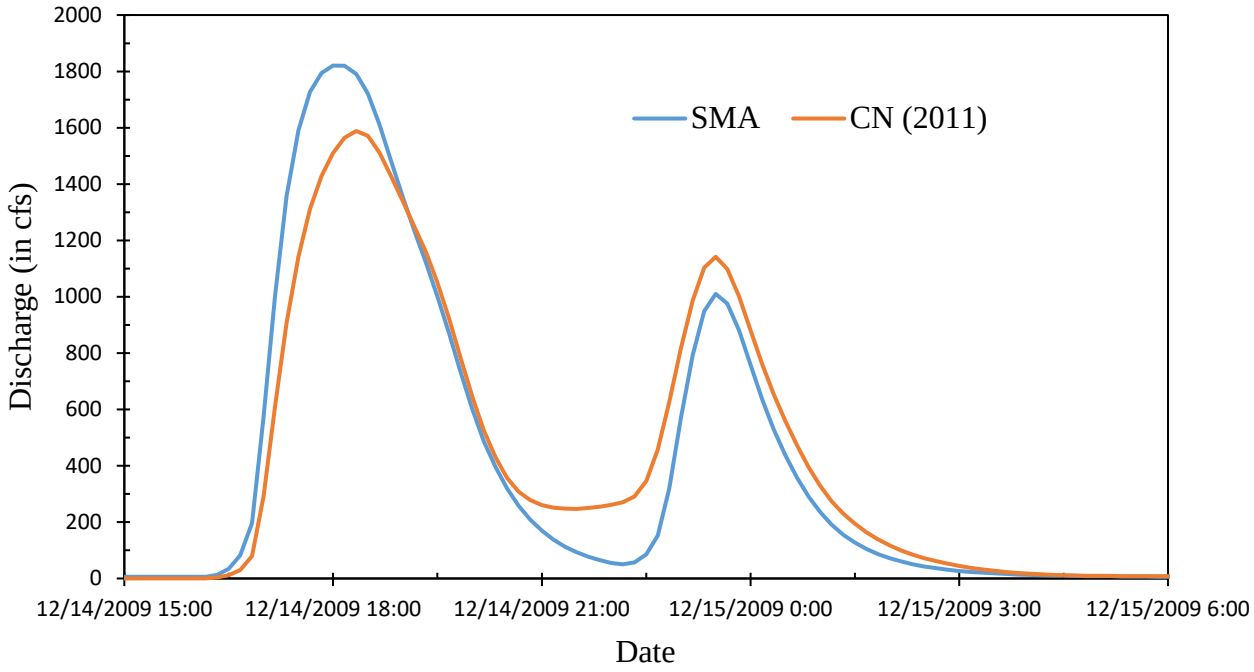

(A)

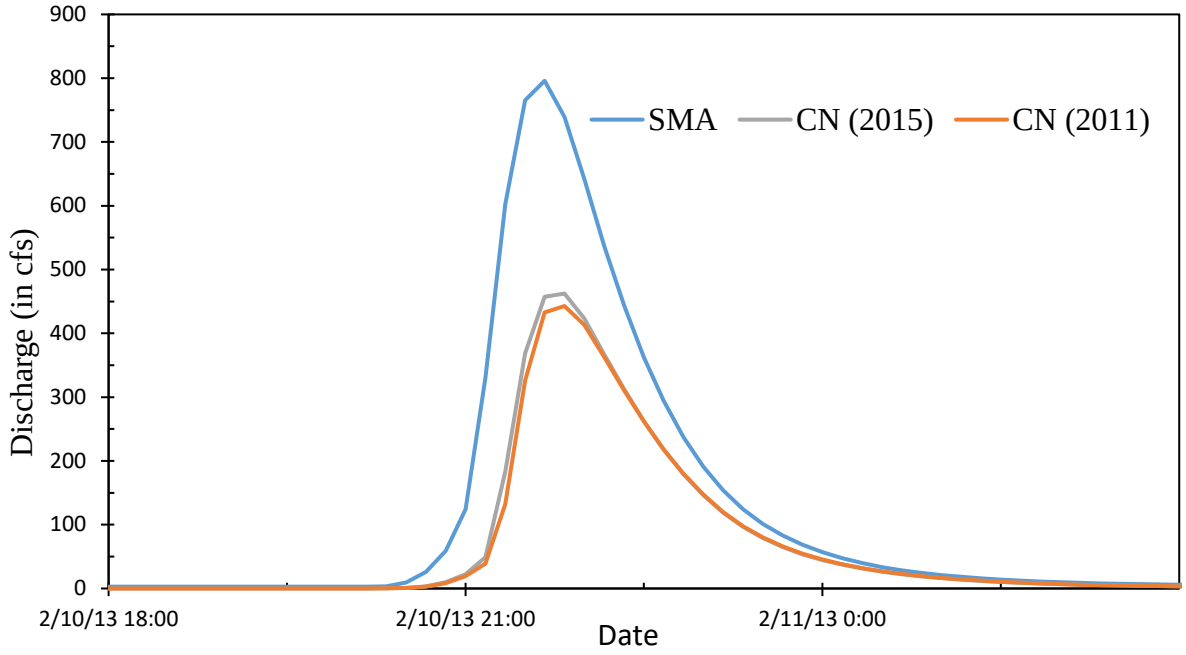

(B)

Figure 5- 16: Comparison of SMA model with uncalibrated event-based CN model for ARC class III condition with storm events. Before 2011 (A) and After 2011 (B)

An attempt was made for calibrating the event-based model using simulated discharge from SMA model "as observed". Since CN for ARC class I and ARC class III depend upon CN for ARC class II, so that, the storm event of 23rd January 2015 (Figure 5-15) corresponding to ARC

class II condition was selected for calibration. CN values for seven subcatchments were varied until CN model discharges matched with SMA model discharges.

This calibrated CN for ARC class II was then, adjusted for dry and wet catchment condition to determine ARC class I and ARC class III CN using Table 5-5 and is listed in Table 5-10. It was found that a 15% increment in ARC class II CN produces the best match between SMA model and CN model discharges. The same increment of 15 % was applied to 2011 ARC class II CN at first and then adjusted for dry and wet catchment condition (Table 5-11).

Table 5- 10: Calibrated 2015 CN values for ARC class I, II, and III

Subbasin	2015 CN	calibrated ARC II CN	calibrated ARC I CN	calibrated ARC III CN
W140	66	76	59	89
W130	75	86	72	94
W120	67	77	59	89
W110	78	90	78	96
W100	75	86	72	94
W90	78	89	77	96
W80	79	90	79	96

Table 5- 11: Calibrated 2011 CN values for ARC class I, II, and III

Subbasin	2011 CN	calibrated ARC II CN	calibrated ARC I CN	calibrated ARC III CN
W140	65	75	56	88
W130	73	84	69	93
W120	67	77	59	89
W110	77	88	75	95
W100	75	86	71	94
W90	77	89	76	96
W80	78	90	78	96

From Figures 5-17, 5-18 and 5-19, it can be seen that the calibrated CN model's output discharge match quite well with the SMA model's discharge for ARC class II and III condition. However, even if, the calibrated CN model produces better match than the uncalibrated event model for ARC class I condition, the calibrated CN model underpredicts the discharge. Furthermore, this underprediction increases as the total 5-day antecedent rainfall decreases (Figure 5-17).

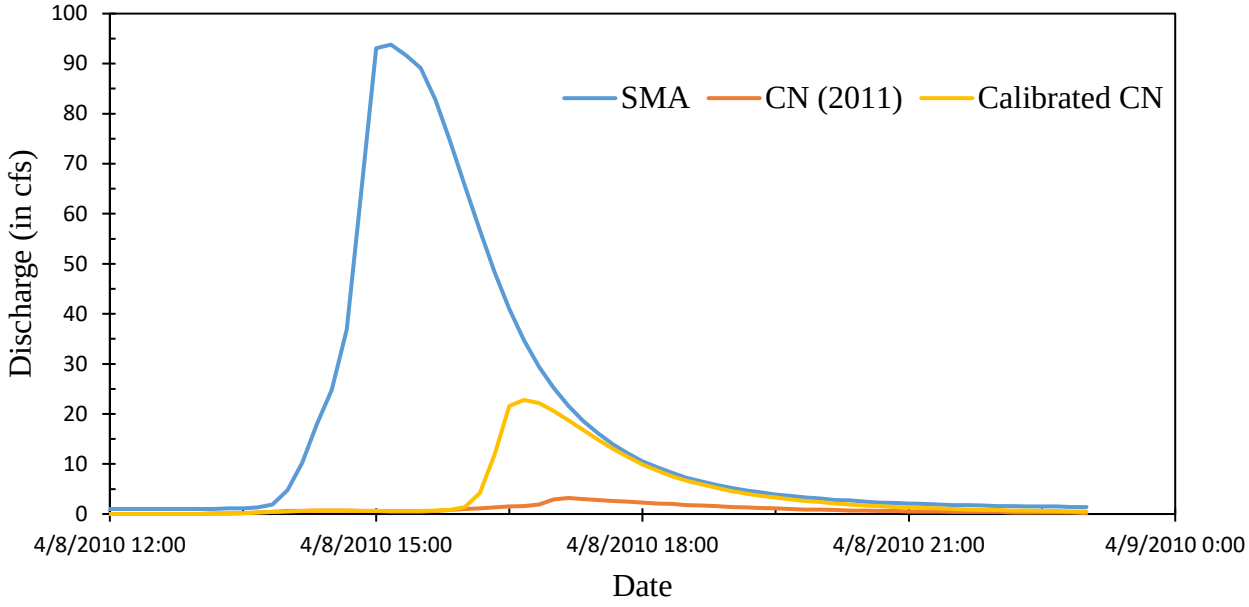

(A)

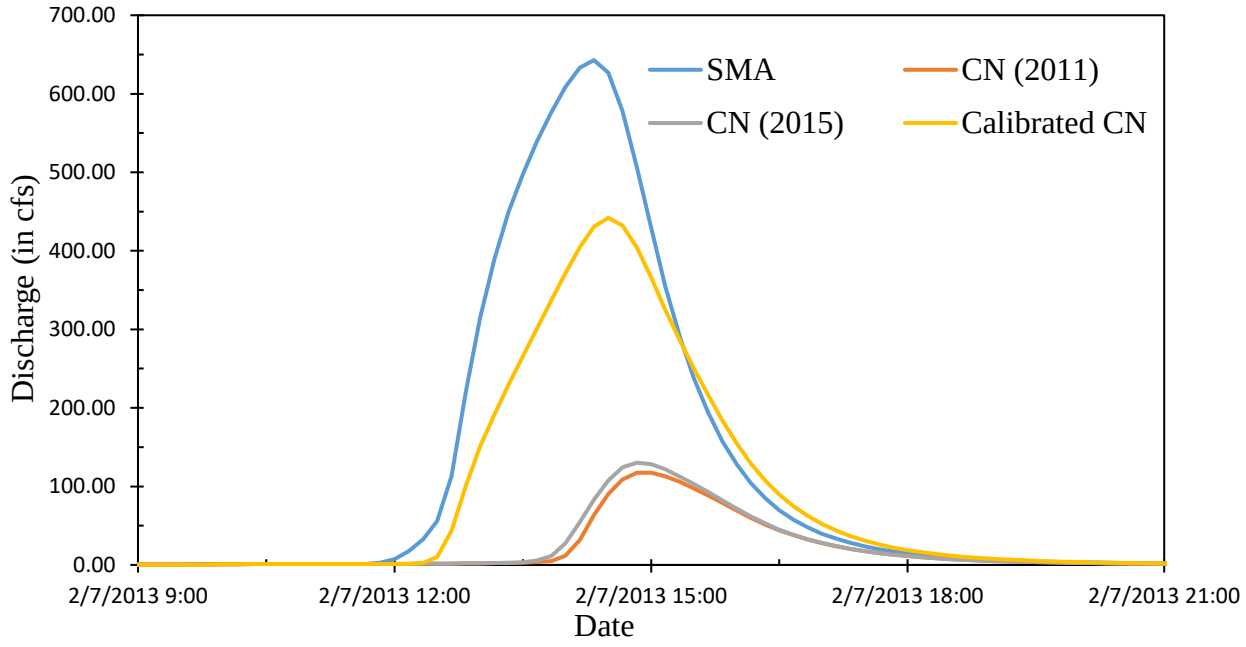

(B)

Figure 5- 17: Comparison of SMA Model with Calibrated CN Model for ARC class I Condition with Storm Events. Before 2011 (A) and After 2011 (B)

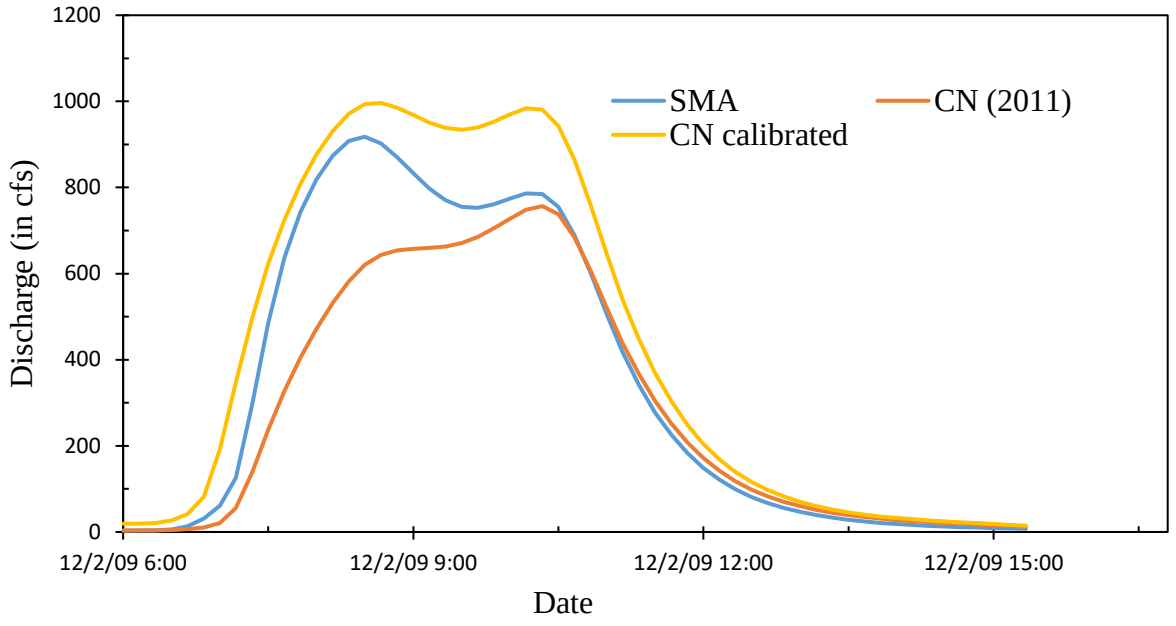

(A)

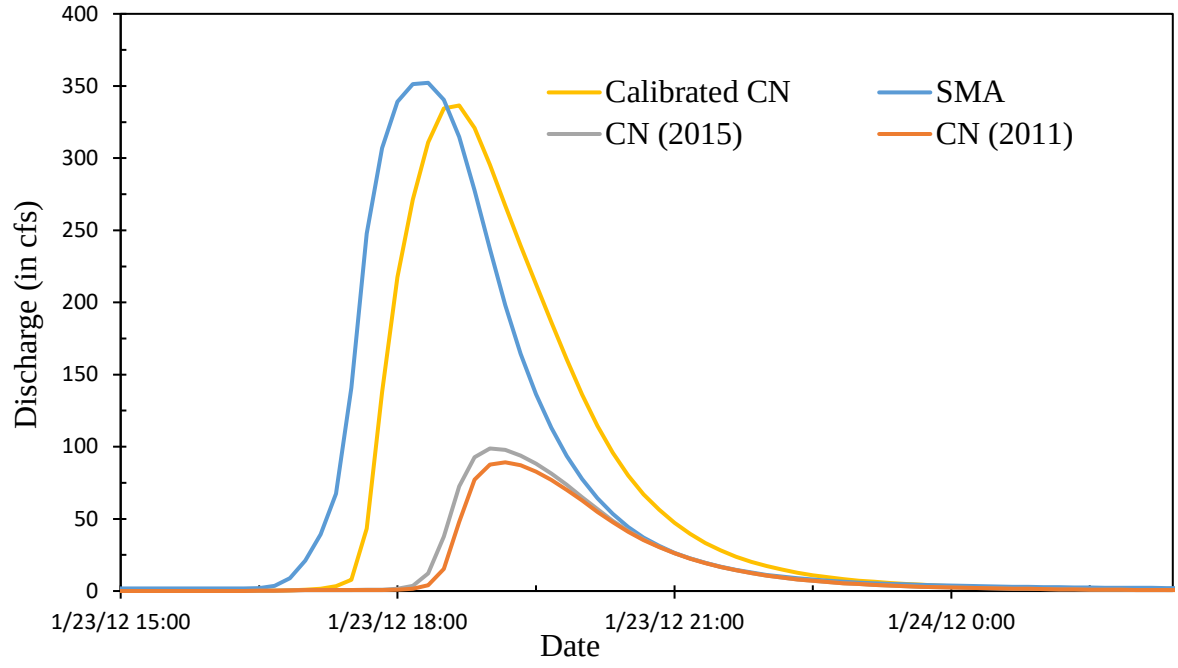

(B)

Figure 5- 18: Comparison of SMA Model with Calibrated CN model for ARC class II condition with Storm Events. Before 2011 (A) and After 2011 (B)

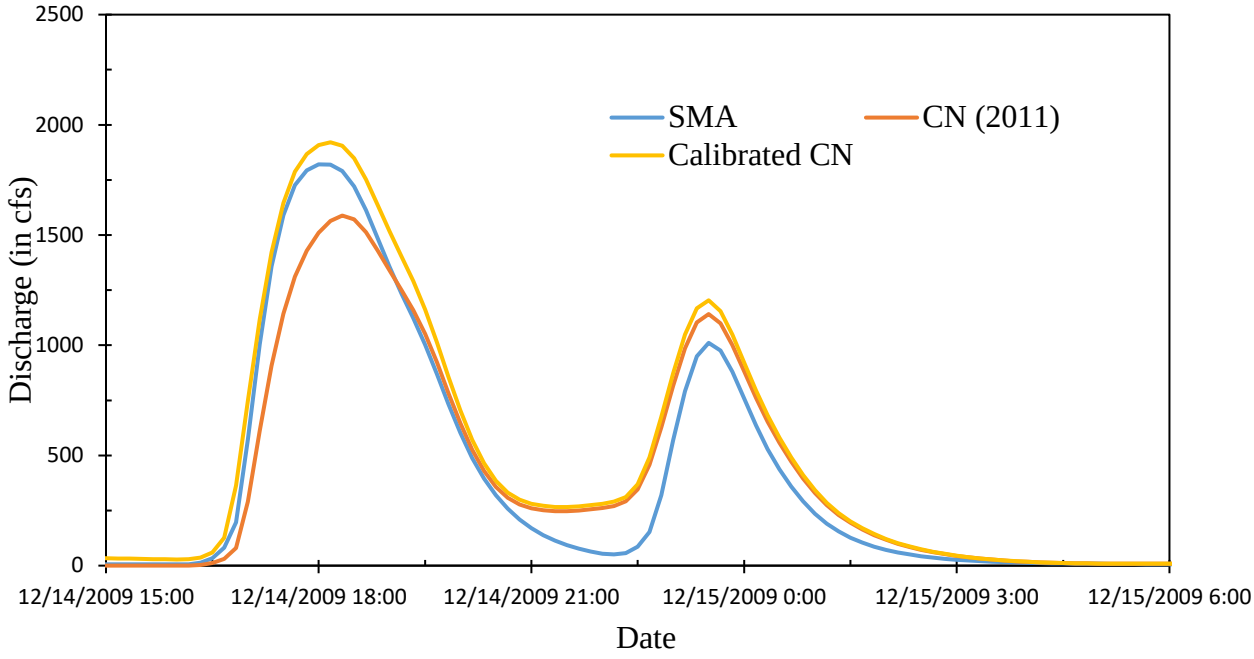

(A)

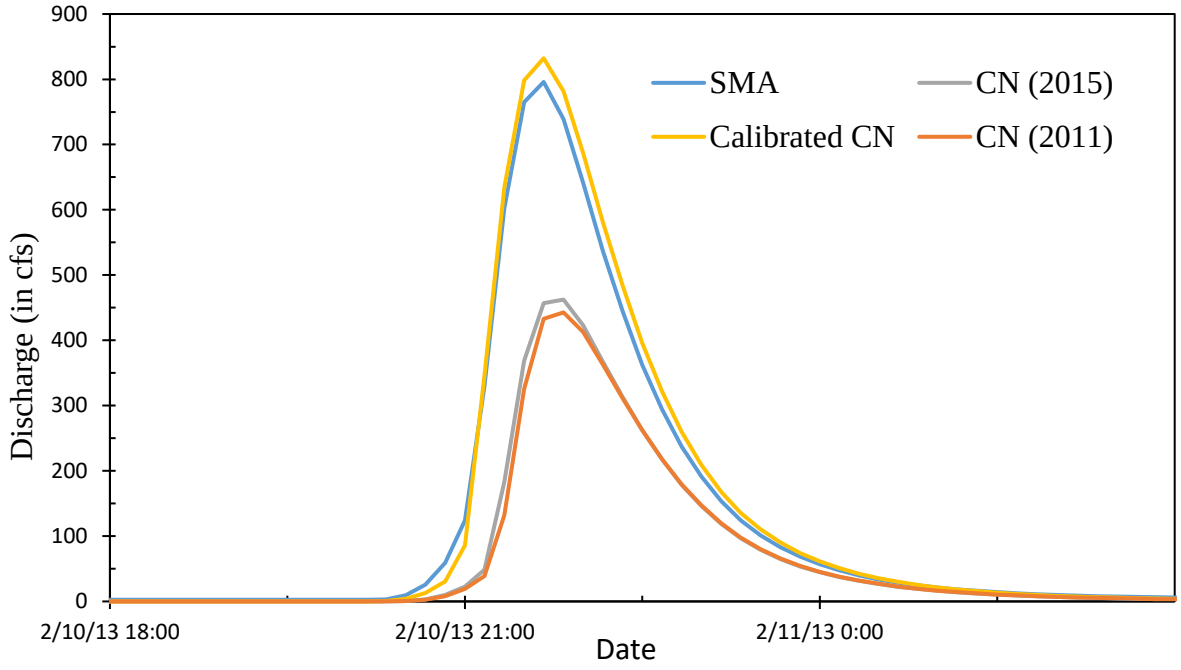

(B)

Figure 5- 19: Comparison of SMA model with Calibrated CN Model for ARC class III Condition with Storm Events. Before 2011 (A) and after 2011 (B)

5.1.4. Sediment yield at Dean Road Bridge

Using the calibrated CN model, sediment yield at the outlet of the Soapstone branch catchment, i.e., Dean Road Bridge was calculated for three different events, i.e., 7th February 2013 (ARC Class I), 23rd January 2012 (ARC Class II), and 10th February 2013 (ARC Class III). For

each event, calibrated CN value and the cover factor of 2011 and 2015 were used to determine the difference in sediment yield due to increasing deforestation and agricultural land expansion in the catchment. Calculation of sediment yield for each event requires the volume of runoff and peak runoff for those events. The value of peak runoff and volume of runoff for each selected event with 2011 and 2015 scenarios is presented in Table 5-12.

Table 5- 12: Peak runoff and volume of runoff for three storm events with 2011 and 2015 scenarios

Event	ARC Class	Rainfall depth (in.)	Rainfall duration (hrs)	2011		2015	
				Peak runoff (cfs)	Volume of runoff (acre-ft)	Peak runoff (cfs)	Volume of runoff (acre-ft)
2/7/2013	I	2.65	11	402.9	83.8	442	92.9
1/23/2012	II	1.34	4	310.7	54.4	336.5	59.2
2/11/2013	III	1.23	1	787.9	98.2	832.2	102.8

Based on the areal average values of K, LS, C, and P factor of the Soapstone branch catchment, sediment yield was calculated for each of the three events listed in Table 5-10. For both 2011 and 2015 catchment condition and the results are shown in Figure 5-20. The sediment yield was estimated to be higher in 2015 due to change of land cover. The increase (%) of sediment yield from 2011 to 2015 was, therefore, calculated and plotted from each event (Figure 5-20). The percentage increase was the highest for the ARC I event, but the sediment yield (in tons) was the highest for the ARC III event.

Furthermore, the sediment yield was also calculated by neglecting the deforestation in the vicinity of stream channel, as shown in Figure 5-21. The sediment yield was the highest for ARC III storm whereas the percentage increase was maximum for ARC I storm condition. Also, it shows that the percentage increase in sediment yield due to other factors is more than 35% from 2011–2015. These increases are due to the fact that other factors such as increase in rangeland area, agricultural area, thinning of forests, etc. had more pronounced effect on producing sediment than the deforestation near stream alone.

The difference between Figure 5-21 and Figure 5-20 gives sediment yield due to the deforestation near stream alone. The major deforestation area estimated from aerial images was 8.4 acres (365973 sq. ft.), which is 1.4 % of the total forest area in the Soapstone Branch watershed and 0.5% of the total watershed area. Estimated stream length in the watershed is about 6.9 km. If we assume the sediment deposition is average 6 ft. in the streams, it has 75010 cubic yards of sediment deposited. During the field visit, it was found that the sediment deposit started much upstream of the river reach nearby the major deforestation and was about 6–7 ft. deep. The field visit along the stream stopped roughly 3 km upstream from the Dean Road Bridge, and no attempt was made to walk further upstream and to determine where the starting point of sediment deposit in the stream was. This indicates the sediment deposit most likely was not due to deforestation alone, which indirectly supports the above finding. Table 5-13 presents the percent change of sediment yield from 2011 to 2015 due to change in different factors viz. runoff energy factor, C factor, etc.

Table 5- 13: Percent changes of sediment yield from 2011 to 2015 due to different factors

Factor	ARC Class I	ARC Class II	ARC Class III
Change of runoff energy factor	11.6	9.6	5.8
Change of C due to all possible changes	95.4	95.4	95.4
Change of C neglecting crop rotation	34.3	34.3	34.3
Change of C neglecting crop rotation and deforestation	29.4	29.4	29.4
Change of C including only deforestation	4.9	4.9	4.9

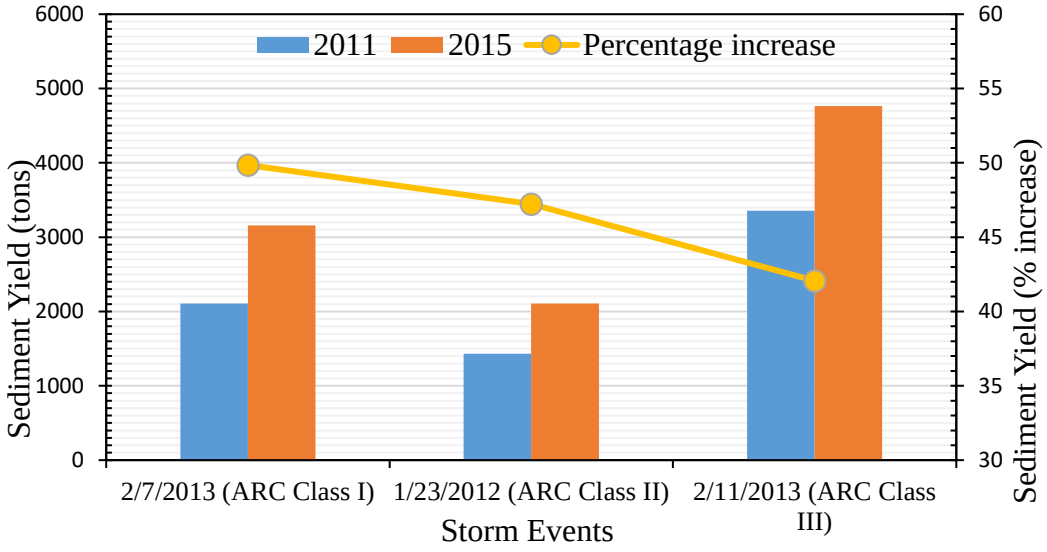

Figure 5- 20: Sediment Yield and Percentage Increase for each ARC Class Condition Storms from the Soapstone Branch Catchment in 2011 and 2015 Scenarios

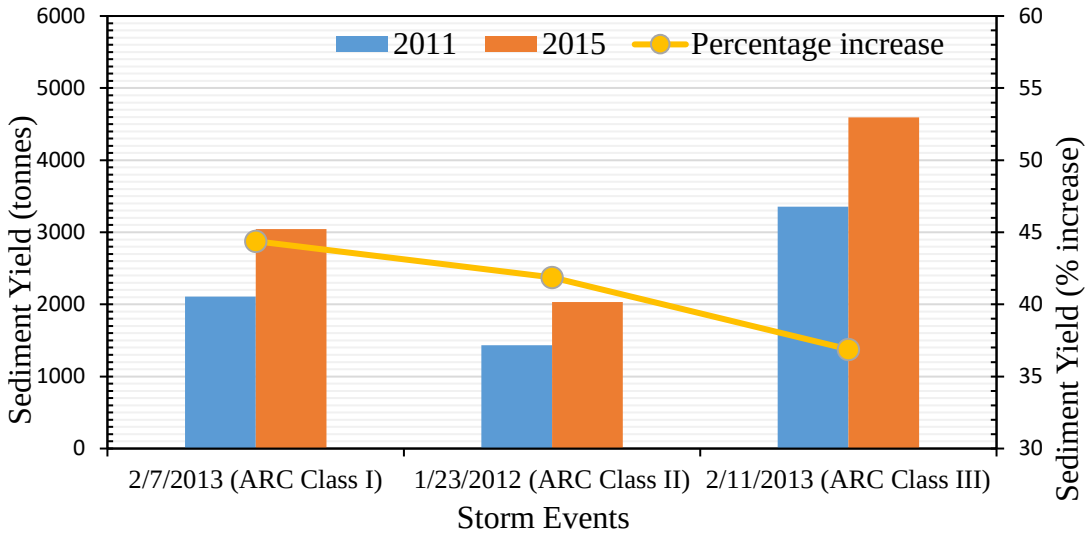

Figure 5- 21: Sediment Yield and Percentage Increase for each ARC Class Condition Storms from the Soapstone Branch Catchment in 2011 and 2015 Scenarios by Neglecting Deforestation

5.2. Hydraulic modeling results

Starting from the hydrological modeling results, the hydraulic modeling of free surface flow intends to assess the ability of modified stream geometries near Dean Road Bridge to transport sediments and avoid aggradation. This is achieved in three steps. Initially, the hydraulic models were assessed in their ability of reproducing stream depth changes based on the HEC-HMS output, which in turn was obtained with rainfall data collected on site. The HEC-HMS outflow hydrographs were used as input data for HEC-RAS 5 or SRH-2D, according to analysis objective. The second step was to focus on studying modeled flow velocity and shear stress results obtained near Dean Road Bridge in its current condition and after a stream modification. Finally, the ability of the proposed stream modification of avoiding sediment retention is tested with the use of hydraulic modeling accounting for sediment transport.

5.2.1. Assessment of model ability to represent hydrographs

HEC-RAS results of depth hydrographs upstream from Dean Road Bridge for two calibration rainfall events are presented in Figures 5-22 and 5-23. Figures 5-24 and 5-25 present the comparable results for the model validation dataset. It is possible to assess that these events have varying intensities, since the stream depth changes ranges from 1.5 ft. up to 4 ft. As pointed earlier, the geometric characteristics of the bridge cross section (Figure 4-18b) were varied to improve the accuracy of peak stream depth representation. Figures 5-22 and 5-23 present the final calibration results using the following channel geometry: Wb = 4 ft., Hb = 0.7 ft., Wh = 60 ft. and n = 0.025 (Figure 4-18b). All validation dataset errors were assessed with this set of parameters.

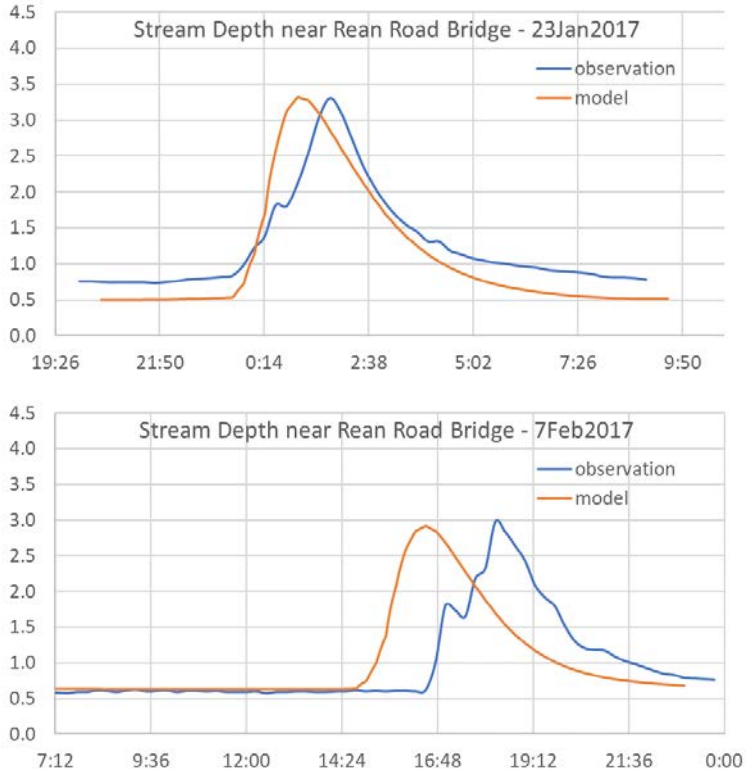

Figure 5- 22: Stream depth hydrographs observed in Soapstone Branch and modeled with HEC-RAS 5 for two calibration rainfall events (1/23 and 2/7/2017) using outflows modeled by HEC-HMS.

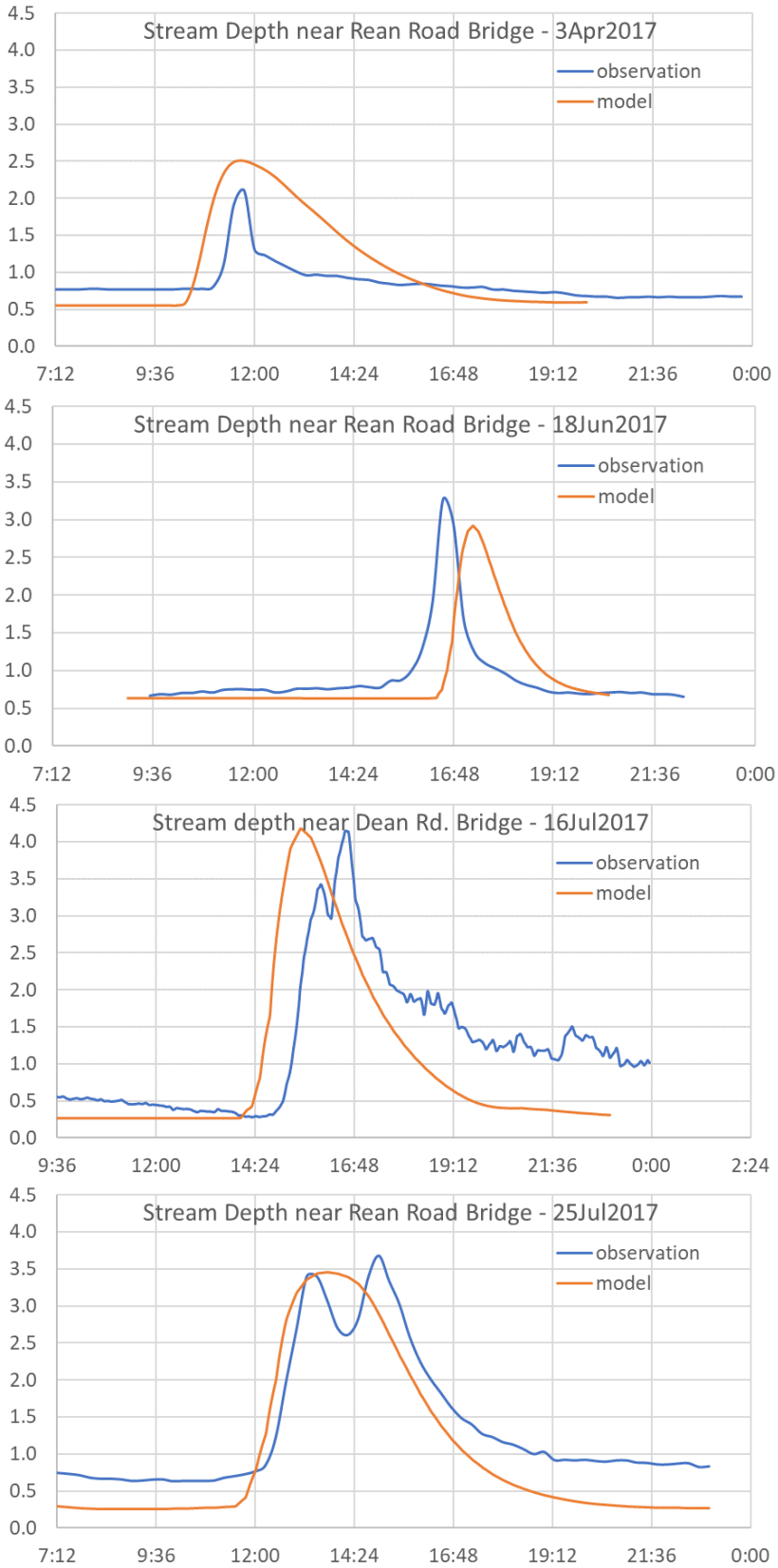

Figure 5- 23: Stream depth hydrographs observed in Soapstone Branch and modeled with HEC-RAS 5 for four calibration rainfall events using outflows modeled by HEC-HMS.

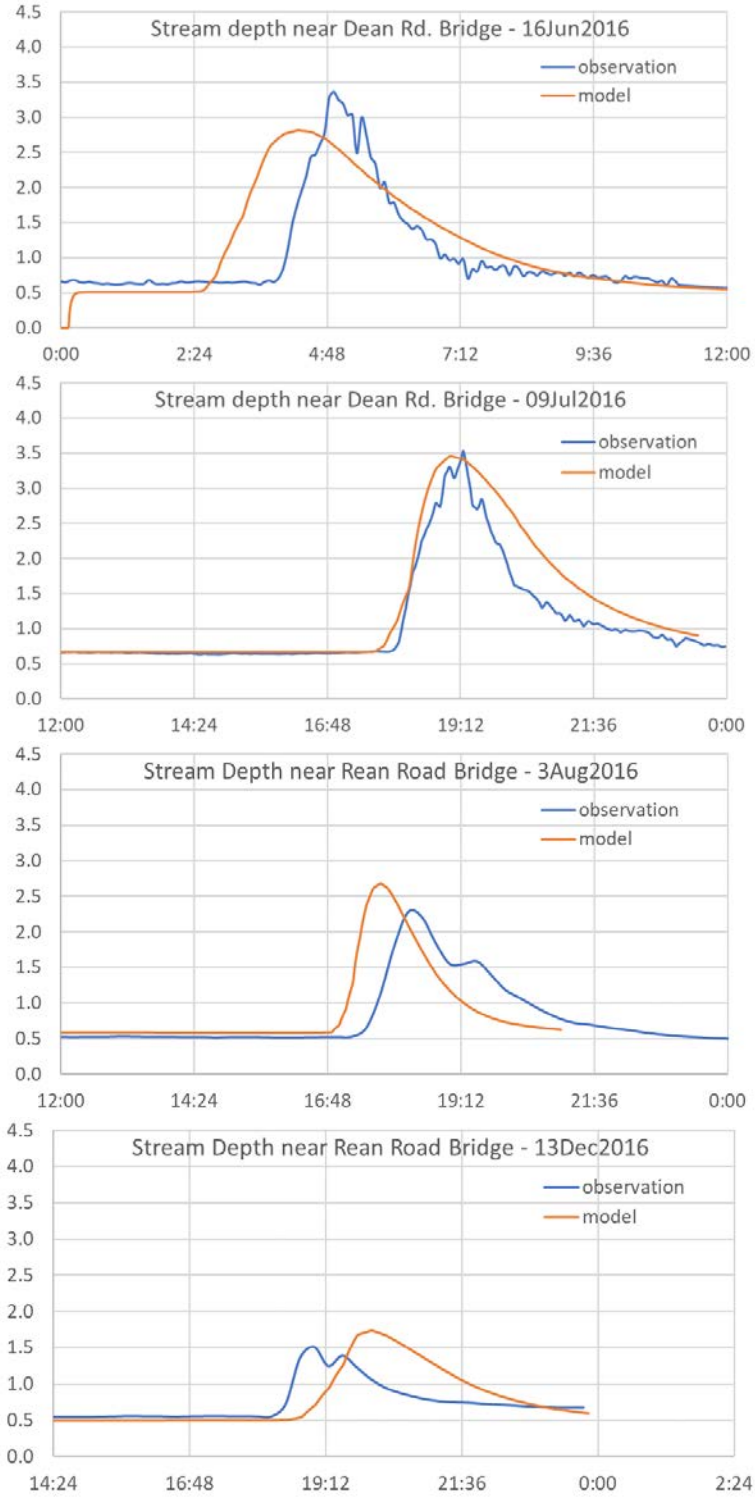

Figure 5- 24: St Stream depth hydrographs observed in Soapstone Branch and modeled with HEC-RAS 5 for four validation rainfall events in 2016 using outflows modeled by HEC-HMS.

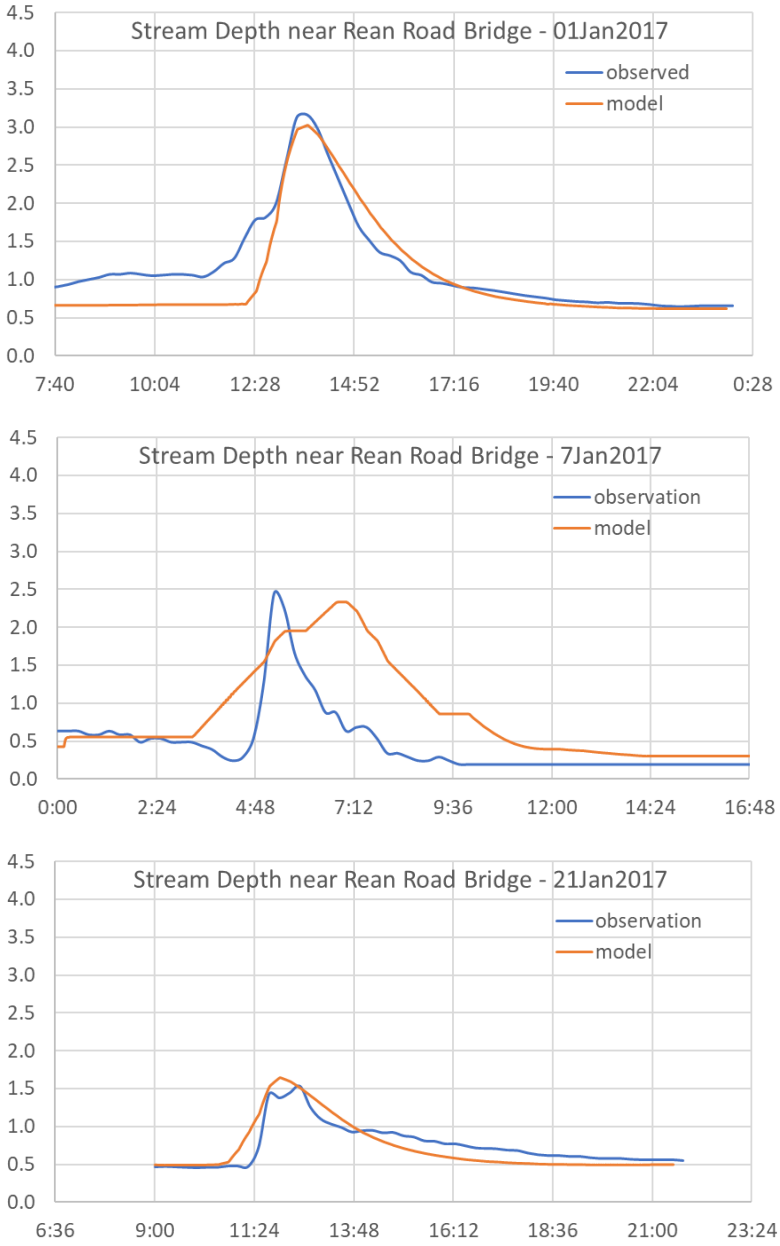

Figure 5- 25: Stream depth hydrographs observed in Soapstone Branch and modeled with HEC-RAS 5 for three validation rainfall events in 2017 using outflows modeled by HEC-HMS.

An evaluation of the modeling results of depth hydrographs indicates that HEC-RAS was in general very accurate in representing the general changes in the stream stage during rainfall events. There is an offset on the observed and simulated peak flow time for some events, but the offset is most likely attributed to inaccuracy of the rainfall-runoff modeling using HEC-HMS such as the amount of rainfall abstraction.

After calibration was concluded, the greatest discrepancy in the peak depth observed in the calibration dataset was 25%, and the average discrepancy was 12%. For the validation dataset, the largest discrepancy was 18%, with an average discrepancy under 10%. Detailed results regarding

the discrepancies in observed and modeled peak flow depth are presented in Table 5-14. Given that the hydraulic model used results from the hydrological model to perform these analysis, it is considered that the modeling calibration and validation was successful.

Table 5- 14: Results of peak flow depth discrepancy between calibration and validation datasets for rainfall events measured at Soapstone Branch Watershed. Depths are considered upstream from the Dean Road Bridge site.

Calibration dataset			
Rain event date	**Measured peak depth (ft.)**	**Modeled peak depth (ft.)**	**Peak flow depth discrepancy**
23-Jan-17	3.3	3.3	0.0%
7-Feb-17	3.0	2.9	3.3%
3-Apr-17	2.2	2.5	13.6%
9-May-17	2.8	2.2	21.4%
18-Jun-17	2.8	3.3	17.9%
16-Jul-17	4.1	4.1	0.0%
25-Jul-17	3.0	3.7	25.4%
Validation dataset			
Rain event date	**Measured peak depth (ft.)**	**Modeled peak depth (ft.)**	**Peak flow depth discrepancy**
16-Jun-16	3.4	2.8	17.6%
9-Jul-16	3.6	3.5	2.8%
3-Aug-16	2.4	2.7	14.9%
13-Dec-16	1.8	1.6	10.9%
1-Jan-17	3.2	3.0	6.3%
7-Jan-17	2.5	2.3	8.0%
21-Jan-17	1.6	1.6	4.5%

5.2.2. Velocity and shear stress results at Soapstone Branch pre and post stream modification

One of the key objectives of this research is to assess whether a solution, other than bridge replacement, can be applied to solve the aggradation issue created by the sediment being transported by Soapstone Branch to Dean Road Bridge. The previous section demonstrated that the hydraulic modeling was successful in representing the flow conditions upstream from the bridge after calibration steps were concluded. This section will perform calculations associated with the shear stress in Soapstone Branch at this present condition, and compare with the shear stress values that would be anticipated with the changing the stream cross section near the bridge, also referred to as stream modification approach.

The proposed stream modification involves using a 2-ft deep, 20-ft wide trapezoidal cross section under the bridge. Upstream from the bridge the stream bed slope is 1%, and after the bridge the slope is 0.10%, with a total length of 240-ft of stream modified. The overarching idea is to

facilitate sediment discharge across the bridge through steeper slope as Soapstone Branch approaches the crossing, and flatter slope downstream from the bridge. With this approach the intervention (stream modification) of channel cross sections in the Soapstone Branch would be limited to the vicinity of the Dean Road Bridge, as is shown in Figures 5-26 to 5-28.

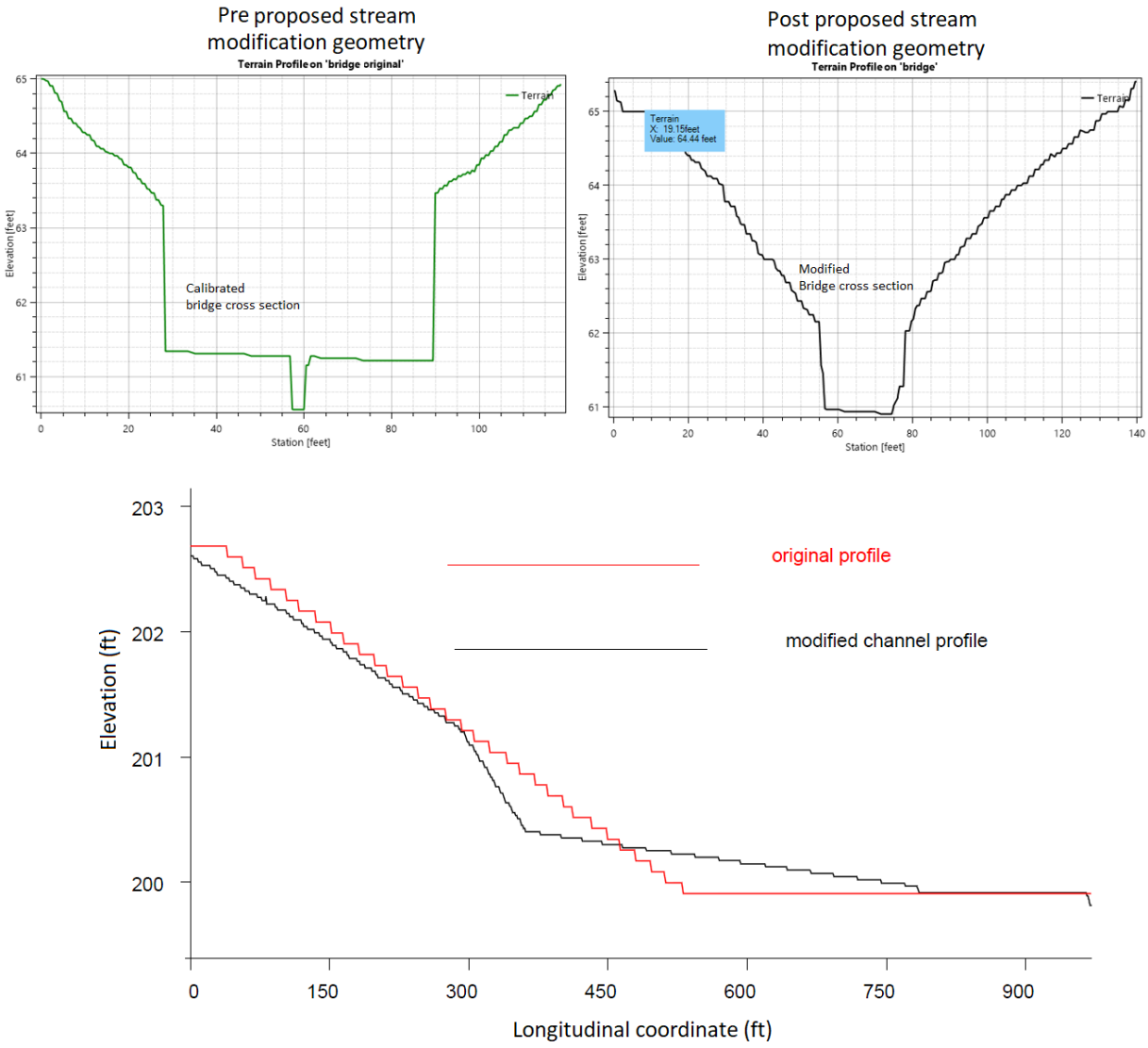

Figure 5- 26: Soapstone Branch cross section under Dean Road Bridge prior to stream modification (top) and after (middle). The new stream profile (bottom) indicates a steeper profile near the Dean Rd. Bridge crossing.

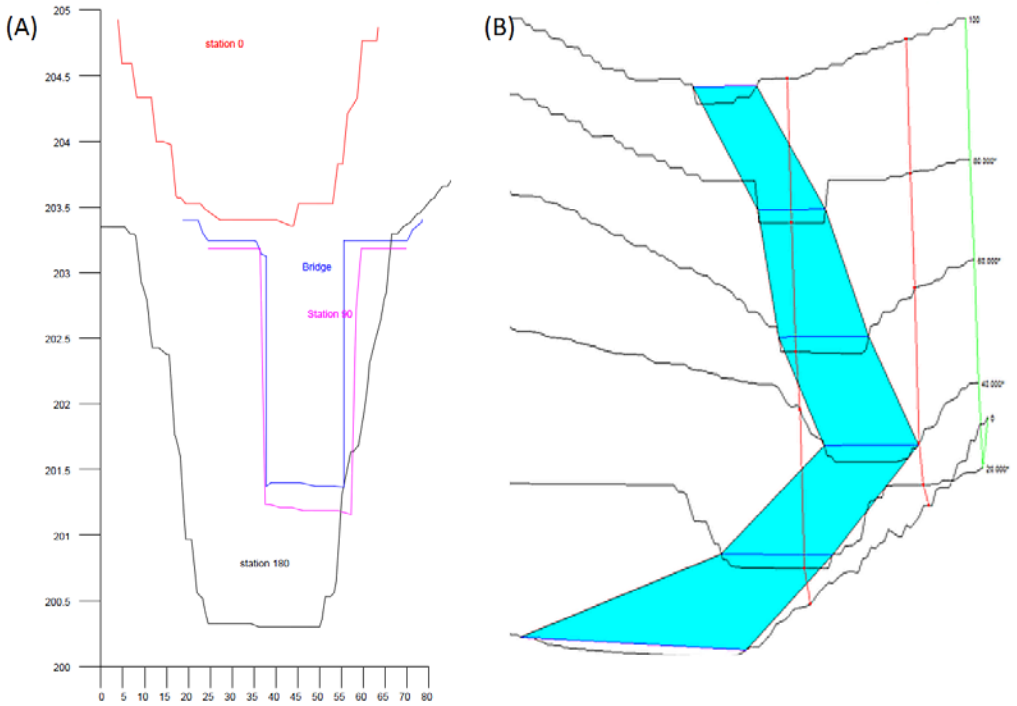

Figure 5- 27: Cross sections of the modified Sopastone Branch (A), and Perspective of flow in Soapstone Branch in the post modification cross section near the bridge site, modeled by HEC-RAS 5 (B).

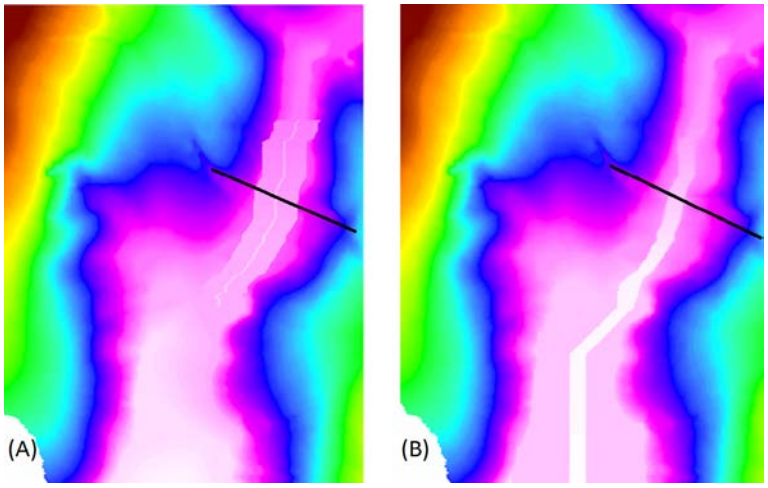

Figure 5- 28: Changes in Soapstone Branch elevation map prior to stream modification (A) and after (B). An more streamlined pathway for sediment discharge is noticed after the modification.

In order to address whether aggradation issue can be mitigated with stream modification, it is necessary to ensure calculate shear stresses in the bottom of the stream for both pre and post-modification scenarios. It is important that the stream modification strategy to result in shear stress levels that are consistently higher than the level that are currently observed in Soapstone Branch. Figures 5-29 to 5-31 present a 2-D representation of the bottom shear stress calculated with the model HEC-RAS 5 for one of the intense rain events (July 9, 2016) that was monitored in Soapstone Branch.

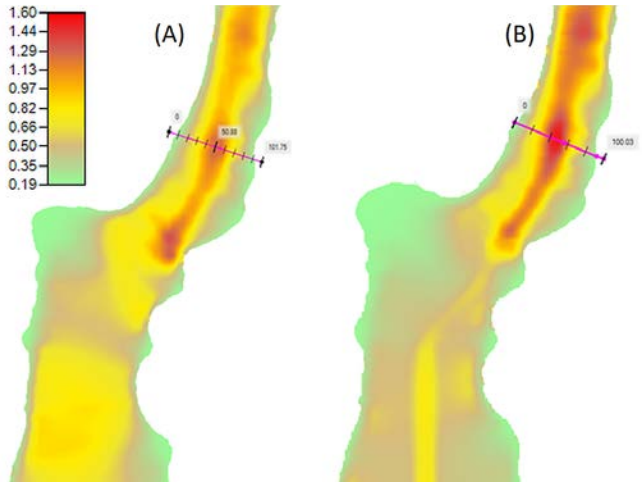

Figure 5- 29: Shear Stress results (in Pascal) at the bottom of the Soapstone Branch in the peak flow for the 7/9/2016 event for pre-stream modification (A) and post stream modification scenarios.

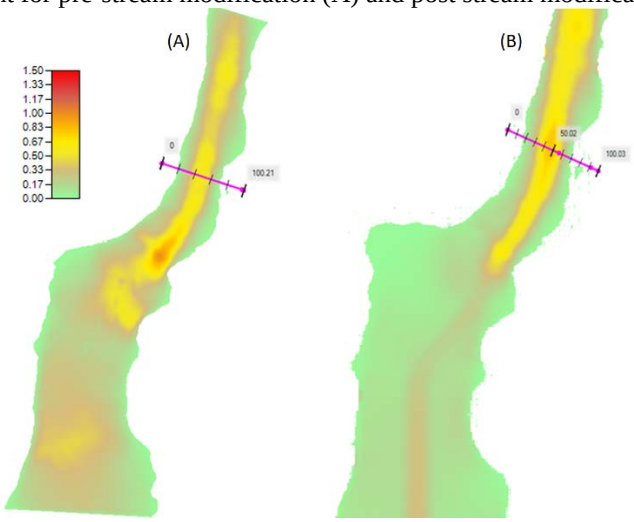

Figure 5- 30: Shear Stress results (in Pascal) at the bottom of the Soapstone Branch for 50% of the peak flow for the 7/9/2016 event for pre-stream modification (A) and post stream modification scenarios.

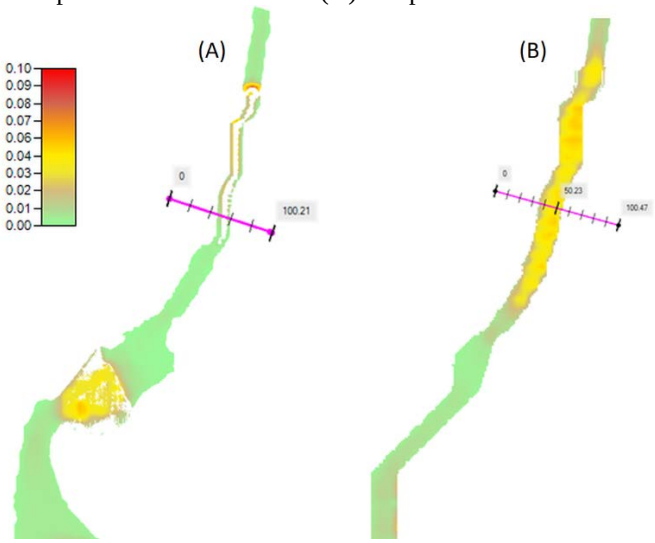

Figure 5- 31: Shear Stress results (in Pascal) at the bottom of the Soapstone Branch for the base flow conditions (1.4 cfs) for pre-stream modification (A) and post stream modification scenarios.

It is noticed that the stream modification alternative increases shear stresses in all three stages Three different conditions are represented in these figures: peak flow conditions (Figure 5-29), 50% peak flow conditions (Figure 5-30) and base flow conditions (Figure 5-31), with current conditions represented with the letter (A), and letter (B) referring to post stream modification conditions. For the flood event, particularly in the vicinity of Dean Road Bridge, which is marked with a magenta line. Most importantly, shear stress levels are higher for the base flow conditions (1.4 cfs), which indicate the ability of the stream modification to allow passage of existing sediment across the bridge even with low flows

While shear stress is a fundamental variable to be studied in this evaluation of sediment motion near Dean Road Bridge, another important assessment would be the actual calculation of sediment motion near the bridge crossing for both pre and post stream modification scenarios. There is a practical difficulty, however, posed by the model used thus far. HEC-RAS 5 is unable as of today (August, 2018) to simulate sediment motion in streams. This research has thus opted to adopt another entirely different model, SRH-2D, developed by the US Bureau of Reclamation, to perform 2-D river flow modeling alongside with sediment motion.

However, prior to start these calculations, it was first necessary to ensure that SRH-2D model results are consistent with the calculated results obtained from HEC-RAS. The mesh generation process for SRH-2D, described in chapter 4, yielded a mesh size that was consistent in dimensions with the HEC-RAS 5 model. Also, the inflow information and boundary conditions adopted in SRH-2D matched the same ones used in the HEC-RAS model. Yet, such assessment is necessary to ensure the validity of calculations. The comparison indicated that the model results were very consistent. As is shown in Figure 5-32, for the 7/9/2016 flood event, depth and velocity predicted by both models near the bridge site are very much in agreement. Moreover, shear stress results for the post stream modification obtained between HEC-RAS and SRH 2D indicate that shear stress levels are in the same range, albeit SRH-2D predicts higher shear levels downstream from the bridge when compared to HEC-RAS. This can be viewed in the results for the 7/9/2016 flood event presented in Figure 5-33 (100% of the peak flow), Figure 5-34 (50% of the peak flow) and in base flow conditions, shown in Figure 5-35. Such consistency enabled the continuation of modeling assessments with focus on sediments to using the SRH-2D model, which is the focus of the next subsection.

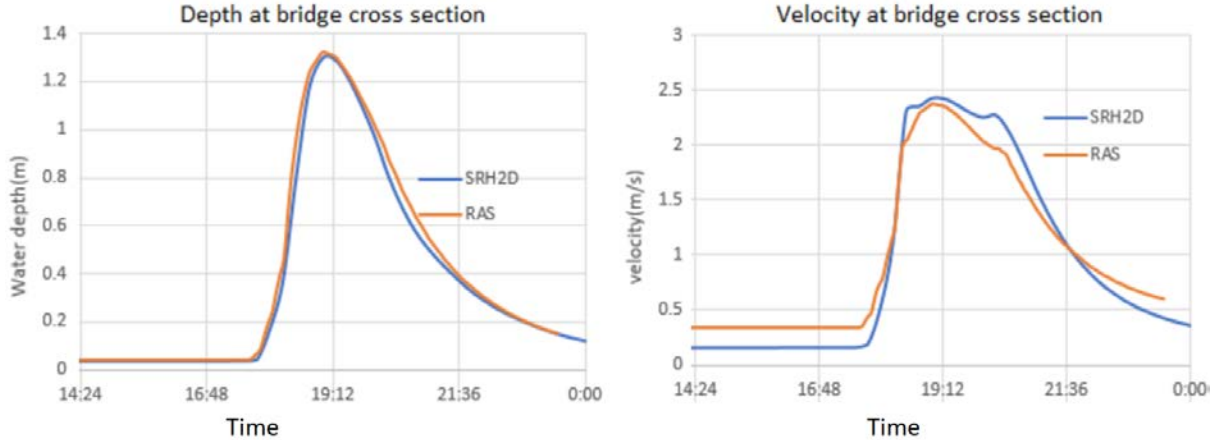

Figure 5- 32: Comparison between the stream flow depth and velocity calculated at the Dean Road Bridge cross section for the 7/9/206 rain event by HEC-RAS 5 model and SRH-2D model.

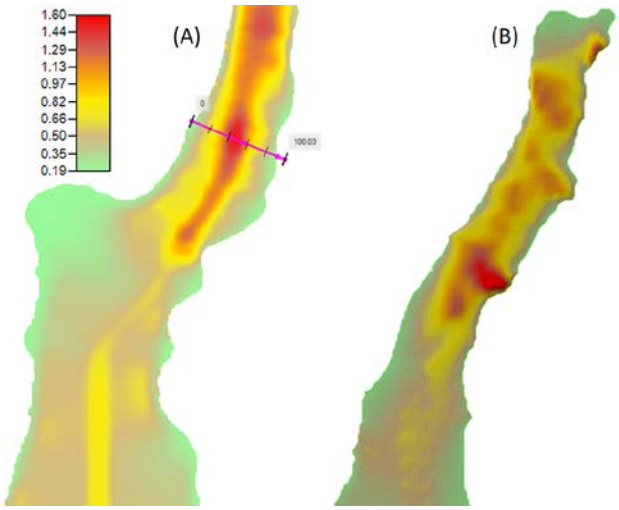

Figure 5- 33: Comparison between the shear stress in Soapstone Branch for the 7/9/206 rain event, at the peak flow conditions, by (A) HEC-RAS 5 model and (B) SRH-2D model.

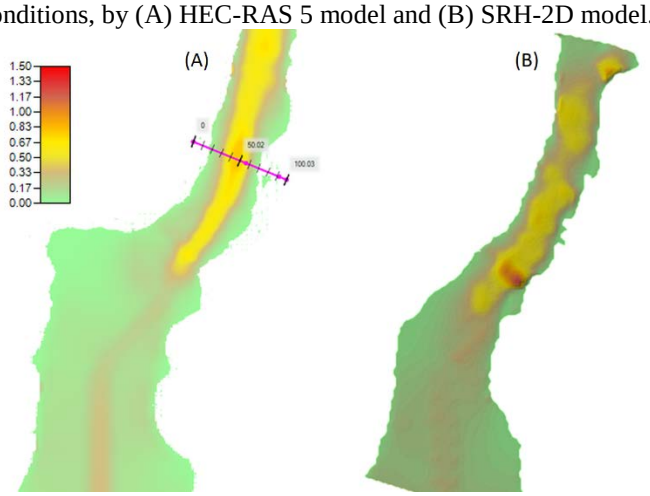

Figure 5- 34: Comparison between the shear stress in Soapstone Branch for the 7/9/206 rain event, at 50% of the peak flow conditions, by (A) HEC-RAS 5 model and (B) SRH-2D model.

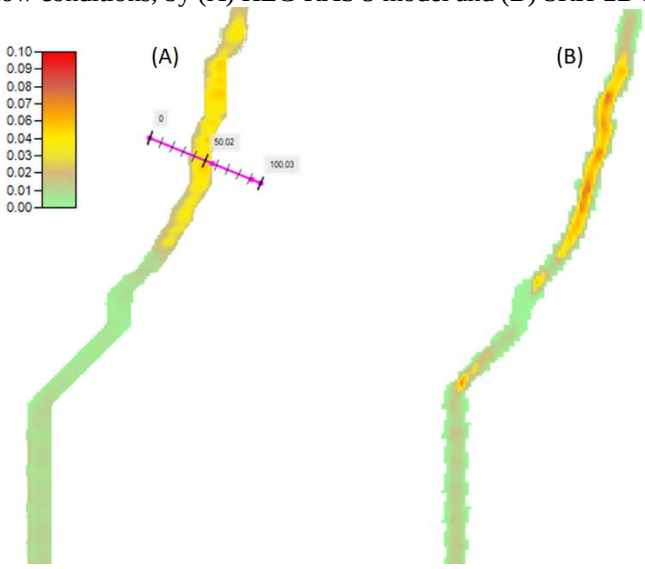

Figure 5- 35: Comparison between the shear stress in Soapstone Branch for the 7/9/206 rain event, at base flow conditions (1.4 cfs), by (A) HEC-RAS 5 model and (B) SRH-2D model.

5.2.3. Calculations of sediment transport in Soapstone Branch by SRH-2D model

All SRH-2D simulations presented in the previous subsection assumed stable stream beds, which is not the case when sediment transport occurs in the stream. To enable the calculation of sediment discharges, SRH-2D requires information of sediment loading in the upstream boundary condition.

During the field data collection phase, samples of stream flow were collected for different rain events. This enabled to correlate stream turbidity along with values of total suspended solids concentration (TSS, expressed in mg/L), each associated with observed stream depths. With stream depth measurements and flow rate results of numerical modeling, it was possible to correlate the observed TSS with varying stream flow values. From this correlation, a TSS-flow expression was developed, based on the field observed values. Values shown in Figure 5-36 indicate that the assumed TSS-flow expression is more conservative than the observed TSS-flow values. The idea is that such correlation could represent other conditions of sediment inflow in Soapstone Branch that are more intense than the ones observed.

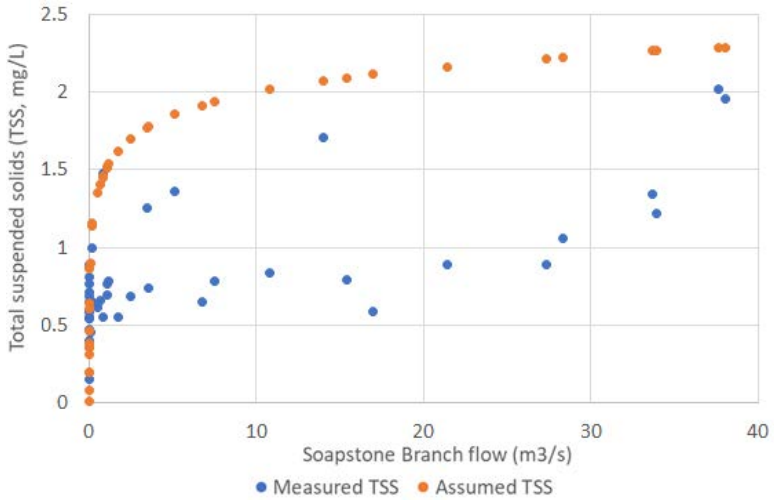

Figure 5- 36: Sediment discharge curve assumed for Soapstone Branch used in the simulation results, derived from the TSS-flow relationship measurements in this research and used in SRH-2D modeling.

Through appropriate conversion, and assuming sediment density as 2,650 kg/m^3, another relationship expressing sediment volumetric flow rate in terms of the stream flow rate was derived for Soapstone Branch. This expression, presented in Figure 5-37, is needed by SRH-2D to perform sediment concentration. Another information that is needed is the particle size distribution for the site, which is presented in Figure 5-38. There is a degree of estimation in sediment discharge given that direct measurement of this parameter was not included in the original project scope.

The assessment of sediment aggradation process was based on a 30.5-day long simulation performed in SRH-2D. This simulation had 2 stages, with separate goals:

- First, it was intended to consider an initial 30 days of the simulation assuming base flow conditions at 1.4 cfs (0.040 m^3/s), associated with low sediment inflows. The goal of this part of the simulation was to verify whether in extended low flow conditions if there would be a long-term tendency of sediment build up near the bridge site, according to the SRH-2D simulation results.

- After this 30-day period, it was assumed that Soapstone Branch would undergo 12-hour of high flow condition associated with a rain event that creates a 25-year return period flow. The rain event that was recorded in July 9, 2016 created a peak flow of 37 m^3/s, or 1,307 cfs. According to Streamstats program (USGS, 2016), this event has an intensity similar to an event with a 25-year return period, as indicated in Table 5-15. The goal of this second stage was to assess how sediment distribution would change as result of a large rain event occurring in Soapstone Branch watershed.
- Finally, another 30-day period of base flows was simulated to evaluate the tendency of the stream to recover from the morphologic changes created by the intense rain event.

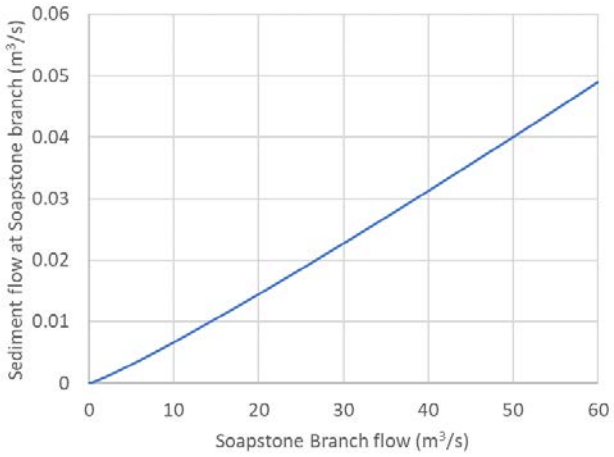

Figure 5- 37: Sediment discharge curve assumed for Soapstone Branch used in the simulation results, derived from the TSS-flow relationship measurements in this research and used in SRH-2D modeling.

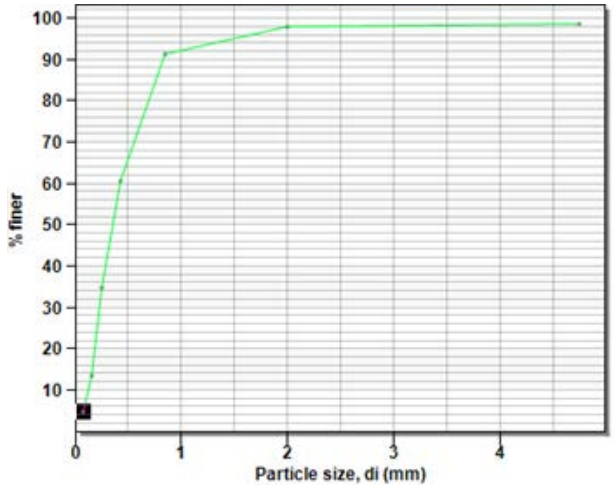

Figure 5- 38: Particle size distribution representative of sediment transported in Soapstone Branch used in SRH-2D modeling.

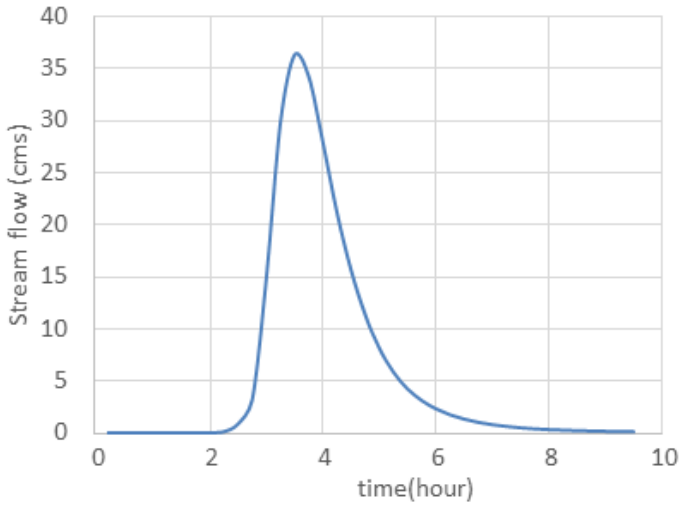

Figure 5- 39: Inflow hydrograph for the 7/9/2016 rain event, with an intensity similar to a 25-yr return period event, and used for the sediment transport assessment with SRH-2D. From 10 to 12 hours, not shown in the graph, flows are near base flow conditions.

Table 5- 15: Streamstats results for Soapstone Branch peak floods for varying return periods. The 25-year flood is similar to the intensity recorded in the July 9, 2016 rain event.

PII: Prediction Interval-Lower, Plu: Prediction Interval-Upper, SEp: Standard Error of Prediction, SE: Standard Error (other -- see report)

Statistic	Value	Unit	SE	SEp	Equiv. Yrs.
1.5 Year Peak Flood	302	ft^3/s	37	37	4
2 Year Peak Flood	394	ft^3/s	33	33	5
5 Year Peak Flood	710	ft^3/s	26	26	11
10 Year Peak Flood	963	ft^3/s	24	24	18
25 Year Peak Flood	1330	ft^3/s	25	25	26
50 Year Peak Flood	1640	ft^3/s	27	27	28
100 Year Peak Flood	1980	ft^3/s	29	29	28
200 Year Peak Flood	2340	ft^3/s	33	33	27
500 Year Peak Flood	2860	ft^3/s	37	37	26

The initial conditions of the simulation (T=0 day), expressed in terms of the stream bed elevation, is presented in Figure 5.40A. Following this initial condition, 30 days of a based flow was assumed to occur. Figure 5.40B presents the same region after 30 days of the base flow (1.4 cfs). The only significant change observed in these days was due to the increased flow velocity downstream from the modified stream near the bridge. This higher velocity resulted in a ripple pattern aligned with the flow direction downstream from the modified stream. But there is no systematic increase in stream bed elevation near the bridge crossing. Figures 5-40C and 5-40D present results 4 hours and 8 hours into the intense rain event that occurs in the simulation after the 30-day base flow period. Results indicate that during the 12 hours very significant changes in stream bottom elevation on Soapstone Branch can occur, but not influence the locations near the bridge or the modified stream.

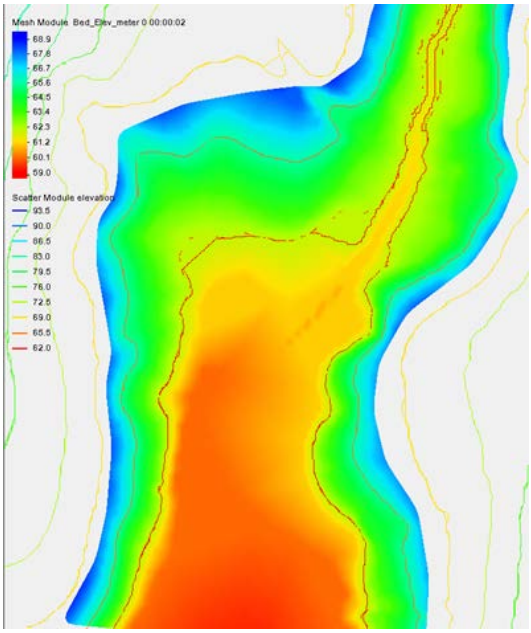

(A) Simulation Start (day 0)

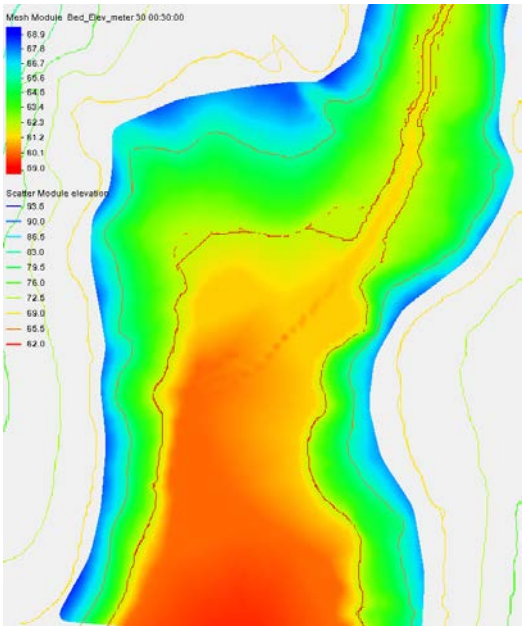

(B) After 30 days of Base flow

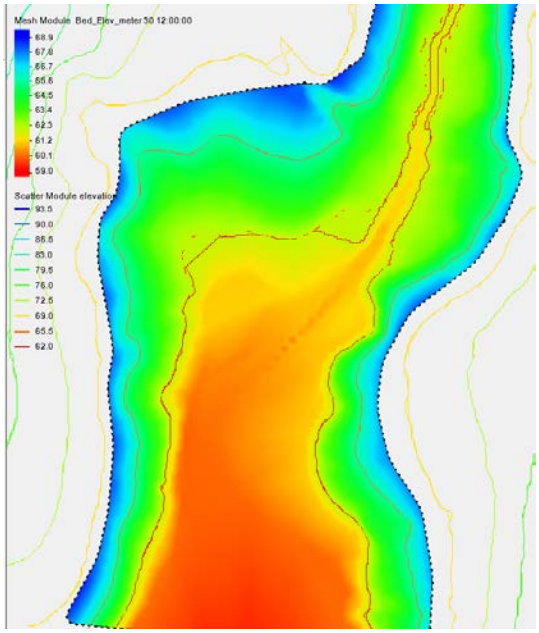

(C) After 30 days, 4 h into the7/9/2016 event

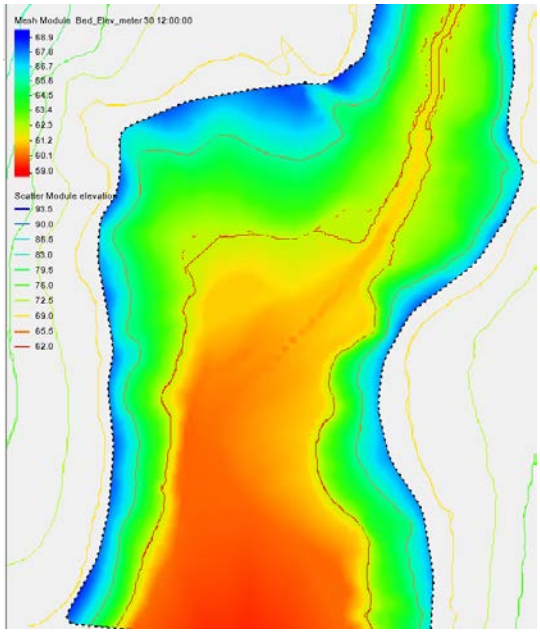

(D) After 30 days, 8 h into the 7/9/2016 event

Figure 5- 40: Predicted streambed elevations yielded by SRH-2D model for a 30.5 day long simulation at various times, from the beginning of the simulation, into 30 days of base flow, and then in two instants after a 12-hour long intense rain event that happened in 7/9/2016.

Figures 5-41 and 5-42 present the incremental changes in bed elevation observed for the 30-day period of base flow or the 12-hour long intense hydrograph, respectively. Values correspond to decreased depth (scour) and red to aggradation. These results show development of sand dunes upstream from the bridge, with stream bed scour to 0.40 m and aggradation to 0.15 m

in the stream bed channel over the 30-day period. After the large rain event, there is some aggradation upstream from the stream modification site, typically under 15 cm. Downstream from the bridge site, the steeper slope created conditions for sediment flushing, and minor scour (under 9 cm) resulted from the large rain event. Following this intense rain event, the model results of an additional 30-day period of base flow, shown in Figure 5-43, show that scour holes are gradually filling up, and aggradation levels are preserved, but not aggradation in the bridge is not observed.

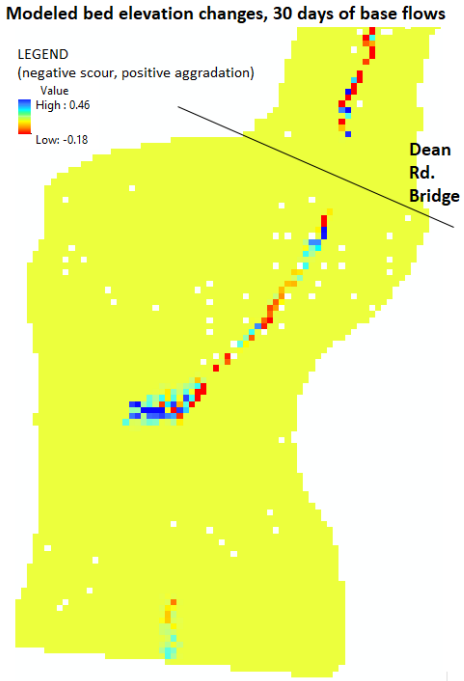

Figure 5- 41 Predicted incremental changes for Soapstone Branch during 30 days of base flow conditions. Red is aggradation, green is scour with respect to original elevation (T=0 days).

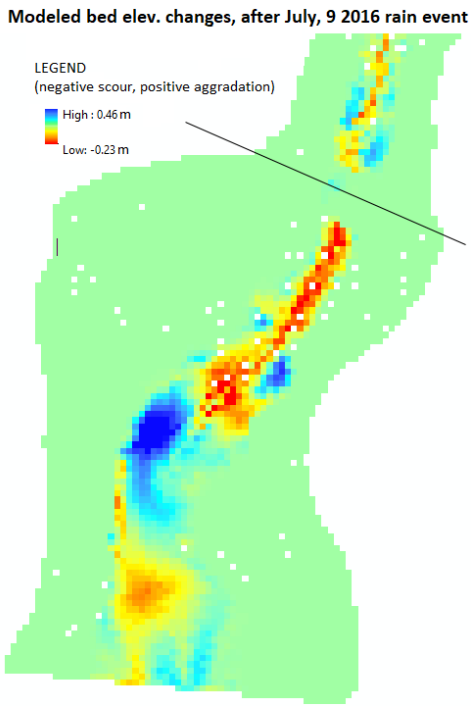

Figure 5- 42: Predicted incremental changes for Soapstone Branch during a 12-h period after the 7/9/2016 rain event. Red correspond to aggradation, green is scour with respect to original elevation (T=0 days).

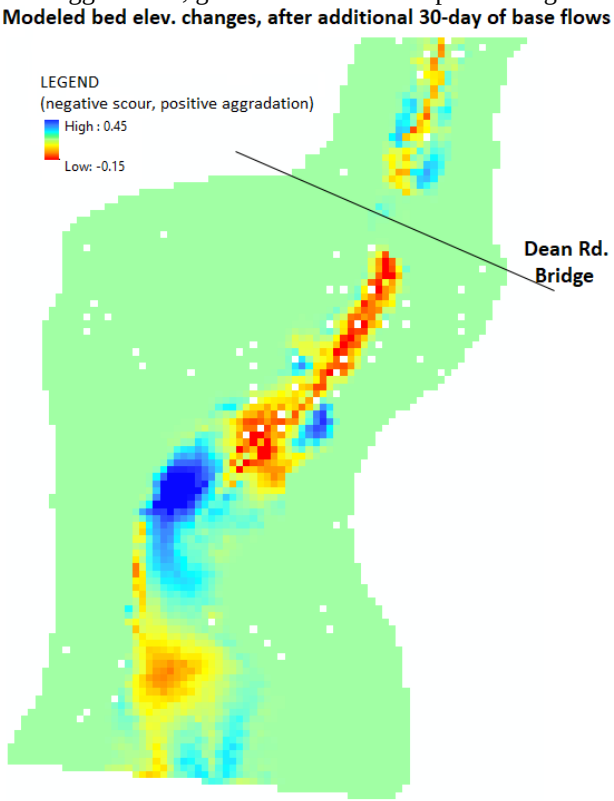

Figure 5- 43: Predicted bed elevation changes for Soapstone Branch after the 7/9/2016 rain event and after another 30 days of base flow. Red correspond to aggradation, green is scour with respect to original elevation (T=0 days).

Figure 5-44 presents the results from 3 points selected downstream from the stream modification region to show the evolution of the elevation changes during the 12 hours of the intense hydrographs. Changes in points A, B and C indicate that scour and aggradation can occur simultaneously, and that most of the observed changes take place as the flow intensity in the stream increased to a maximum, from 6 to 10 hours of the hyetograph.

In summary, these results indicate that the stream modification can be an effective strategy in pushing sediments from the location where the bridge is, creating a region with minor scour downstream from the modified stream. The minor aggradation upstream from the bridge occuring during base flows is likely to be removed with the tendency for scour during base flow conditions. Provided that the sources for sediment upstream from Soapstone Branch can be reduced or mostly eliminated, a solution based on stream modification could be successful.

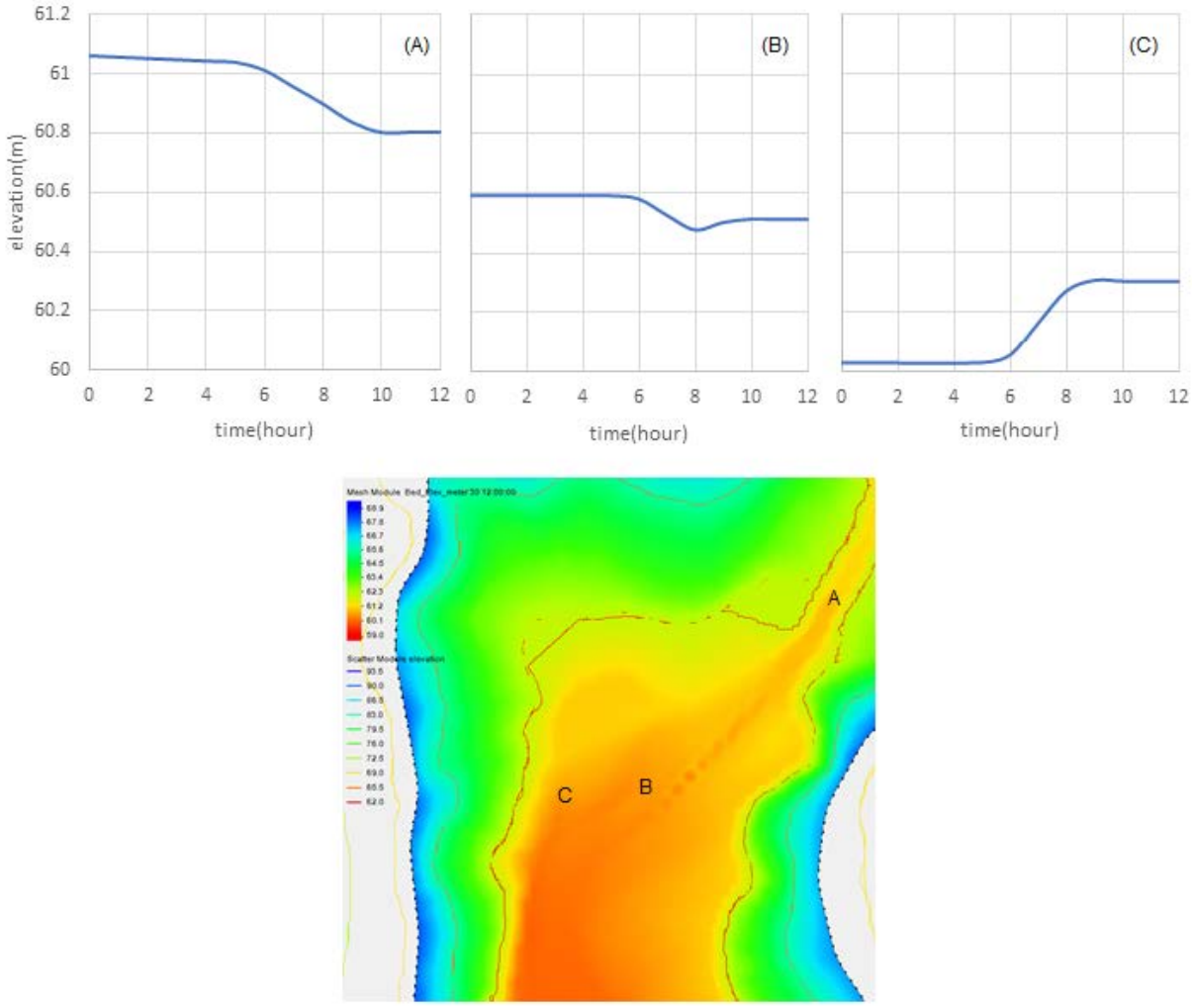

Figure 5- 44: Evolution of stream bed elevation for points A, B and C located downstream from the stream modification region of Soapstone Branch.

5.2.4. Latest changes in Dean Road Bridge and related numerical modeling

During September 2018 the research team returned to Soapstone Branch watershed one last time to retrieve the sensors used in the investigation and determined that a temporary steel bridge has been placed immediately downstream from the existing Dean Road Bridge. This bridge was placed at a higher elevation, following a sequence of rain events that damaged further the old Dean Road Bridge over Soapstone Branch. This temporary bridge, constructed in a steel, is presented in Figure 5-45.

Figure 5- 45: Temporary steel bridge placed in parallel to the old Dean Road Bridge over Soapstone Branch.

It was determined that the bridge is supported directly on the two embankments that were constructed to a higher grade elevation, enabling the structure to avoid immediate overtopping. The embankments are fitted with riprap to difficult the erosion created by the Soapstone Branch peak flows. These embankments create a contraction to Soapstone Branch geometry that was not considered in previous modeling efforts. Thus a new group of numerical simulations were added to this research effort, also using SRH-2D.

This new SRH-2D model was built with field estimates of the new bridge geometry. The bed elevation of the channel bank right downstream of the channel is raised 8ft higher than the original elevation and was set to be unerodable. The bottom width of the main channel was assumed as 30-ft wide, and side slopes were assumed as 1V:2H. The inflow conditions assumed for the 50-year rain event in subsection 5.2.3 were repeated for this simulation. The simulation result shows that there may be aggradation at east side of the channel and a small amount of scour the west side of the channel. Following a 25-year return period rain event, this aggradation may amount to 15 cm, with a corresponding scour of 2 cm, as is illustrated in Figure 5-46.

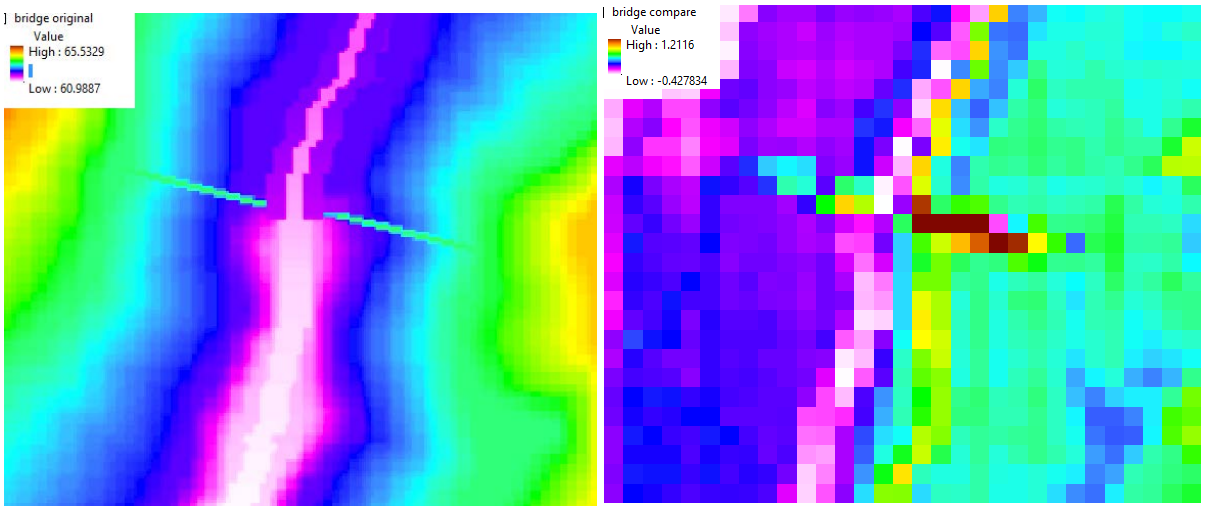

(A) (B)

Figure 5- 46: (A) New terrain elevation (estimated) near Dean Road bridge; and (B) change in stream level due to scour (negative) and aggradation (positive) resulting from the temporary steel bridge construction. East embankment results shows aggradation, while west embankment shows scour.

Signs of this aggradation process are actually already observable in that there is an accumulation of sediment in the east bank, downstream from the bridge, as is shown in Figure 5-47. This bank is approximately already 1 ft above the water level in the stream. In Figure 5-47 this bank presents a breach, which is caused by the discharge of stormwater drainage flows from the east part of Dean Road. To some extent, this outcome is expected given that a needed change in the stream bed slope, to help flush sediments away from Dean Road bridge, was not performed with the construction of this temporary bridge.

This actually, is another source of potential problems in this temporary steel bridge solution. There are clear signs of erosion in the bridge approaches, particularly the one in the east end of the bridge. Moreover, a culvert discharging stormwater flow from Dean Road without proper energy dissiparion is eroding the newly built approaches for the temporary steel bridge, as is shown in Figure 5-48. Without immediate intervention in the bridge this erosion process will continue and may compromise the integrity of the bridge and lead to a catastrophic failure.

Figure 5- 47: Aggradation signs on the east side of Soapstone Branch, downstream from temporary steel bridge

Figure 5- 48: Surface erosion in the eastern embankment and erosion created by stormwater flows from Dean Road, creating slope failures immediately upstream from the temporary steel bridge.

6. Permitting considerations related to Soapstone Branch and Dean Road Bridge conveyance improvements

Section 404 of The Clean Water Act established a federal regulatory program designed to protect Waters of the U.S. The Clean Water Act delegates oversight authority to the Environmental Protection Agency (EPA) and day-to-day management authority to the U.S. Army Corps of Engineers (USACE) to regulate Waters of the U.S.

If a project includes proposed actions deemed to be "placement of dredged or fill material" in Waters of the U.S., a Section 404 permit must first be obtained from the USACE. Placement of fill has been interpreted by the USACE and the courts to include a broad category of impacts not limited to filling activities. Other activities considered to be impacts include construction of culverts, draining, and soil disturbance.

6.1. Waters of the U.S.

The Clean Water Act addresses a variety of categories of waters. In the project area, the pertinent types are wetlands and streams.

6.1.1. Wetlands

Jurisdictional wetlands may be identified by the methodology presented in the Corps of Engineers Wetlands Delineation Manual (1987). This manual defines wetlands as:

> "Those areas that are inundated or saturated by surface or ground water at a frequency and duration sufficient to support, and that under normal circumstances do support a prevalence of vegetation typically adapted for life in saturated soil conditions. Wetlands generally include swamps, marshes, bogs, and similar areas."

The 1987 Manual specifies a three-parameter approach for the identification of wetlands. Wetlands must be dominated by hydrophytic vegetation, have hydric soils, and exhibit defined wetland hydrology. Methodology and indicators for each of the three parameters is contained in the manual. The "Regional Supplement to the Corps of Engineers Wetland Delineation Manual: Atlantic and Gulf Coastal Plain Region (Version 2.0)" (2010) provides supplemental information applicable to the subject area.

6.1.2. Streams

Unlike the identification of wetlands, there is not comprehensive guidance for the identification of jurisdictional streams. In order to be considered a jurisdictional stream, a drainage feature must exhibit the following three criteria:

1. Defined Bed
2. Defined Banks
3. Ordinary High Water Mark

Soapstone Branch exhibits all 3 of these characteristics and is a jurisdictional stream. During a site visit on June 16, 2016, at least three additional jurisdictional tributaries to Soapstone Branch were observed upstream of the Dean Road crossing.

In 2008, the USACE and EPA issued guidance titled "Clean Water Act Jurisdiction Following the U.S. Supreme Court's Decision in Rapanos v. United States & Carabell v. United States," that included new stream classifications. Soapstone Branch would be considered a Relatively Permanent Water (Perennial).

6.1.3. Impacts to Waters of the U.S.

The Clean Water Act authorizes the USACE to regulate "placement of fill or dredged material" in Waters of the U.S. The USACE and the courts have long interpreted this phrase to include a wide variety of activities including the placement of earthen fill, placement of culverts, construction of utility lines, placement of armor, construction of dams, dikes or levees, impoundment of water, mechanized land clearing, and conversion of forested wetlands to maintained areas.

Construction and land management activities in or around Waters of the U.S. should be evaluated to determine if they are considered to be impacts by the USACE. If so, authorization by a Department of the Army Permit may be necessary.

6.2. Section 404 Permits

6.2.1. General Permits (Nationwide Permits)

For proposed activities that will only have minimal adverse effects, a General Permit may be appropriate. These permits may be issued on a state, regional, or nationwide basis. The Nationwide Permit (NWP) is a specific type of General Permit that covers most activities with minimal adverse effects in the Mobile District; it is likely that activities associated with the proposed project could be authorized by NWPs. These permits are organized into categories by land use and proposed activities. NWPs that could be useful for the Soapstone Branch project include Nationwide Permits 3 (Repair, rehabilitation, or replacement of previously authorized, currently serviceable structures or fills), 13 (Bank Stabilization), 14 (Linear Transportation Projects), 27 (Aquatic Habitat, Restoration, Enhancement, and Establishment Activities), and/or 39 (Commercial and Institutional Developments).

By definition, NWPs only authorize activites with minimal adverse effects. Therefore, many NWPs only authorize activities within defined limits. These limits should be reviewed on a case by case basis, but generally impacts greater than 0.5 acres of Waters of the U.S. and/or 300 feet of stream channel are not authorized by NWPs. In some cases, it may be possible to request a waiver to these limits.

USACE review of NWPs is limited to 45 days. However, it should be noted that in the event that the USACE requests additional information, the USACE's review may be paused until that issue is resolved. A common delay occurs when the USACE commonly requests documentation of a project's compliance with Section 107 of the National Historic Preservation Act. This often

necessitates an archaeological/historical survey and agency review. These issues have the potential to extend the USACE review months beyond the 45-day review window.

6.2.2.Individual Permits

Proposed activities that are potentially significant must be authorized by an Individual Permit (IP); there are no limits to the impacts that may be authorized by an IP. All appropriate regulatory agencies (USACE, U.S. Environmental Protection Agency, U.S. Fish & Wildlife Service, National Marine Fisheries Service, National Oceanic and Atmospheric Administration, Alabama Department of Environmental Management, Alabama Historic Commission/State Historic Preservation Officer, etc.) review IPs, and there is no time limit to the review. In general, applicants request IPs when their projects may not be authorized by a NWP due to the quantity or nature of impacts.

6.2.3. Compensatory Mitigation

Compensatory mitigation is usually required as a condition of a USACE Permit. Mitigation is intended to compensate for the loss of quantity and function of Waters of the U.S. due to the permitted activity. Mitigation must be "in-kind." Wetland mitigation offsets wetland impacts and stream mitigation offsets stream impacts.

The Mobile District of the USACE uses various assessment tools to track the amount of mitigation required for various activities as "credits." Mitigation credits may be purchased from an approved mitigation bank or provided by the applicant. In either case, certain restoration, enhancement, or preservation activities must be conducted on wetlands or streams in order to "generate" the appropriate wetland credits or stream credits.

Most projects in the Mobile District provide mitigation credits through the purchase of credits from a mitigation bank. However, mitigation credits can be very expensive and have the potential to be a significant portion of a project's budget. In many cases, the required mitigation credits may render a project unfeasible.

Compensatory mitigation is not always required as a condition of a Department of the Army Permit.

6.3. Potential impacts to Soapstone Branch

Any intervention in Soapstone Branch should be evaluated to determine if USACE notification and permit authorization is required. The following sections discuss two alternatives that may be employed, and the permitting concerns associated with them. The potential for activities in adjacent areas has also been addressed.

6.3.1. Alternative 1 – Replace Structure on Existing Alignment

If the Dean Road structure over Soapstone Branch could be replaced within the footprint of the existing structure, the replacement would be authorized by NWP 3 (Repair, rehabilitation, or

replacement of previously authorized, currently serviceable structures or fills). USACE notification and mitigation are not required.

If a new structure is installed over Soapstone Branch at a different location or if the culvert length is increased, authorization under NWP 14 (Linear Transportation Projects) would be required. This would require a Pre-Construction Notification (permit application) to the USACE and mitigation.

If the existing structure were removed and replaced with a bridge that spans the entire channel, the USACE would view the activity as a removal of old impact. No notification or mitigation would be required.

6.3.2. Alternative 2 - In-stream Intervention,

In-stream intervention measures could involve a combination of techniques, including the placement of armor, grading/reshaping the stream bottom, and /or a construction of a sediment trap.

Armor - The banks of Soapstone Branch could be armored with rip-rap, stone, or another hardened material in order to prevent further bank erosion. This activity is authorized by NWP 13 (Bank Stabilization) without notification if the total length of armor is less than 500 feet, the discharge is less than 1 cubic yard/running foot, and material is not discharged in to special aquatic sites (including riffle-pool sequences). If the proposed activity does not meet any of the above conditions, a Pre-Construction Notification to the USACE would be required for authorization by NWP 13. Whether or not mitigation would be required would depend on the USACE evaluation of the design.

Grading - Grading or shaping the stream bottom could be performed under authorization by NWP 27 (Aquatic Habitat, Restoration, Enhancement, and Establishment Activities) if the activity were determined by the USACE to constitute aquatic habitat restoration. This would require appropriate natural channel design including the use of an ecological reference site and accepted techniques and design principles. Activities authorized by NWP 27 are not considered impacts; therefore, mitigation is not required.

Grading or shaping of the stream bottom that does not conform to natural channel design principles may require authorization under an IP. These activities would be considered impacts and would require mitigation.

Sediment Trap - Although NWP 43 (Stormwater Management Facilities) may authorize sediment traps in certain circumstances, it specifically excludes the construction of new stormwater management facilities in perennial streams. Therefore, construction of a

sediment trap within the channel of Soapstone Branch would require authorization under an IP and mitigation would be required.

6.3.3. Activities in Adjacent Areas

Location of offline stormwater management facilities outside of the channel will avoid stream impacts. However, care should be taken to utilize non-wetland areas if possible in order to avoid wetland impact and the need to permit those facilities. In addition, other construction activities such as haul roads, staging areas, etc. should also be located outside wetland areas in order to achieve avoidance of impacts.

Identification of adjacent wetland areas should be conducted early in the design process in order to facilitate avoidance.

7. Conclusions and recommendations for future studies

This research was motivated by a serious aggradation problem occurring on the Dean Road bridge in Dale County, as it crosses Soapstone Branch catchment, a tributary of Little Choctawhatchee River. Historical aerial imageries of the catchment revealed increasing deforestation occurring in a short period of time 2011–2015, some of which near or at the stream banks. The research involved the development of a field investigation, use of hydrological modeling tools and hydraulic modeling tools. The goals involved the quantification of changes in sediment yield in the past years, as well to assess whether a stream modification strategy could result in a sustainable means for sediment discharge in the cross section.

HEC-HMS hydrological model was applied alongside with MUSLE for quantifying the change in discharge and then sediment yield due to human activities was explored in this study. Apart from topographic and physiographic factors required for computing sediment yield, discharge data at catchment outlet is required. Soapstone branch catchment being an ungauged catchment lacked discharge time series information. Initial attempts of installing an Area-Velocity sensor in the catchment for obtaining discharge data failed due to severe aggradation occurring after each event and sensor getting buried. As an alternative to obtain discharge data, hydrological modeling using parameter transfer approach from nearby gauged donor catchment draining to Choctawhatchee River was undertaken. However, parameters in curve number method are highly sensitive and predominant land use types in the donor catchment and the Soapstone Branch catchment are variable. Due to these reasons, a less-sensitive SMA model which depends mostly on soil data was used for parameter transfer.

A continuous SMA model was developed for the donor catchment (Choctawhatchee River catchment draining near Newton, Alabama) using land cover and soil data. Due to the limitation of precipitation data, the model was run from January 2009–September 2015, where the period of study was partitioned into nine months of warmup and three years of both calibration and validation each. For identification of sensitive parameters for ease in calibrating the model, a sensitivity analysis was performed. Based on this sensitivity analysis, six most sensitive parameters were selected for manual and automated calibration. The NSE value of 0.73 and PBIAS of -10.4% during the calibration period and a NSE value of 0.63 and PBIAS of 3.8% during the validation period were obtained. This suggested that the model is capable of simulating streamflow well.

These modeling parameters were then transferred to the Soapstone Branch catchment to be used with the hydrological model. Precipitation data from the nearby Dothan regional airport prior to 2016 was used together with the installed rain gauge data since 2016. The model was run from January 2009–December 2016 with nine months of warmup period. Due to lower sensitivity of SMA model to changes in land cover and MUSLE being an event based sediment yield model, an event based method was required.

Two event based curve number models were initially developed, based on land cover information from 2011 and 2015. Apart from land cover and soil data, CN model is highly affected by antecedent runoff condition (ARC). Therefore, those two event based models were then, expanded into six different CN models considering three ARC classes for each one of them. Six

corresponding storm events were selected and simulated and results were compared against SMA model results. Following a calibration process, most CN models yielded results that matched the SMA model results, which enabled the study of the sediment yield using the MUSLE approach.

Three storm events corresponding to each ARC class types after 2011 were simulated using 2011 and 2015 land cover scenario. An increase in peak runoff and volume of runoff due to land cover change from 2011–2015 was found for each of these events. A final application of MUSLE together with CN model revealed an increase of more than 40% in sediment yield due to land cover changes in the catchment. Furthermore, a hypothetical scenario with assumption of no major deforestation in the vicinity of stream reveals an increase of sediment yield of more than 35 % from 2011 to 2015. This suggests increase in rangeland area, agricultural land, thinning of forests, etc. have pronounced effects on sediment yield.

Another outcome from these research was the development of a hydraulic modeling of Soapstone Branch near Dean Road Bridge. Based on the stream flows calculated from the hydrological model, the main goal was to compute shear stress near the bridge crossing at current conditions and after a stream modification strategy. The stream modification intended to facilitate sediment discharge through increasing the stream bed slope as Soapstone Branch approached Dean Road Bridge.

The first step needed to achieve this goal was to perform a calibration of the hydraulic model, which involved choosing an adequate Manning roughness factor. However, flow conditions near the bridge are specially challenging due to varying amount of sediment accumulated under the bridge during a flooding event. The varying flows result in a partial clearing of the sediment under the bridge during a rain event, leading to pressurized flows under the bridge. In addition, overtopping may also occur if the flow rates are large. Various geometry surrogates to represent the behavior of the observed depth-discharge for a variety of rain events. A geometry was found that successfully represented the head discharge near the bridge site, enabling a study on shear stresses at other areas near Dean Road Bridge.

The numerical simulations to investigate shear stresses at Soapstone Branch compared the existing condition and the conditions after the stream modification was introduced. It was shown that the proposed stream modification yielded consistently larger values of shear stress in the stream near the bridge site. This indicates that this alternative would facilitate the transport of sediment near the bridge site, mitigating the aggradation process.

One shortcoming of this stage of the research was the inability of the hydraulic model (HEC-RAS 5) to simulate sediment transport in this two-dimensional simulation framework. To overcome this issue another hydraulic model, SRH-2D, was used in this work. Comparisons were made between HEC-RAS 5 and SRH-2D results in terms of flow depth and velocity, and modeling results were shown to be very consistent with each other. Thus SRH-2D shear stress predictions were generated and results of simulated shear stress from both models compared fairly well. The last stage of the hydraulic modeling process involved using SRH-2D model for an extended (30.5-day long) simulation that represented one month of base flows followed by an intense rain event. These results showed that no significant aggradation occurred near the bridge site during the initial 30 days (aggradation under 15 cm or 0.5 ft.). The intense rain event results in minor aggradation upstream from the bridge (typically under 20 cm or 0.7 ft.) and minor scour downstream (less than 9 cm or 3.5 in.). This indicates that the proposed alternative can be sustainable, avoiding the need

of channel dredging that is currently in place. This stream modification strategy also is likely to be significantly less expensive than an alternative involving the replacement of Dean Road Bridge.

Whether a stream modification strategy or a bridge replacement alternative is used, any intervention in Soapstone Branch will require adequate permitting. The different types of required permits, associated with different interventions in Soapstone Branch, are presented in this work. However, one point to be considered is that the sources of sediments in the watershed need to be controlled to prevent further complications on Dean Road Bridge, or even in bridges located downstream in the Little Choctawhatchee River or the Choctawhatchee River. This involves communication and coordination of efforts with landowners within the watershed, particularly the ones with land at the edge of the stream.

The continuation of this research developed in this effort could involve the following:

- Monitoring of other bridge or culvert crossings in the State of Alabama that are experiencing similar aggradation issues, and apply the methodology used in this study to evaluate alternatives to solve the aggradation issue.
- Development of the 2nd stage of research in rivers downstream from Soapstone Branch to determine if the aggradation issues created in the nearby watersheds are impacting these bridge conveyance capacity.
- Improve the methodology used in the present research by exploring other alternatives to perform hydrological studies and sediment yield analysis. With this methodology, map bridge crossings across the State of Alabama that are more at risk of being impacted by aggradation processes.
- Perform a detailed analysis of the role of streambank failure mechanism in the amount of sediment generation in Soapstone Branch.

Lastly, a temporary steel bridge structure was placed in Dean Road to attempt to remedy the issues with the overtopping and damage to the existing Dean Road Bridge. However, as this research pointed out, aggradation still continues to occur on the site given that the stream slope was not changed. Moreover, there are signs of erosion created by stormwater drainage issues at the newly constructed embankments of the temporary steel bridge, which in turn can impact its safety. It is recommended to study and implement alternatives to remedy these drainage issues as soon as possible.

References

Aricö C. and Tucciarelli, T. (2008) “Diffusive modeling of aggradation and degradation in artificial channels” *Journal of Hydraulic Engineering*, ASCE

Arneson, L.A.; Zevenbergen, L.W.; Lagasse, P.F. and Clopper P.E. (2012), *Evaluating Scour at Bridges,* 5th edition, Federal Highway Administration Report No. FHWA-HIF-12-003 HEC-18

Bashar, K. E., and A. F. Zaki. "SMA Based Continuous Hydrologic Simulation of the Blue Nile." *A paper published in the International Conference of UNESCO Flanders FUST FRIEND/NILE Project" Towards a Better Cooperation”. Sharm El-Sheikh, Egypt*. 2005.

Bennett, T. H. (1998). *Development and application of a continuous soil moisture accounting algorithm for the Hydrologic Engineering Center Hydrologic Modeling System (HEC-HMS*). University of California, Davis.

Bossler, J. D., Jensen, J. R., McMaster, R. B., and Rizos, C. (2004). *Manual of geospatial science and technology*, CRC Press.

Brown, G. W. and Krygier, J. T. (1971) “Clear-Cut logging and Sediment Production in the Oregon Coast Range” *Water Resources Research,* V. 7 N. 5, pp. 1189 – 1198

Brunner, G. W. (2010). *HEC-RAS River Analysis System: Hydraulic Reference Manual*. US Army Corps of Engineers, Institute for Water Resources, Hydrologic Engineering Center.

Brunner, G. W. (2018). *HEC-RAS River Analysis System: Supplemental to HEC-RAS Version 5.0 User's Manual.* US Army Corps of Engineers, Institute for Water Resources, Hydrologic Engineering Center.

Brunner, G. W. and Gibson, S. (2005). Sediment Transport Modeling in HEC RAS. *Proc. 2005 ASCE EWRI World Water and Environmental Resources Congress*, Anchorage, AK

Castro, J. and Reckendorf F. (1995) *Effects of Sediment on the Aquatic Environment: Potential NRCS Actions to Improve Aquatic Habitat – Working Paper No. 6*. Natural Resources Conservation Service and Oregon State University – Department of Geosciences

Colman, E. (1947). "A Laboratory Procedure For Determining The Field Capacity of Soils." *Soil Science*, 63(4), 277-284.

Cosby, B., Hornberger, G., Clapp, R., and Ginn, T. (1984). "A statistical exploration of the relationships of soil moisture characteristics to the physical properties of soils." *Water Resources Research*, 20(6), 682-690.

Farnsworth, R. K., and Thompson, E. S. (1983). *Mean monthly, seasonal, and annual pan evaporation for the United States*, US Department of Commerce, National Oceanic and Atmospheric Administration, National Weather Service.

Feldman, A. D. (2000). *Hydrologic modeling system HEC-HMS: technical reference manual*, US Army Corps of Engineers, Hydrologic Engineering Center.

Fleming, M. (2002). "*Continuous hydrologic modeling with HMS: parameter estimation and model calibration and validation."* Msc Thesis, Tennessee Technological University.

Fleming, M., and Vincent N. (2004) "Continuous hydrologic modeling study with the hydrologic modeling system." *Journal of Hydrologic Engineering* 9.3 : 175-183.

Gitas, I. Z., Douros, K., Minakou, C., Silleos, G. N., and Karydas, C. G. (2009). "Multi-temporal soil erosion risk assessment in N. Chalkidiki using a modified usle raster model." *EARSeL eProceedings*, 8(1), 40-52.

Ghimire, G. and DeVantier, B. (2016) “Sediment Modeling to Develop a Deposition Prediction Model at the Olmsted Locks and Dam Area”. *Proceedings of ASCE EWRI World Environmental and Water Resources Congress*. pp. 410-420.

Gibson, S. A., J. H. Pak, and M. J. Fleming. (2010) "Modeling watershed and riverine sediment processes with HEC-HMS and HEC-RAS." *Watershed management conference*. 2010.

Harbor, J. (1995) “Engineering geomorphology at the cutting edge of land disturbance: erosion and sediment control on construction sites” *Geomorphology* V. 31 pp. 247–263

Heeren, D. M.; Mittelstet, A. R.; Fox, G. A.; Storm, D. E.; Al-Madhhachi, A. T.; Midgley, T. L.; Stringer, A. F.; Stunkel, K. B.; and Tejral, R. D. (2012) "Using rapid geomorphic assessments to assess streambank stability in Oklahoma Ozark streams." *Transactions of the ASABE* 55.3 (2012): 957-968.

Hogan S. (2015) “Advancements in Two-Dimensional Floodplain Modeling with SRH-2D” *Presentation on the 2015 Association of State Flood Plain Managers Conference, 06/04/2015.*

Holberg, J. A. (2015). "*Downward model development of the soil moisture accounting loss method in HEC-HMS: Revelations concerning the soil profile*." Purdue University.

Johnson, P. A.’; Hey, R. D.; Horst, M. W. and Hess, A. J. (2001) “Aggradation at Bridges” *Journal of Hydraulic Engineering*, ASCE, V. 127, N. 2, pp. 154 –157

Johnston, P., and Pilgrim, D. (1976). "Parameter optimization for watershed models." *Water Resources Research*, 12(3), 477-486.

Kinnell, P. I. A. (2005) "Why the universal soil loss equation and the revised version of it do not predict event erosion well." *Hydrological Processes* 19.3: 851-854.

Kuok, K. K., Mah, D. Y., and Chiu, P. (2013). "Evaluation of C and P factors in universal soil loss equation on trapping sediment: case study of Santubong River." *Journal of Water Resource and Protection*, 5(12), 1149.

Lagasse, P.F.; Clopper P.E., Pagán-Ortiz, J.E., Zevenbergen, L.W., Arneson L.A., Shall, J.D. and Girard L.G. (2009), *Bridge Scour and Stream Instability Countermeasures*, 3nd Edition, Federal Highway Administration Report No. FHWA NHI HEC-23.

Lagasse, P.F.; Zevenbergen, L.W.; Spitz, W.J. and Arneson L.A. (2012), *Stream Stability at Highway Structures,* 4th edition, Federal Highway Administration Report No. FHWA-HIF-12-004 HEC-20

Lai, Y.G. (2010). “Two-Dimensional Depth-Averaged Flow Modeling with an Unstructured Hybrid Mesh,” *Journal of Hydraulic Engineering*, ASCE, V. 136 N.1, pp. 12-23.

McCuen, R. H. (2005). *Hydrologic analysis and design*, Prentice-Hall, Englewood Cliffs, N.J.

Meselhe, E., Habib, E., Oche, O., and Gautam, S. (2009 "Sensitivity of conceptual and physically based hydrologic models to temporal and spatial rainfall sampling." *Journal of Hydrologic Engineering* 14.7: 711-720.

Morgan, R.P. (2009) “Soil erosion and conservation”. John Wiley & Sons.

NASS, U.-. (1997). "Usual Planting and Harvesting Dates for US Field Crops." *Agricultural Handbook*, 628.

Oudin, L., Andréassian, V., Perrin, C., Michel, C., and Le Moine, N. (2008). "Spatial proximity, physical similarity, regression and ungaged catchments: A comparison of regionalization approaches based on 913 French catchments." *Water Resources Research*, 44(3).

Pak, J.; Fleming, M.; Scharffenberg, W.; and Ely, P. (2008) "Soil erosion and sediment yield modeling with the hydrologic modeling system (HEC-HMS)." *Proceedings of ASCE EWRI World Environmental and Water Resources Congress*.

Pak, J.; Fleming, M.; Scharffenberg, W.; Gibson, S.; and Brauer, T. (2015) "Modeling Surface Soil Erosion and Sediment Transport Processes in the Upper North Bosque River Watershed, Texas." *Journal of Hydrologic Engineering* DOI 10.1061/(ASCE)HE.1943-5584.0001205, 04015034.

Pandeya, A.; Himanshua, S. K. Mishraa, S. K.; and Singh, V. P (2016) "Physically based soil erosion and sediment yield models revisited." *CATENA* 147, 595-620.

Pannell, D. J. (1997). "Sensitivity analysis: strategies, methods, concepts, examples." *Agric Econ*, 16, 139-152.

Richardson, E.V., Simons, D.B., and Lagasse, P.F. (2002). *River Engineering for Highway Encroachments*, *Highway in the river environmen*t, Federal Highway Administration Report No. FHWA NHI 01-004 HDS 6.

Rawls, W. J., Brakensiek, D., and Saxtonn, K. (1982). "Estimation of soil water properties." *Transactions of the ASAE*, 25(5), 1316-1320.

Roy, D.; Begam, S.; Ghosh S.; and Jana, S. (2013) "Calibration and validation of HEC-HMS model for a river basin in Eastern India." *ARPN Journal of Engineering and Applied Sciences* 8.1 33-49.

Seiden, Z. T., and Schwartz. J. (2013) "A Review of Erosional Processes along a River Continuum: Watershed-scale Implications for River Restoration Planning." *Proceedings of ASCE EWRI World Environmental and Water Resources Congress.*

Service, U. S. N. R. C. (1995). Soil Survey Geographic (SSURGO) Data Base: Data Use Information, National Cartography and GIS Center.

Smith, D. D. (1941). "Interpretation of soil conservation data for field use." Agric. Engg., 22, 173-175.

Song, X. M., Kong, F. Z., and Zhu, Z. X. (2011). "Application of Muskingum routing method with variable parameters in ungauged basin." Water Science and Engineering, 4(1), 1-12.

Speth, J. G. "Towards an effective and operational international convention on desertification." [Unpublished] 1994. Presented at the Third INC-D Session of the Intergovernmental U.S. Army Corps of Engineers (2015). *Hydrologic Modeling System HEC-HMS Applications Guide*. USACE Report No. CPD-74C

Wang, J.; Briaud, J.L.; Li, Y.; Chen, H.C. and Nurtjahyo, P. (2004) *NCHRP Report 516: Pier and Contraction Scour in Cohesive Soils* ISBN 978-0-309-26929-2, National Academies Press

USDA, N. (1972). "*National Engineering Handbook*." Hydrology Section, 4, 4-10.

U.S. Geological Survey (2016) he StreamStats program, online at http://streamstats.usgs.gov, accessed on July, 2018.

Viessman, W., and Lewis, G. L. (2003). Introduction to hydrology, Pearson Education, Upper Saddle River, N.J.

Williams, J. R. (1975) "Sediment-yield prediction with universal equation using runoff energy factor." In *Present and Prospective Technology for Predicting Sediment Yield and Sources*, Vol. ARS-S-40 p. 244-252.

Wischmeier, W.H., and D.D. Smith. (1965) *Predicting rainfall-erosion losses from crop land east of the Rocky Mountains: Guide for selection of practices for soil and water conservation*. U.S. Dep. of Agriculture, Agriculture. Handbook No.282.

Yang, Chih Ted (1996) *Sediment Transport – Theory and Practice*, McGraw-Hill press, 396 p.

Zhang, Y., and Chiew, F. H. (2009). "Relative merits of different methods for runoff predictions in ungauged catchments." Water Resources Research, 45(7).

Zhang H., and. Kahawita R. (1986) “Nonlinear Model for Aggradation in Alluvial Channels”. *Journal of Hydraulic Engineering*, ASCE

Zingg, A. W. (1940). "Degree and length of land slope as it affects soil loss in run-off." Agric. Engng., 21, 59-64.